Reviews in Mineralogy & Geochemistry
Vol. 57, pp. 241-290, 2005



# Modular Microporous Minerals: Cancrinite-Davyne Group and C-S-H Phases

**Elena Bonaccorsi and Stefano Merlino**

*Dipartimento di Scienze della Terra*
*Università di Pisa*
*Pisa I-56126, Italy*
*elena@dst.unipi.it merlino@dst.unipi.it*

In this chapter, we illustrate and discuss two distinct groups of microporous phases: the cancrinite group and the C-S-H compounds of the tobermorite and gyrolite families. The compounds in the first group present a three-dimensional purely tetrahedral framework with, apart from a single exception, Si:Al ratio equal to 1; in the mineralogical classifications they are included among feldspathoids and are generally "regarded …… distinct from zeolites, in part, at least, because of the presence of large volatile anions" (Coombs et al. 1998). The members of the second group are characterized by mixed frameworks built up by silicon (and aluminum) tetrahedra and calcium polyhedra. A common feature of both groups is the modular character of their frameworks, which are built up through various stacking ways of a single module (as in the minerals of the cancrinite-davyne family) and two or more modules as in the case of the C-S-H phases.

## CANCRINITE-DAVYNE GROUP

### Structural aspects

The minerals belonging to the cancrinite group (Merlino 1984; Deer et al. 2004) are feldspathoids with a Si:Al ratio equal to 1, with the only exception of cancrisilite, which has Si:Al = 7:5 (Khomyakov et al. 1991a,b). The available structural data for the phases with Si:Al = 1 indicate that silicon and aluminum regularly alternate in the tetrahedral sites, in accordance with the Loewenstein rule. The structural cavities host alkaline and earth-alkaline cations, and a wide variety of extra-framework anions, as well as $H_2O$ molecules. Their framework is characterized by layers containing six-membered rings of tetrahedra (Fig. 1). Every ring is linked to three similar rings in the preceding layer and to three rings in the succeeding one. If the position of the rings in the first layer is called "A," and the two possible alternative positions in the adjacent layers are "B" and

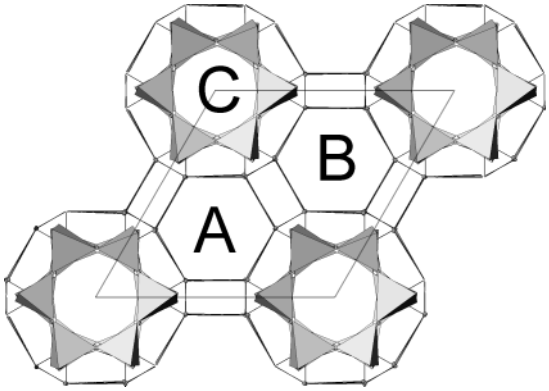


**Figure 1.** Schematic drawing of the layer of six-membered rings which builds up the minerals of the cancrinite group; the positions A, B and C are indicated.

1529-6466/05/0057-0008$05.00 DOI: 10.2138/rmg.2005.57.8

"C," following the notation of the closest-packed structures, the resulting framework can be described by a sequence of A, B, C symbols, without consecutive repetition of letters. Another group of phases exists, in which six-membered rings may overlap, forming a double ring, or a hexagonal prism. In this case, the stacking sequence symbol contains pairs of A, B and/or C letters, as in the well-known offretite (AAB... stacking sequence), gmelinite (AABB...), and chabazite (AABBCC…) zeolites. Formally, all these natural or synthetic phases as well as the members of the cancrinite group belong to the so-called ABC-6 family of crystal structures (Gies et al. 1999). The natural phases of this wide group are listed in Table 1.

By examining Table 1, it is evident that the minerals traditionally included in the cancrinite group could be divided in two subgroups on the basis of the stacking sequence of layers. The simplest sequence AB… characterizes many natural and synthetic phases including cancrinite, vishnevite, and davyne. On the contrary, other trigonal or hexagonal phases show more complex stacking sequences of layers, which give rise to the occurrence of different cages. The known minerals with complex sequences have 4, 6, 8, 10, 12, 14, 16, and 28 layers for *c* translation; moreover, domains showing 14, 18 and 24 layer sequences were observed in TEM images (Rinaldi and Wenk 1979; Rinaldi 1982). All these phases with complex sequences were originally named "cancrinite-like" minerals by Leoni et al. (1979), and, later on, they were usually grouped together within the "cancrinite group."

***The phases with AB… stacking sequence.*** There are nine natural phases which display the same kind of framework, built up by the AB... sequence of six-membered rings of tetrahedra. Eight phases are aluminosilicates; tiptopite, instead is a beryllophosphate with formula $[(Li_{2.9}Na_{1.7}Ca_{0.7})(OH)_2(H_2O)_{1.3}](K_2)(Be_6P_6O_{24})$ (Peacor et al. 1987).

The framework of the nine phases is characterized by channels delimited by 12-membered rings of tetrahedra running along [001], denoted as $[6^612^{2/2}]$ in the IUPAC nomenclature (McCusker et al. 2001), and by columns of base-sharing cancrinite cages, denoted as $[4^66^5]$ but also known as ε-cages or undecahedral cages (Fig. 2).

While the extra-framework content of the channel varies to a large extent in the different minerals, in the small cancrinite cages only two different situations have been observed: either water molecules bonded to sodium cations or chlorine anions bonded to calcium cations occur (see below). Consequently, the minerals will be grouped just taking into account this crystal chemical difference.

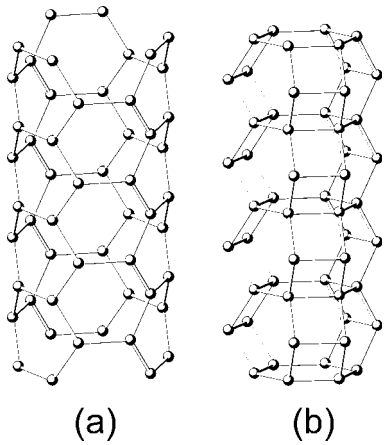


**Figure 2**. Open channel (a) and column of base-sharing cancrinite cages (b), running along the [001] direction in the AB... framework. Only the tetrahedral sites are indicated.

*The cancrinite-vishnevite series.* On the basis of crystal chemical considerations Pauling (1930) put forward the first hypothesis on the crystal structure of cancrinite; and it was confirmed and refined by Jarchow (1965). Later on, many other structural refinements of natural and synthetic cancrinites have been performed, and many other chemical data have been collected, allowing for a sound definition of its compositional range. The crystal chemical formula of cancrinite may be written as:

$$[(Na,Ca)_{5\text{-}6}(CO_3)_{1.4\text{–}1.7}][Na_2(H_2O)_2][Si_6Al_6O_{24}]$$

where the first part of the formula refers to the content of the large channel, the second to the cancrinite cages, and the last one represents the framework

composition. In the large channel, the amount of allowable carbonate groups is limited by the occurrence of short contacts between two adjacent carbonate groups. By assuming the distance between two carbonate groups in aragonite [2.87 Å] as the lowest possible C-C distance in cancrinite, a maximum content of 1.78 $CO_3$ groups may be calculated. This value is in agreement with the published chemical analyses (cf. Fig. 3). The ordering of the carbonate groups and vacancies, possibly related to the ordering of neighboring sodium and calcium cations, can give rise to the occurrence of satellite reflections (Jarchow 1965; Brown and Cesbron 1973; Foit et al. 1973; Grundy and Hassan 1982; Hassan and Buseck 1992) pointing to commensurate superstructures with multiple *c* values, as well as to incommensurate structures.

Actually, almost all the natural cancrinites contain also significant amounts of $SO_4$ anions (Fig. 3), substituting the carbonate groups. The end-member of this substitutional series is the mineral vishnevite, of chemical formula

$$[(Na,Ca)_{6-x}K_x(SO_4)][Na_2(H_2O)_2][Si_6Al_6O_{24}]$$

The presence of one sulfate group per unit cell, instead of 1.4÷1.7 carbonate groups, allows for the introduction of significant amounts *x* of potassium cations within the channel. In vishnevite of the type locality $x = 1$ (Hassan and Grundy 1984), and the potassium cation is statistically distributed in the Na1 cation site. However, up to three K cations could occupy three symmetry related sites in the channel, which regularly alternate with three (Na,Ca) sites surrounding the sulfate groups (Pushcharovskii et al. 1989). The apparently disordered distribution of these atoms inside the channel, with two split cation sites and two statistically occupied sulfur sites, depends on the lack of long-range correlation of this ordered sequence in the different channels; actually, a (Na,Ca):K ratio close to 1 greatly favors a long range ordering of sulfate groups and extra-framework cations also within adjacent channels; consequently, superstructure reflections requiring $a_{sup} = \sqrt{3}\ a$ occur. In agreement with this statement, the "high-potassium vishnevite" from Synnyrksii, Russia (Pushcharovskii et al. 1989), which contains about 3 $K^+$ cations per unit cell, has cell parameter $a = 22.24$ Å (Bonaccorsi 1992). A potassium rich phase with $a = \sqrt{3}\ a_{vish} = 22.1$ Å was originally found at Pitigliano (Italy) and named pitiglianoite (Merlino et al. 1991).

In all these phases – cancrinite, vishnevite, pitiglianoite – the cancrinite cages contain sodium cations and water molecules. The sodium cations are strongly bonded to three framework oxygen atoms and to one water molecule (bond distances of 2.30–2.45 Å), in

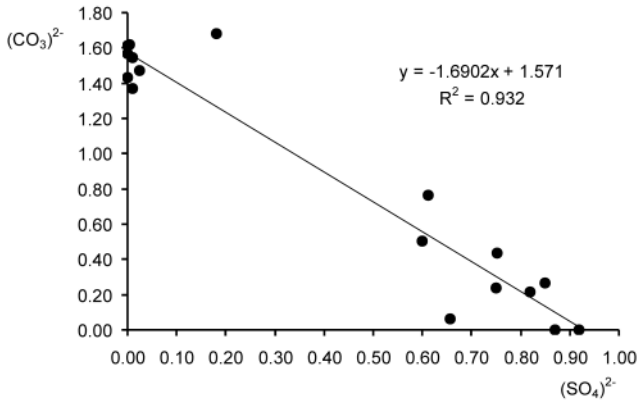


**Figure 3.** Correlation between $(CO_3)^{2-}$ and $(SO_4)^{2-}$ contents in minerals of the cancrinite-vishnevite series. Modified from Ballirano et al. (1998).

**Table 1.** The ABC-6 family of minerals. *N* = number of the layers for unit cell. In italics synthetic phases with no natural counterpart.

| *Phase* | *Stacking sequence* | *N* | *S.G.* | *a* (Å) | *c* (Å) | *Z* | *Ideal chemical formula (on the basis of 12 tetrahedral cations)* |
|---|---|---|---|---|---|---|---|
| ***Single six-membered rings*** | | | | | | | |
| sodalite | (ABC) | 3 | $P\bar{4}3n$ | 8.882 | | 1 | $(Na_8Cl_2)(Si_6Al_6O_{24})$ |
| haüyne | (ABC) | 3 | $P\bar{4}3n$ ($P23$) | 9.082 | | 1 | $[Na_6Ca_2(SO_4)_2](Si_6Al_6O_{24})$ |
| nosean | (ABC) | 3 | $P\bar{4}3n$ | 9.090 | | 1 | $[Na_8(SO_4)(H_2O)](Si_6Al_6O_{24})$ |
| lazurite | (ABC) | 3 | $P\bar{4}3n$ | 9.074 | | 1 | $\{(Na,Ca)_8[(SO_4),S,Cl,(OH)]_2\}(Si_6Al_6O_{24})$ |
| helvite | (ABC) | 3 | $P\bar{4}3n$ | 8.291 | | 1 | $(Mn_8S_2)(Be_6Si_6O_{24})$ |
| genthelvite | (ABC) | 3 | $P\bar{4}3n$ | 8.120 | | 1 | $(Zn_8S_2)(Be_6Si_6O_{24})$ |
| danalite | (ABC) | 3 | $P\bar{4}3n$ | 8.213 | | 1 | $(Fe_8S_2)(Be_6Si_6O_{24})$ |
| bicchulite | (ABC) | 3 | $P\bar{4}3n$ | 8.829 | | 1 | $[Ca_8(OH)_8](Al_8Si_4O_{24})$ |
| tugtupite | (ABC) | 3 | $I\bar{4}$ | 8.640 | $c$ = 8.874 | 1 | $(Na_8Cl_2)(Al_2Be_2Si_8O_{24})$ |
| tsaregorodsevite | (ABC) | 3 | $I222$ | 8.984 | $b$ = 8.937<br>$c$ = 8.927 | 1 | $[N(CH_3)_4]_2(Si_{10}Al_2O_{24})$ |
| cancrinite | (AB) | 2 | $P6_3$ | 12.615 | 5.127 | 1 | $[(Ca,Na)_6(CO_3)_{1\text{-}1.7}][Na_2(H_2O)_2](Si_6Al_6O_{24})$ |
| vishnevite | (AB) | 2 | $P6_3$ | 12.685 | 5.179 | 1 | $[(Na_6(SO_4)][Na_2(H_2O)_2](Si_6Al_6O_{24})$ |
| hydroxycancrinite | (AB) | 2 | $P3$ | 12.740 | 5.182 | 1 | $[Na_6(OH)_2][Na_2(H_2O)_2](Si_6Al_6O_{24})$ |
| cancrisilite | (AB) | 2 | $P6_3mc$ | 12.575 | 5.105 | 1 | $Na_7Al_5Si_7O_{24}(CO_3)\cdot 3H_2O$ |
| pitiglianoite | (AB) | 2 | $P6_3$ | 22.121 | 5.221 | 1 | $[(Na_4K_2)(SO_4)][Na_2(H_2O)_2](Si_6Al_6O_{24})$ |
| davyne | (AB) | 2 | $P6_3/m$ or $P6_3$ | 12.705 | 5.368 | 1 | $[(Na,K)_6(SO_4)_{0.5\text{-}1}Cl_{1\text{-}0}](Ca_2Cl_2)(Si_6Al_6O_{24})$ |
| microsommite | (AB) | 2 | $P6_3$ | 22.142 | 5.345 | 3 | $[Na_4K_2(SO_4)](Ca_2Cl_2)(Si_6Al_6O_{24})$ |
| quadridavyne | (AB) | 2 | $P6_3/m$ | 25.771 | 5.371 | 4 | $[(Na,K)_6Cl_2](Ca_2Cl_2)(Si_6Al_6O_{24})$ |
| tiptopite | (AB) | 2 | $P6_3$ | 11.655 | 4.692 | 1 | $[(Li_{2.9}Na_{1.7}Ca_{0.7})(OH)_2(H_2O)_{1.3}](K_2)(Be_6P_6O_{24})$ |
| bystrite | (ABAC) | 4 | $P31c$ | 12.855 | 10.700 | 2 | $[(Na,K)_7Ca](Si_6Al_6O_{24})(S^{2-})_{1.5}\cdot H_2O$ |
| liottite | (ABABAC) | 6 | $P\bar{6}$ | 12.87 | 16.096 | 3 | $[(Na,K)_{5.3}Ca_{2.7}](Si_6Al_6O_{24})(SO_4)_{1.7}Cl_{1.3}$ |

| | | | | | | | |
|---|---|---|---|---|---|---|---|
| afghanite | (ABABACAC) | 8 | $P31c$ | 12.801 | 21.412 | 4 | $[(Na,K)_{5.5}Ca_{2.5}](Si_6Al_6O_{24})(SO_4)_{1.5}Cl_{1.5}$ |
| franzinite | (ABCABACABC) | 10 | $P321$ | 12.904 | 26.514 | 5 | $[(Na,K)_6Ca_2](Si_6Al_6O_{24})(SO_4)_2\cdot 0.4H_2O$ |
| tounkite | (ABABACACABAC) | 12 | $P3$ | 12.755 | 32.218 | 6 | $[(Na,K)_5Ca_3](Si_6Al_6O_{24})(SO_4)_{1.7}Cl_{1.3}$ |
| marinellite | (ABCBCBACBCBC) | 12 | $P\bar{6}2c$ or $P31c$ | 12.88 | 31.761 | 6 | $[(Na,K)_7Ca](Si_6Al_6O_{24})(SO_4)_{1.3}Cl_{0.3}\cdot H_2O$ |
| farneseite | (ABCABABACBACAC) | 14 | $P6_3/m$ | 12.878 | 37.007 | 7 | $[(Na,Ca,K)_8](Si_6Al_6O_{24})(SO_4)_{1.7}(Cl,H_2O)_{0.9}$ |
| giuseppettite | (ABABABACBABABABC) | 16 | $P31c$ | 12.858 | 42.306 | 8 | $[(Na,K)_{7.25}Ca_{0.75}](Si_6Al_6O_{24})(SO_4)_{1.25}Cl_{0.25}\cdot H_2O$ |
| sacrofanite | (ABCABACACABACBAC BACABABACABC) | 28 | $P\bar{6}2c$ | 12.865 | 74.24 | 14 | $[Na,K,Ca]_8(Si_6Al_6O_{24})(SO_4)_{1.86}Cl_{0.14}\cdot 0.57H_2O$ |
| ***Double six-membered rings*** | | | | | | | |
| gmelinite | (AABB) | 4 | $P6_3/mmc$ | 13.756 | 10.048 | 1 | $(Na_2,Ca)_4(Al_8Si_{16}O_{48})\cdot 24H_2O$ |
| chabazite | (AABBCC) | 6 | $R\bar{3}m$ | 13.803 | 15.075 | 1 | $Ca_6Al_{12}Si_{24}O_{72}\cdot 36H_2O$ |
| willhendersonite | (AABBCC) | 6 | $P\bar{1}$ | $a = 9.206$<br>$b = 9.216$<br>$c = 9.500$ | $\alpha = 92.3$<br>$\beta = 92.7$<br>$\gamma = 90.1$ | 1 | $Ca_6K_6Al_{18}Si_{18}O_{72}\cdot 30H_2O$ |
| *SAPO-56* | *(AABBCCBB)* | *8* | $P\bar{3}1c$ | *13.757* | *19.936* | *1* | $TMHD_{3.26}(Al_{23.5}P_{19.5}Si_{4.9})O_{96}$ |
| *AlPO4-52* | *(AABBCCAACCBB)* | *12* | $P\bar{3}1c$ | *13.73* | *28.95* | *1* | $7.2[(TEA^+)(H2PO_4^-)]\cdot[Al_{36}P_{36}]O_{144}$ |
| ***Alternated single and double six-membered rings*** | | | | | | | |
| offretite | (AAB) | 3 | $P\bar{6}m2$ | 13.261 | 7.347 | 1 | $KCaMg[Al_5Si_{13}O_{36}]\cdot 16H_2O$ |
| erionite | (AABAAC) | 6 | $P6_3/mmc$ | 13.15 | 15.05 | 1 | $Na_2K_2Ca_3[Al_{10}Si_{26}O_{72}]\cdot 30H_2O$ |
| bellbergite | (ABBACC) | 6 | $P6_3/mmc$, $P6_3mc$, or $P\bar{6}2c$ | 13.244 | 15.988 | 1 | $(K,Na,Sr)_2Sr_2Ca_2(Ca,Na)_4Al_{18}Si_{18}O_{72}\cdot 30H_2O$ |
| levyne | (AABCCABBC) | 9 | $R\bar{3}m$ | 13.338 | 23.014 | 1 | $Ca_8Na_{2.1}K_{0.9}[Al_{19}Si_{35}O_{108}]\cdot 50H_2O$ |
| ***One double and two single rings regularly alternated*** | | | | | | | |
| *STA-2* | *(ABBCBCCACAAB)* | *12* | $R\bar{3}$ | *12.726* | *30.939* | 1 | $(Mg_6Al_{30})P_{36}O_{144}\cdot 3R^{2+}\cdot 22H_2O$ |

a substantially tetrahedral coordination, whereas three other oxygen atoms and the water molecule on the other side form weaker bonds (bond distances greater than 2.8 Å). The column of cancrinite cages contains Na-$H_2O$···Na-$H_2O$··· sequences; this atomic distribution excludes the occurrence of a horizontal symmetry plane (the space group of all these phases is $P6_3$), and results in a generally short *c* parameter (5.1 ÷ 5.2 Å).

*Davyne, microsommite, quadridavyne.* Davyne, microsommite and quadridavyne host $Ca^{2+}$ and $Cl^-$ in the cancrinite cages, instead of $Na^+$ and $H_2O$. The calcium cation lies on the base of the cancrinite cages, and has a bi-pyramidal coordination, forming six bonds with the framework oxygen atoms in the base of the cage, and two equal bonds with the chlorine anions which occupy the center of two base-sharing cancrinite cages. The resulting Ca-Cl-Ca-Cl-… chain along [001] is compatible with the $P6_3/m$ space group, which was actually found in davyne and quadridavyne (Bonaccorsi et al. 1990; Bonaccorsi et al. 1994). Moreover, the *c* parameter (5.36 Å) of davyne, microsommite and quadridavyne is significantly higher than that (5.20 Å) of the cancrinite-vishnevite phases.

These minerals differ as regards the kind of the extra-framework anions which are placed in the large channel, microsommite being the sulfate-rich and quadridavyne the chloride-rich end-member of the substitutional series $(Na,K)_6(SO_4)Ca_2Cl_2Si_6Al_6O_{24}$ – $(Na,K)_6(Cl_2)Ca_2Cl_2Si_6Al_6O_{24}$, whereas davyne has an intermediate composition. Moreover, davyne may also contain significant amounts of carbonate groups (Ballirano et al. 1998; Binon et al. 2004). The peculiarity of this series is the different ordering which takes place in the two end-members, resulting in different superstructures. The relationships among the unit cells of the three phases are sketched in Figure 4.

The structural results obtained for davyne from Vesuvius (Bonaccorsi et al. 1990; Hassan and Grundy 1990), indicate that the sodium and potassium cations located in the channel occupy two different sites, external and internal respectively. Up to one sulfate can be placed in the large channel, with the S atom occupying one of two symmetry-related sites, ½ *c* apart. As only the external cation sites may be occupied at the same level of the sulfate group, to prevent too short contact distances, an ordered distribution of two distinct clusters, the former built up by a ($SO_4$) anion surrounded by three Na cations, the latter built up by three (K,Na) cations, may be hypothesized. The observed disordered distribution of the two groups is the consequence of two factors, both occurring in davyne: (i) the ordering of these groups in the channels can be realized in two geometrically equivalent ways, and adjacent channels display them statistically; and (ii) the substitution of one sulfate group by two chlorine anions, as well as by carbonate groups, could break the ordered sequence within a channel. In microsommite, where such substitutions are not present, the channels are internally ordered and the scheme of ordering

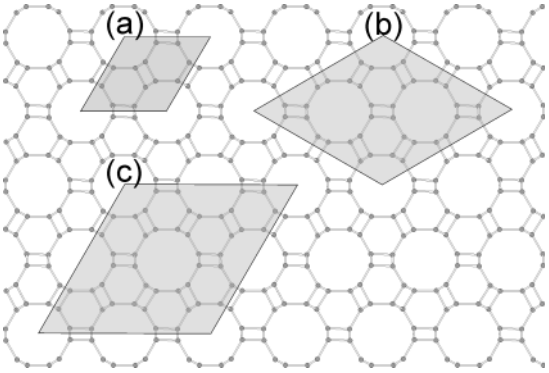


**Figure 4.** Relationships among the unit cell of (a) davyne, (b) microsommite and (c) quadridavyne, as seen along [001].

is correlated in adjacent channels, so that they are no longer equivalent by translation, and a superstructure develops. Such long-range ordering depends on the temperature, and a davyne-like phase can be obtained by heating microsommite up to 750°C (Bonaccorsi et al. 2001).

A similar thermal behavior has been observed in quadridavyne, the sulfate-free end member of the series. The crystal structure of quadridavyne is not known in detail, as the superstructure reflections are generally very weak. Preliminary structural data were published together with the description of the mineral (Bonaccorsi et al. 1994), indicating a possible ordering scheme for the chlorine anions and the alkali cations inside the channels.

*Cancrisilite, hydroxycancrinite.* These two phases are substantially similar to the minerals of the cancrinite-vishnevite series as regards the content of the cancrinite cages ($Na^+$ and $H_2O$), but they differ for the other chemical components.

Hydroxycancrinite (Nadezhina et al. 1991; Khomyakov et al. 1992) is the natural counterpart of the widely synthesized "basic cancrinite," containing sodium and (OH) groups within the large channel.

Cancrisilite (Khomyakov et al. 1991a,b) is the only member of the group which shows a Si:Al ratio different from 1. Its simplified crystal formula is $Na_7[Al_5Si_7O_{24}](CO_3)\cdot 3H_2O$, cell parameters $a$ = 12.573, $c$ = 5.105 Å and space group $P6_3mc$.

***The phases with complex sequences of layers.*** Nine minerals were found which may be described as a more or less complex sequence of six-membered single rings (Table 1). Their $c$ parameters correspond to 4, 6, 8, 10, 12, 14, 16, 28 layers. Generally, only one mineral exists for a given number of layers, except the case of marinellite and tounkite, which are structurally different phases presenting the same number of layers (twelve).

The complex-sequence phases may be also conveniently described by examining the different cages stacked along the [001] direction in three distinct columns, corresponding to the A, B and C positions, respectively. In Table 2, the sequences of cages occurring in the different structures are listed, whereas a schematic drawing of the existing structures is reported in Figure 5. The common feature of all these cages is that they are delimited by six-membered and four-membered rings only, at variance with the cages that occur in other phases of the ABC-6 family, which contain also eight-member rings.

The thickness of the cages along $c$ correspond to 2, 3, 4, 6, 8 layers of six-member rings, respectively. Cages corresponding to 5 or 7 layers were never found, probably because they are unsuitable to host an integer number of sulfate groups. As each kind of cage has similar features in the different minerals, a short description of the cages and of their chemical content in these minerals will be presented hereafter.

*Cancrinite cage.* The cancrinite cage, $[4^6 6^5]$ according to the IUPAC rules, has a thickness along $c$ corresponding to two layers. All the minerals with complex sequences of layers contain an even number of cancrinite cages, which, as already seen in the phases with AB... stacking sequence, may host either water molecules or chlorine anions (Fig. 6a and 6b, respectively). In the former case (franzinite, marinellite, giuseppettite, and partially in sacrofanite), the site in the center of the cage may be partially occupied, pointing to a water content lower than the maximum allowable. In the latter case (bystrite, liottite, afghanite, tounkite), the site is fully occupied. A minor substitution of chlorine by fluorine anions has been observed in liottite and afghanite.

*Sodalite cage.* The sodalite cage, $[4^6 6^8]$ in the IUPAC nomenclature, is well known, as it constitutes the building unit of the sodalite group minerals (see Depmeier 2005), as well as of other zeolitic phases, where it can host many types of extra-framework atoms. In the phases

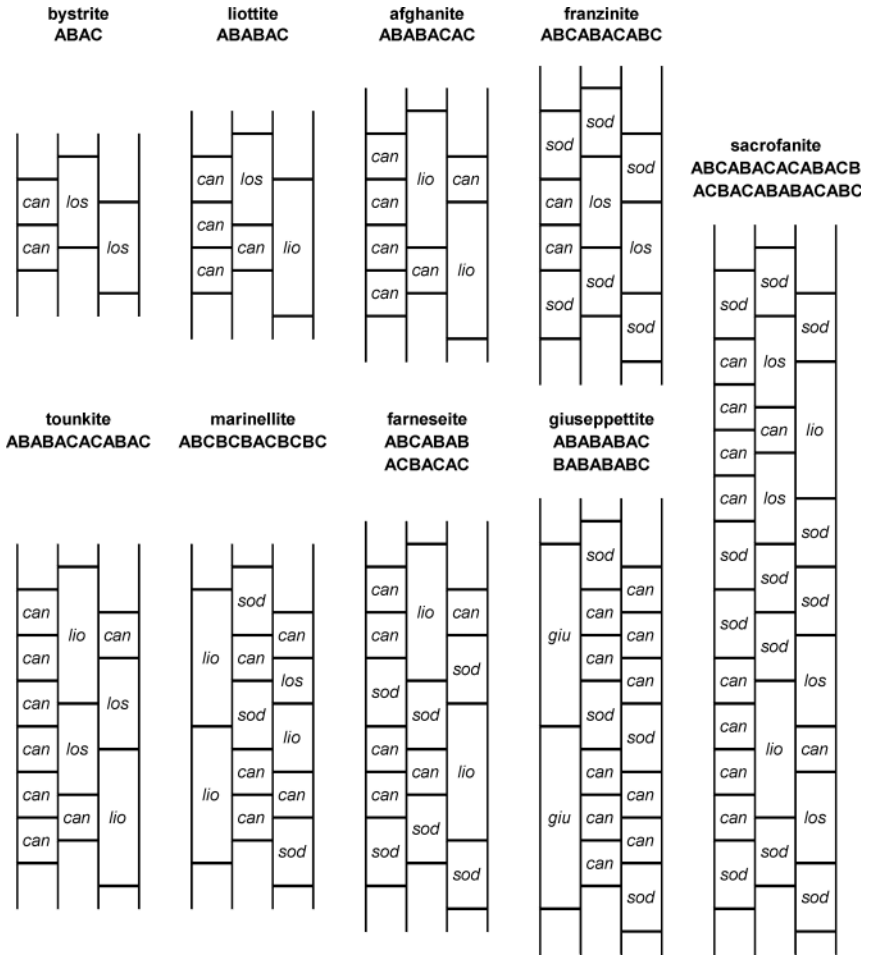


**Figure 5.** Schematic drawing of the sequences of cages in the cancrinite group minerals showing complex sequences of layers.

of the cancrinite group this kind of cage hosts generally one sulfate group in the center of the cage, whereas (Na,Ca) cations are distributed in split sites near the center of the eight six-membered faces of the cage (Fig. 7a). Typically, the atom distribution within this kind of cage is highly disordered, from both the chemical and geometrical points of view. In marinellite and giuseppettite, the sodalite cages host both sulfate and chlorine anions (Fig. 7a and 7b, respectively). In those cases, the ordering of sulfate and chlorine anions in different sodalite cages causes a decreasing of symmetry from $P\bar{6}2c$ to $P31c$.

*Losod cage.* The losod cage was first described by Sieber and Meier (1974) in the synthetic compound "Losod," which is a four-layer phase isostructural with bystrite. It has symbol $[4^6 6^{11}]$ and has a thickness of four layers. The minerals which contain losod cages (Fig. 8a) are bystrite itself, liottite, franzinite, tounkite and sacrofanite. Apart from bystrite, which probably contains a significant amount of $S^{2-}$ anions, in the other minerals this kind of cage is able to host two sulfate groups. They are surrounded by three (Ca,Na) cations, which may be shared by other neighboring cages, and are separated by groups of three cations.

**Table 2.** Structures of the complex sequence phases. The sequences of cages along the three columns are indicated by a sequences of number, corresponding to the width of the cages in terms of layers (2 = cancrinite cage, 3 = sodalite cage and so on).

| *Phase* | *N* | *Zdhanov symbol* | *number and kind of cages in the unit cell* | *0, 0, z* | *1/3, 2/3, z* | *2/3, 1/3, z* | *Ref.* |
|---|---|---|---|---|---|---|---|
| bystrite | 4 | \|(2)\|(2)\| | 2 *los*, 2 *can* | 22 | 4 | 4 | (1) |
| liottite | 6 | \|21\|12\| | 1 *lio*, 1 *los*, 4 *can* | 222 | 24 | 6 | (2) |
| afghanite | 8 | \|1(2)1\|1(2)1\| | 2 *lio*, 6 *can* | 2222 | 26 | 62 | (3) |
| franzinite | 10 | 82 | 2 *los*, 6 *sod*, 2 *can* | 3223 | 343 | 433 | (4) |
| tounkite | 12 | (2)211(2)112 | 2 *lio*, 2 *los*, 8 *can* | 222222 | 264 | 624 | (5) |
| marinellite | 12 | \|1(4)1\|1(4)1\| | 2 *lio*, 4 *sod*, 6 *can* | 66 | 23223 | 22323 | (6) |
| farneseite | 14 | \|1(5)1\|1(5)1\| | 2 *lio*, 6 *sod*, 6 *can* | 322322 | 6323 | 3236 | (7) |
| giuseppettite | 16 | \|11(4)11\|11(4)11\| | 2 *giu*, 4 *sod*, 10 *can* | 88 | 2232223 | 2223223 | (8) |
| sacrofanite | 28 | \|12(8)21\|12(8)21\| | 2 *lio*, 4 *los*, 12 *sod*, 10 *can* | 322223322223 | 34243363 | 36334243 | (9), (10) |

*References:* (1) Pobedimskaya et al. 1991; (2) Ballirano et al. 1996b; (3) Ballirano et al. 1997; (4) Ballirano et al. 2000; (5) Rozenberg et al. 2004; (6) Bonaccorsi and Orlandi 2004; (7) Camara et al. 2004; (8) Bonaccorsi 2004; (9) Ballirano 1994; (10) Ballirano and Bonaccorsi (*pers. commun.*)

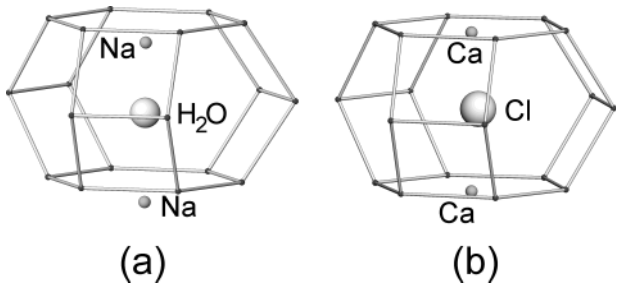


**Figure 6**. Cancrinite cages hosting Na and $H_2O$ (a) and Ca and Cl (b).

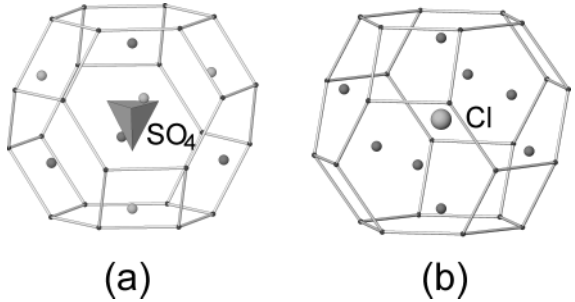


**Figure 7**. Sodalite cages hosting (a) one sulfate group and (b) one chloride anion in the center of the cage. (Na,Ca) cations are represented as small grey circles.

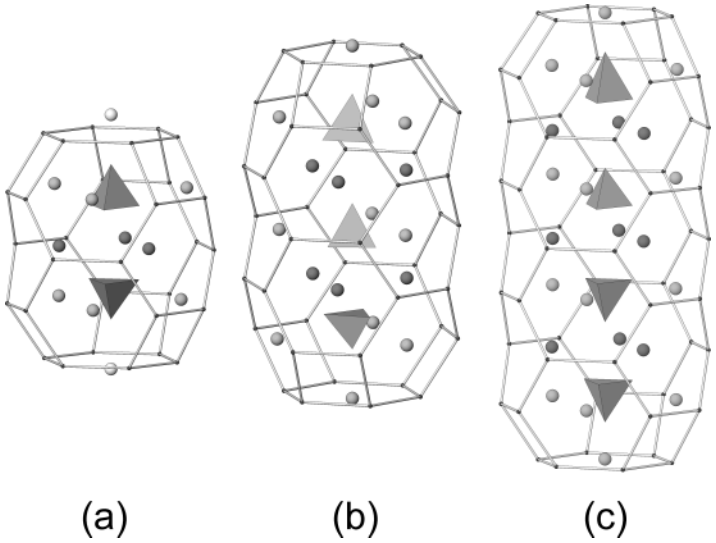


**Figure 8.** (a) Losod cage, containing two $SO_4$ groups; (b) liottite cage, with three $SO_4$ groups; (c) giuseppettite cage, 21 Å long; it contains four $SO_4$ groups. In the various cages, triples of cations (filled small circles) follow each other along [001].

*Liottite cage.* This 6-layer cage, $[4^6 6^{17}]$ is present in liottite, afghanite, tounkite, marinellite, sacrofanite, as well as in a 14-layer new phase (Camara et al. 2004) [the new mineral and its name, farneseite, have been recently approved by the IMA Commission on New Minerals and Mineral Names, IMA No. 2004-043]. The liottite cage contains three sulfate groups (Fig. 8b).

*Giuseppettite cage.* This 8-layer long cage, with symbol $[4^6 6^{23}]$, was found so far only in giuseppettite, where it contains four sulfate groups (Fig. 8c).

***Relationships between chemistry and stacking sequences.*** The occurrence of so numerous phases showing different stacking sequences and number of layers in the unit cell raises the problem of the stability fields, and of the chemical and physical factors which influence the crystallization.

An earlier trial to set some geometrical constraints on the chemical content in the different cages was attempted by Ballirano et al. (1996a). Those authors recognized that phases showing different stacking sequences display also different chemical composition, especially as regards the extra-framework anion content. In their model, the small cancrinite cages host a chloride anion, whereas the larger cages host sulfate groups (1, 2, 3 and 4 in sodalite, losod, liottite and giuseppettite cages, respectively). According to those authors the $SO_4$ group seems to play a major role, as "…it tends to fill completely the available voids within the framework."

More recently, Sapozhnikov et al. (2004) built a reasonable structural model of tounkite, one of the two 12-layer members of the group, just on the basis of similar crystal chemical considerations. They observed that the phases containing more than one $Cl^-$ anion per 12 (Si+Al) tetrahedral cations, namely liottite and afghanite, display uninterrupted columns of cancrinite cages in their framework. Moreover, their normalized *c* parameter, namely their actual *c* parameter divided by *N*/2 (*N* is defined in Table 1) is higher than the normalized *c* parameter of the phases with a lower chlorine content (for example franzinite, marinellite, giuseppettite). The authors emphasized the role of the chloride anions in determining the stacking sequence of

the different phases. As tounkite shows a high chlorine content, as well as large normalized *c* parameter, they assumed and afterwards successfully confirmed (Rozenberg et al. 2004) that a continuous column of cancrinite cages should be present in its structure.

In both the mentioned approaches, the occurrence of a well-defined stacking sequence is related to the presence of different amounts of extra-framework anions. In fact, while the sum of the extra-framework cations is equal to 8 per 12 tetrahedral cations in all the idealized formulas of the cancrinite group phases, the sum of the extra-framework anions and of the $H_2O$ molecules is variable, ranging from 2 to 3 in the phases with complex sequences of layers. This variability does not depend on the possible partial occupancy of the anion sites, but is a consequence of the set of different types of cages present in the various structures. In Figure 9, the extra-framework chemical content of the minerals with complex sequence of layers is plotted in a ($SO_4$) vs. (Cl + $H_2O$) diagram. As additional information, also the anion contents of several sodalite group minerals (ABC... stacking sequence) and cancrinite group minerals (AB... stacking sequence) are plotted in the same diagram.

The minerals with the simple AB... stacking sequence may host the greatest amount of extra-framework anions and/or water molecules. As reported above, for example, microsommite, davyne and quadridavyne, respectively, all contain two chlorine anions within the cancrinite cages, whereas in the large channel one sulfate group (occurring in microsommite) may be partially or completely substituted by two chlorine anions (in davyne and quadridavyne). Similarly, vishnevite and pitiglianoite contain two $H_2O$ molecules in the cancrinite cages and one $SO_4$ group in the channel. On the contrary, the sum of the extra-framework anions and water molecules in minerals with ABC... stacking sequence (sodalite group) is ideally equal to 2.

The phases with more complex sequence of layers occupy a different field in the plot of Figure 9. They are able to host more anions than the minerals of the sodalite group and more sulfate groups than the phases with AB... stacking sequence. For example, the framework of afghanite, 8-layer member with stacking sequence ABABACAC..., is formed by six cancrinite cages, containing 6 $Cl^-$ anions, and two liottite cages, each one hosting three $(SO_4)^{2-}$ group. The formula of afghanite, on the basis of 12 (Si+Al) tetrahedral cations, may be written as $[(Na,K)_{5.5}Ca_{2.5}](Si_6Al_6O_{24})(SO_4)_{1.5}Cl_{1.5}$, where the sum of the extra-framework anions is

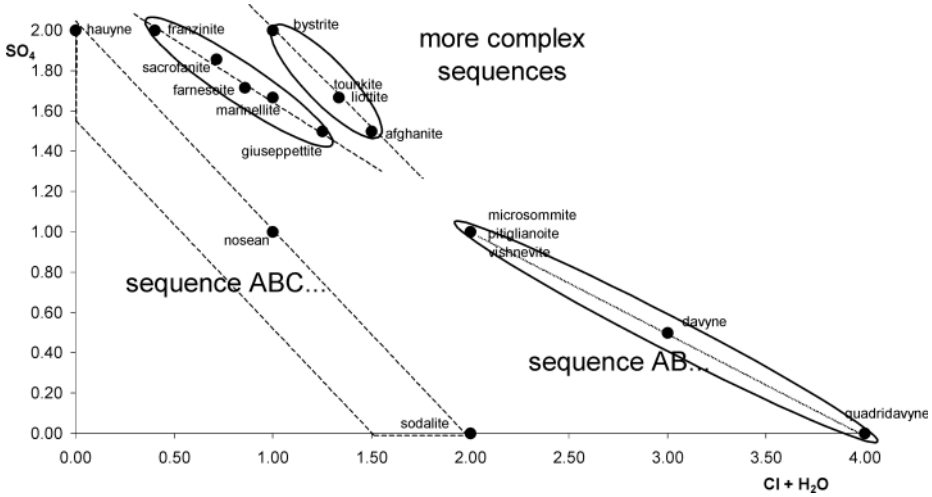


**Figure 9.** Different compositional fields of the phases formed by the stacking of layers with six-membered single rings.

exactly 3. On the other hand, the framework of franzinite, 10-layer member with stacking sequence ABCABACABC..., is formed by two cancrinite, six sodalite and two losod cages. The formula of franzinite is $[(Na,K)_6Ca_2](Si_6Al_6O_{24})(SO_4)_2 \cdot 0.4H_2O$, where the sum of the extra-framework anions and water molecules is 2.4. As a rule, the occurrence of sodalite cages reduces the amount of extra-framework anions which can be hosted in a structure.

By looking at the diagram of Figure 9, it can also be observed that the points corresponding to the complex-sequence phases present two different trends, suggesting a possible regularity in the stacking sequence of layers on the basis of the $(SO_4)$:$(Cl+H_2O)$ ratio. One trend comprises bystrite, liottite, afghanite and tounkite. These phases are characterized by the absence of sodalite cages, a high chlorine content, a great normalized *c* parameter around 5.36 Å (Sapozhnikov 2004) and a sum of extra-framework anions ideally equal to 3. The second trend includes franzinite, marinellite, farneseite, giuseppettite and sacrofanite. Their frameworks are characterized by the occurrence of sodalite cages; moreover, they host a lower amount of chlorine anions, and a sum of extra-framework anions and water molecules ranging from 2.3 to 2.7 per formula unit. Additionally, their normalized *c* parameter is always below 5.30 Å.

These considerations, together with the relationships between the size of the cages and their chemical content discussed in a preceding section, could be useful both for descriptive and structure modeling purposes. For example, on the basis of a good chemical analysis giving the exact amount of the extra-framework anions and water molecules, and knowing the number of the layers from the cell parameter *c*, the number of the possible cages in the structure could be evaluated.

**Genesis of natural compounds**

The genesis of the cancrinite-group minerals and the main localities of occurrence are exhaustively accounted for in Deer et al. (2004), and also the recently found minerals of the group (marinellite and farneseite) have occurrences similar to those there described for other complex-sequence minerals.

The most common occurrence of cancrinite as primary phase is in nepheline syenite intrusions, where it crystallizes in the late stage as hydrothermal product in the presence of fluids containing "volatile" components such as carbonate, sulfate and/or chloride anions. Cancrinite occurs also as replacement of nepheline or minerals of the sodalite group. Similar occurrences, even if less common, were reported for vishnevite.

Cancrinite and cancrinite-group minerals formed also in the contact zone between alkaline rocks and limestone. Several minerals with complex sequences of layers are found in ejected skarn blocks in Italian volcanic areas (afghanite, in the Somma-Vesuvius area; liottite, afghanite, franzinite, and farneseite in Monti Vulsini volcanic field, afghanite, franzinite, marinellite, giuseppettite, sacrofanite in the Monti Sabatini volcanic area). Few of these minerals were found also in other localities. Afghanite was first found in Sar-e-Sang lapislazuli mine, Afghanistan, and later in several other localities in contact metamorphic deposits (Ivanov and Sapozhnikov 1975; Hogarth 1979), including Zabargad Island, Egypt (Bonaccorsi et al. 1992). Giuseppettite was also claimed to occur in the Oslo Rift, Norway (Jamtveit et al. 1997), but it was identified only by means of a microprobe analysis.

**Thermal behavior**

Few studies were performed to characterize the structural modification of cancrinite and related phases by increasing temperature. The structural modifications of carbonate cancrinite upon heating are related to the dehydration and to the consequent movement of the sodium cations in the cancrinite cages (Ballirano et al. 1995; Hassan et al. 2005). The non-linear

increase of the cell parameters, and the discontinuity observed at about 500°C were related (Hassan et al. 2005) to the different thermal mechanisms operating in cancrinite. A different behavior upon heating was observed in pitiglianoite (Merlino and Bonaccorsi, unpublished results), where the dehydration process, in the temperature range 200–350°C, corresponds to a significant decrease of the cell volume (Fig. 10).

The linear thermal expansion coefficients up to 650°C were obtained for davyne from two localities and for microsommite (Bonaccorsi et al. 1995). The observed discontinuity in the thermal expansion of the *c* parameter of microsommite was related to the tilting of the tetrahedra connected along [001] and to the occurrence of a purely displacive phase transition with symmetry change from $P6_3$ to $P6_3/m$ at about 200°C.

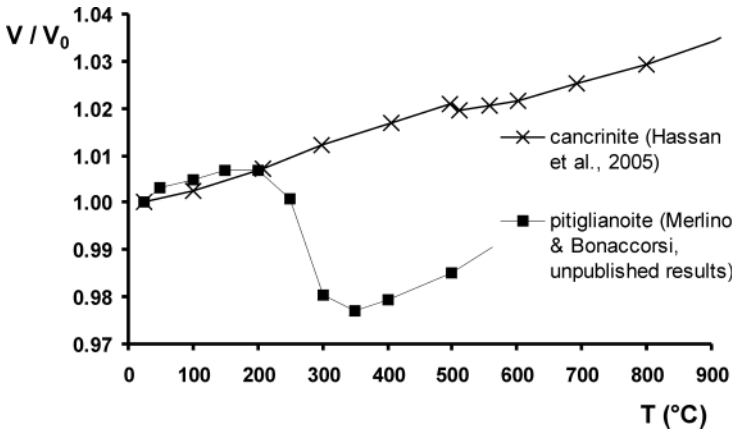


**Figure 10.** Relative variations of the unit cell volume with increasing temperature for cancrinite (crosses) and pitiglianoite (filled squares).

**Synthetic cancrinites**

Many synthetic compounds were obtained, showing the same framework topology of cancrinite, and with a wide variability as regards both the extra-framework species and the tetrahedral cations. A list of these compounds may be found in the paper by Sirbescu and Jenkins (1999); additional entries are reported in Table 3. Phases with chemical compositions very similar to those of natural cancrinite can be readily synthesized by hydrothermal reaction of oxides and carbonates, or from gels and carbonates; cancrinite was also obtained by hydrothermal methods starting from a mixture of kaolinite, NaOH and $NaHCO_3$.

After the first approach of Eitel (1922), several other authors studied synthetic $CO_3$-bearing cancrinite either from a structural point of view (Nithollon and Vernotte 1955; Smolin et al. 1981; Emiraliev and Yamzin 1982; Buhl 1991; Hackbarth et al. 1999) or in order to define its stability field (Barrer and White 1952; Edgar and Burley 1963; Edgar 1964; Zyryanov 1982; Hackbarth et al. 1999; Sirbescu and Jenkins 1999).

As far as structural aspects are concerned, no significant differences were observed with respect to the natural samples (Grundy and Hassan 1982; Ballirano and Maras 2004). The refined occupancy factors for the carbon sites within the channel appears to be lower than in natural cancrinites, pointing to only one carbonate group per formula unit instead of 1.4–1.6 (see also Fig. 3). Moreover, no superstructure reflections were observed in these synthetic $CO_3$-bearing samples, in agreement with their lower $CO_3$ content; in fact, the possible ordering

**Table 3**. Synthetic cancrinites which are not already listed in Sirbescu and Jenkins (1999).

| *Crystal-chemical formula* | | | *a* | *c* | *S.G.* | *Ref.* |
|---|---|---|---|---|---|---|
| *Channel* | *Cage* | *Framework* | | | | |
| $Na_6H_{0.88}(CO_3)_{1.44}$ | $Na_2(H_2O)_2$ | $[Al_6Si_6O_{24}]$ | 12.644 | 5.146 | $P6_3$ | (1) |
| $Na_{5.3}CO_3$ | $Na_2$ | $[Al_6Si_6O_{24}]$ | 12.659 | 5.153 | $P6_3$ | (2) |
| $Na_6CO_3{\cdot}1.4(H_2O)$ | $Na_2(H_2O)_2$ | $[Al_6Si_6O_{24}]$ | 12.713 | 5.186 | $P6_3$ | (3) |
| $Na_{5.5}(OH)_{1.5}{\cdot}5.6H_2O$ | $Na_2(H_2O)_2$ | $[Al_6Si_6O_{24}]$ | 12.756 | 5.198 | $P6_3$ | (4) |
| $Na_{5.6}(HCO_3)_{1.2}(CO_3)_{0.2}$ | $Na_2(H_2O)_2$ | $[Al_6Si_6O_{24}]$ | 12.725 | 5.177 | $P6_3$ | (5) |
| $Na_6(OH)_2$ | $Na_2(H_2O)_2$ | $[Al_6Si_6O_{24}]$ | 12.735 | 5.182 | $P6_3$ | (6) |
| $Na_{5.6}(NO_3)_{1.6}$ | $Na_2(H_2O)_2$ | $[Al_6Si_6O_{24}]$ | 12.668 | 5.166 | $P6_3$ | (7) |
| $Na_6(NO_3)_2{\cdot}2H_2O$ | $Na_2(H_2O)_2$ | $[Al_6Si_6O_{24}]$ | 12.68 | 5.18 | Not rep. | (8) |
| $Na_6(S_2O_3)$ | $Na_2(H_2O)_2$ | $[Al_6Si_6O_{24}]$ | 12.624 | 5.170 | $P3$ | (9) |
| $Na_6(S_2O_3){\cdot}H_2O$ | $Na_2(H_2O)_2$ | $[Al_6Si_6O_{24}]$ | 12.73 | 5.02 | Not rep. | (8) |
| $Na_6(SO_4){\cdot}H_2O$ | $Na_2(H_2O)_2$ | $[Al_6Si_6O_{24}]$ | 12.674 | 5.173 | Not rep. | (8) |
| $Na_6S{\cdot}2H_2O$ | $Na_2(H_2O)_2$ | $[Al_6Si_6O_{24}]$ | 12.669 | 5.187 | Not rep. | (8) |
| $Na_6(OH)_2{\cdot}0.54Se$ | $Na_2$ | $[Al_6Si_6O_{24}]$ | 12.670 | 5.165 | $P6_3$ | (6) |
| $Na_{2.5}(Se_2)^{2-}{}_{0.15}(Se_2)^{-}{}_{0.20}$ | $Na_2(H_2O)_2$ | $[Al_4Si_8O_{24}]$ | 12.639 | 5.157 | Not rep. | (10) |
| $Li_{4.5}{\cdot}4.9H_2O$ | $Cs_{1.50}$ | $[Al_6Si_6O_{24}]$ | 12.433 | 4.969 | $P6_3$ | (11) |
| $Li_{2.75}Tl_{1.25}{\cdot}2.0H_2O$ | $Tl_2$ | $[Al_6Si_6O_{24}]$ | 12.442 | 4.988 | $P6_3$ | (11) |
| $Li_{5.47}(OH)_{1.47}{\cdot}7.8(H_2O)$ | $Cs_2$ | $[Al_6Si_6O_{24}]$ | 12.416 | 4.970 | $P6_3$ | (12) |
| $Na_6Ge(OH)_6$ | $Na_2(H_2O)_2$ | $[Al_6Ge_6O_{24}]$ | 13.023 | 5.204 | $P6_3$ | (13) |
| $Na_6Ge(OH)_6$ | $Cs_2$ | $[Al_6Ge_6O_{24}]$ | 12.968 | 5.132 | $P6_3$ | (14) |
| $Na_6Ge(OH)_6$ | $Cs_2$ | $[Ga_6Ge_6O_{24}]$ | 12.950 | 5.117 | ($P6_3mc$) | (14) |
| $Na_6(OH)_2{\cdot}5H_2O$ | $Cs_2$ | $[Zn_6P_6O_{24}]$ | 12.794 | 5.066 | $P6_3$ | (15) |
| $Fe^{3+}Na{\cdot}6H_2O$ | $(Cs,K)_2$ | $[Zn_6P_6O_{24}]$ | 12.492 | 4.999 | $P6_3$ | (16) |
| $Na_6(OH)_2{\cdot}5.3H_2O$ | $Cs_2$ | $[Co_6P_6O_{24}]$ | 12.851 | 5.047 | $P6_3$ | (17) |

*References:* (1) Kanepit and Rieder 1995; (2) Burton et al. 1999; (3) Hackbarth et al. 1999; (4) Fechtelkord et al. 2003; (5) Gesing and Buhl 2000; (6) Bogomolov et al. 1992; (7) Buhl et al. 2000; (8) Hund 1984; (9) Lindner et al. 1995; (10) Lindner et al. 1996; (11) Norby et al. 1991; (12) Fechtelkord et al. 2001; (13) Belokoneva et al. 1986; (14) Lee et al. 2000; (15) Bienok et al 1998; (16) Yakubovich et al. 1986; (17) Bienok et al 2004

of one carbonate group per unit cell should simply correspond to a decrease of symmetry from $P6_3$ to $P3$ (Emiraliev and Yamzin 1982).

The stability of cancrinite as a function of $T$ and $X(CO_2)$ of the vapor phase was investigated at constant pressure by Sirbescu and Jenkins (1999). By increasing $T$ and $X(CO_2)$, cancrinite breakdowns to nepheline, calcite and $H_2O$, according to the reaction

$$\underset{\text{cancrinite}}{Na_6Ca_{1.5}[Al_6Si_6O_{24}](CO_3)_{1.5}{\cdot}1.1H_2O} = \underset{\text{nepheline}}{6\ NaAlSiO_4} + \underset{\text{calcite}}{1.5\ CaCO_3} + \underset{\text{fluid}}{1.1\ H_2O}$$

The thermodynamic analysis of this reaction allowed an evaluation of the enthalpy and entropy of cancrinite (Sirbescu and Jenkins 1999).

A so-called basic cancrinite, which corresponds to the hydroxycancrinite composition (Nadhezina et al. 1991; Khomyakov et al. 1992), has been obtained from a gel of composition $Na_2O$, $Al_2O_3$, $2SiO_2$, $xH_2O$ and aqueous NaOH in excess at 390°C (Barrer and White 1952; Barrer et al. 1970). The occurrence of both $H_2O$ molecules and $OH^-$ groups, as well as of two sites for the sodium cations, have been found within the structural channel of this sample. Similar structural results, except for the occurrence of only one cation site within the channel, were obtained for other synthetic basic cancrinites (Bresciani Pahor et al. 1982; Hassan and Grundy 1991).

Structural studies are also available for the nitrate cancrinite, with chemical formula $Na_{7.5}[Al_6Si_6O_{24}](NO_3)_{1.5}\cdot 2H_2O$. It was synthesized by hydrothermal reaction of kaolinite, NaOH and $NaNO_3$ (Barrer and White 1952) and later obtained in several different experiments (Hund 1984; Buhl et al. 2000). Different conclusions were reached as regards the position of the nitrate group within the cancrinite framework. While the early provisional data of Barrer and White (1952) suggested that $NO_3$ groups could be located mainly in the cancrinite cages, more recent results rule out this possibility, pointing out that $NO_3$ groups are located only in the channels, exactly as it happens for the $CO_3$ groups (Buhl et al. 2000).

A phase with composition $K_3Na_5(Si_6Al_6O_{24})(SO_4)_{0.67}(OH)_{0.67}\cdot 2.3–2.7H_2O$ and supercell parameters corresponding to pitiglianoite and microsommite was synthesized by Klaska and Jarchow (1977), who named it sulfate-hydrocancrinite.

Among the synthetic products containing more "exotic" guest species, the Cs-bearing cancrinites are particularly interesting as they were shown to contain the cesium cations entrapped in the center of the cancrinite cages (Norby et al. 1991; Fechtelkord et al. 2001; Bieniok et al. 2004). Here, the $Cs^+$ cation is strongly bonded to 12÷15 framework oxygen atoms with bond distances ranging from 3.2 to 3.7 Å, and is virtually not exchangeable. These properties, and the observation that cancrinite crystallizes as a secondary phase in the alteration process of kaolinite under particular conditions of high alkalinity, were the basis for environmental studies in the sedimentary soils near waste storage tanks (Chorover et al. 2003; Mashal et al. 2004). While the extensive uptake of $Cs^+$ into the crystal structure of newly formed nitrate cancrinite could be a promising way for immobilizing this radionuclide, the colloidal nature of the alteration products including cancrinite may actually facilitate the movement of $Cs^+$ in the soils (Zhuang et al. 2003).

More recently, several efforts have been made to synthesize cancrinite from organic solvents, in order to obtain a free channel system after removing, by heating, the small organic precursor molecules. Organic solvents successfully used to crystallize cancrinite are 1,3 and 1,4 butane-diol (Liu et al. 1993; Milestone et al. 1995; Burton et al. 1999; Fechtelkord et al. 2003).

ECR-5 (Vaughan 1986) is a cancrinite structure-type material obtained under application of ammonia and aqueous ammonia solutions; it has a high silica content and an increased adsorption capacity compared to conventional cancrinite. The same silica-rich phase was successively obtained in ammonia-free solutions (Vaughan 1991), disposing of a major pollution problem during the synthesis process.

An additional method successfully used to obtain synthetic cancrinite, together with sodalite and other zeolitic phases, makes use of molten salts (Park et al. 2000).

***Other synthetic phases.*** While a wide literature exists on synthetic compounds isostructural with cancrinite, few synthetic products are known with more complex stacking sequence. Actually, they were obtained only for the stacking sequence ABAC..., corresponding to the natural phase bystrite.

The compound "Losod" was synthesized and its crystal structure was proposed (Sieber and Meier 1974) before the natural counterpart was characterized by Pobedimskaya et al. (1991), who also refined the crystal structure. Losod has chemical formula $Na_6Si_6Al_6O_{24}\cdot 9H_2O$, and cell parameter $a$ = 12.906, $c$ = 10.541 Å. The proposed space group for Losod was $P6_3/mmc$ (Sieber and Meier 1974), but the probable ordering of Si and Al in the tetrahedral sites could lower the symmetry to either $P\bar{6}2c$ or $P31c$ (Baur 1991).

Later on, two other synthetic compounds with ABAC… framework type (LOS) were crystallized, a sodium aluminogermanate containing carbonate groups and water molecules in the cages (Sokolov et al. 1978, 1981; Baur 1991) and a lithium beryllophosphate, containing ($HPO_4$) and water molecules in the cages (Harrison et al. 1993).

So far, no phases have been synthesized with a framework corresponding to the more complex sequence of layers listed in Table 2. On the other hand, many synthetic compounds were obtained and characterized as formed by layers of six-membered rings with more or less complex stacking sequences but containing double six-membered rings of tetrahedra together with single ones. For example synthetic phases have been found to be isostructural with gmelinite, chabazite, offretite, erionite, bellbergite, and levyne, as reported in the Database of Zeolite Structures (*http://www.iza-structure.org/databases/*; website maintained by Baerlocher and McCusker). Moreover, other synthetic phases belonging to the ABC-6 family with double rings exist, which do not correspond to any natural counterpart (SAPO-56, AlPO4-52, STA-1; their stacking sequences are reported in Table 1).

**Ionic exchanges**

The cancrinite framework is composed by a large channel running along [001], delimited by 12-membered rings of tetrahedra and with a free diameter of about 6 Å, and by columns of cancrinite cages, delimited by 6- and 4-membered rings of tetrahedra (Fig. 2). As a consequence of this structural arrangement, it could be deduced that the extra-framework ions located within the channel are exchangeable and, on the contrary, the small openings of the cancrinite cages prevent the substitution of the guest species, at least at low temperature and for some cations. The experimental data partially confirm these hypotheses. However, the occurrence of stacking faults in the AB... sequence, with the insertion of a 6-membered ring in position C, could dramatically reduce the ionic exchange capacity of cancrinite. Another obstacle to the cation diffusion within the channel is the presence of other ionic species, which may block the structural micropores.

Complete exchange reactions Na ↔ Li and Na ↔ Ag occur between fused lithium and silver nitrates, respectively, and a synthetic basic-cancrinite (Barrer and Falconer 1956) to give completely exchanged Li- and Ag-cancrinites. These samples were used in successive cation exchanges in solutions containing salts of the ions Li, Na, K, Rb, Cs, Ag and Tl. While 100% exchanged cancrinites were obtained with Li, Na, and Ag, only partial exchanges were realized with K, Tl and Rb, and no exchange at all with Cs. Moreover, the complete and reversible exchange reaction between $Li^+$ and $Na^+$ was studied in solution at different temperatures; the calculated Arrhenius energy of activation of the process was estimated to be 13.3 kcal/mol, and the activity coefficient of the reaction was 1.85 (Barrer and Falconer 1956).

The cation exchange reactions between the Na-rich davyne from Zabargad (Bonaccorsi et al. 1992) and different molten salts was studied by the present authors (Bonaccorsi 1992; Merlino and Bonaccorsi, unpublished results), in order to investigate the role of the large cations in the order-disorder transition between davyne and microsommite. Single crystals of davyne with chemical composition $Na_{5.5}Ca_{2.5}[Si_6Al_6O_{24}](SO_4)Cl_{2.5}$ and cell parameters $a$ = 12.74, $c$ = 5.34 Å were kept in fused KI at 680–710°C for 24 hours. The reaction which took place is represented by the following equation, in which the contents of the channel, cage and

tetrahedral framework are between square parentheses for the solid phases:

$$[Na_{5.5}Ca_{0.5}(SO_4)\,Cl_{0.5}][Ca_{2.0}Cl_{2.0}][Si_6Al_6O_{24}] + 3KI \leftrightarrow$$
davyne liquid

$$[K_{3.0}Na_{2.0}Ca_{0.5}(SO_4)][Ca_{2.0}Cl_{2.0}][Si_6Al_6O_{24}] + 3\,NaI + 0.5NaCl$$
microsommite liquids

The main conclusions of these experiments were: (i) only the cations located in the channel are involved in the exchange process; (ii) when sufficient amounts of large cations substitute the small Na cations within the channel, a long range microsommite-like ordering takes place, and a supercell with $a = \sqrt{3}\ a_{dav}$ is observed. Very similar results were obtained with $NaTlSO_4$ at 750°C, whereas the exchange reaction with $NaKSO_4$ at 950°C could not be studied: the resulting phase had a different framework, possibly of the sodalite type.

## C-S-H COMPOUNDS

The calcium silicate hydrates system, with about thirty stable crystalline phases, besides to ill-crystallized materials, is well more complex than the MgO(FeO)-$SiO_2$-$H_2O$ system. Most of the crystalline phases occur as minerals and display OD features and polytypic forms. According to Taylor (1964), "one reason for the greater complexity of the CaO-$SiO_2$-$H_2O$ system perhaps lies in the greater ionic radius and in the more electropositive character of calcium, which permit a number of different types of coordination with oxygen. $Mg^{2+}$ and $Fe^{2+}$, in contrast, are nearly always octahedrally coordinated."

The terminology used in dealing with C-S-H phases, including the expression C-S-H phases itself, has been introduced and developed by cement chemists. In fact the relevance of part of these compounds in the hydration processes of cements, and of Portland cement in particular, stimulated their interest and produced a wide number of research programs aimed at understanding the structural arrangements, the crystal chemical features and the formation processes of the calcium silicate hydrates.

C-S-H compounds are generally obtained in the laboratory through hydrothermal treatment of amorphous or semicrystalline products showing different CaO:$SiO_2$ proportions. This ratio (C:S in the cement chemistry terminology) and the temperature are the main—although not unique—parameters controlling the formation of the different crystalline phases. Figure 11 presents a schematic stability diagram, in the C:S range 0.6 to 1.0, and temperature range up to 300°C, showing the relative stabilities of part of C-S-H phases (Shaw et al. 2000). In this diagram C-S-H(I) indicates poorly crystalline materials formed during the hydration of Portland cement and corresponding, according to Taylor (1986, 1992), to tobermorite-like structures.

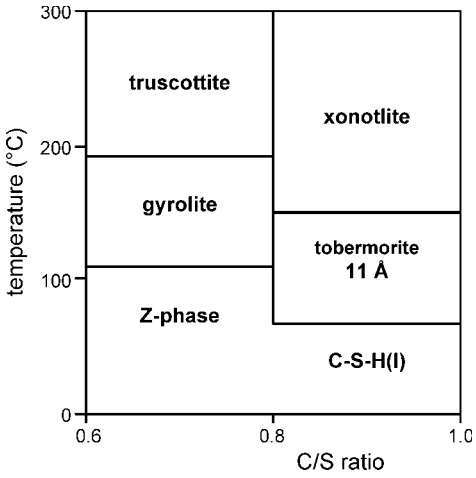


**Figure 11**. Schematic diagram showing the relative stability of part of the C-S-H compounds prepared under hydrothermal conditions (modified from Fig. 1 in Shaw et al. 2000).

Our attention will be particularly devoted to the minerals, and corresponding

synthetic phases, of the tobermorite and gyrolite groups. Actually not all of them are microporous. In the tobermorite group microporosity characterizes tobermorite 11 Å (in both normal and anomalous forms) and clinotobermorite, whereas their dehydration products do not present pores of suitable dimensions, and the hydration product of tobermorite 11 Å, namely tobermorite 14 Å, is a layer structure, although a peculiar one, as it will be shown in the following, easily transformed into the structure-type of tobermorite 11 Å by heating at 80–100°C. In the group of gyrolite, besides microporous compounds (truscottite, reyerite, fedorite, K-phase) there are layer structures, gyrolite and Z-phase, which, however, may transform, by dehydration, into microporous phases. The close structural relationships among the various phases in both groups, as well as the relatively easy conversion of the layer structures to microporous structures by dehydration, suggest to present and discuss in this chapter all the phases occurring in both structural groups.

## NATURAL AND SYNTHETIC COMPOUNDS OF THE TOBERMORITE GROUP

### Historical outlook

The particular interest in the structure and crystal chemistry of the tobermorite compounds stemmed not only from their close relationships with the C-S-H phases formed during the hydration processes of Portland cement, but also from their properties as cation exchangers (at least for tobermorite 11 Å) and potential applications in nuclear and hazardous waste disposal. That has stimulated a broad series of studies to obtain a deep knowledge of the structural aspects of these minerals, with special consideration of tobermorite 11 Å for its central position in the family and the ambiguity of its behavior in dehydration processes.

In 1880 Heddle described a hydrate calcium silicate found in three localities of Scotland, two near Tobermory, Mull island, and one at Dunvegan, Skye island; the name tobermorite was given to that compound. Afterwards tobermorite has been discovered in two other Scottish localities by Heddle (1893) and Currie (1905) and subsequently in various localities all over the world, generally occurring as alteration product of calcium carbonate rocks and as vesicle fillings in basalts.

Claringbull and Hey (1952) re-examined the specimens of Heddle; they confirmed that tobermorite was a valid species and observed a close similarity between the diffraction patterns of tobermorite and that of C-S-H-I (calcium silicate hydrate) compounds synthesized and studied by Taylor (1950) and Heller and Taylor (1951, 1952). Moreover they suggested some similarity with crestmoreite, a supposed phase described by Eakle (1917) as occurring in Crestmore (California, USA), together with another phase, riversideite, which would differ from crestmoreite only for the lower water content. Flint and coworkers (1938), by investigating specimens of riversideite and crestmoreite concluded that they are the same and proposed to drop out the name riversideite. Subsequently Taylor (1953a) demonstrated that crestmoreite (and riversideite as well) is an association, at submicroscopic scale, of tobermorite "with different hydration states" and wilkeite, a presently discredited species corresponding to phosphatian fluorellestadite.

Parallel to the researches carried out on natural phases of the tobermorite group, chemists interested in the nature of the compounds produced in the hydration processes of Portland cement studied C-S-H-I (calcium silicate hydrate) phases and found that they occur in three hydration states, called tobermorite 14 Å, tobermorite 11 Å and tobermorite 9 Å (Taylor 1953b). The notations 9 Å, 11 Å and 14 Å refer to the characteristic basal spacings of 9.3, 11.3 and 14.0 Å which these phases present in their X-ray powder diffraction patterns.

An important contribution in understanding the relationships among the various phases and in assessing the nomenclature has been given by McConnell (1954). In samples from Ballycraigy, County Antrim, North Ireland, he found the pure 11 Å phase, as well as the mixed 11 Å –14 Å hydrates. He carried out a careful study of the behavior of the mixed material on heating, indicating that tobermorite 14 Å transforms to tobermorite 11 Å ($5CaO{\cdot}6SiO_2{\cdot}5H_2O$) in the temperature range 80-100°C; then tobermorite 11 Å transforms to tobermorite 9 Å ($5CaO{\cdot}6SiO_2{\cdot}1H_2O$) at 300°C. McConnell assumed that the product studied by Eakle (1917) (riversideite – crestmoreite) was actually the 9 Å phase, transformed into the more hydrated terms due to the lack of proper preservation. Finally he observed that the composition of the more hydrated term, which appears at Ballycraigy as a natural gel, was identical to that of plombierite, a mineral with gelatinous character defined by Daubrée (1858), who found it at Plombières, Vosges, France. In conclusion McConnell proposed to assign the following names: *riversideite* to the 9 Å phase, *tobermorite* to the 11 Å phase, *plombierite* to the 14 Å phase.

More recently clinotorbermorite, another member of the group, has been found at Fuka, Japan, by Henmi and Kusachi (1989, 1992); it was subsequently found at Wessels mine, South Africa, and studied by Hoffmann and Armbruster (1997). Also clinotobermorite, which has a basal spacing of ~11 Å, does shrink, as "normal" tobermorite (actually it was found that some specimens of tobermorite 11 Å do not shrink on dehydration and are referred to as "anomalous") upon heating at 300°C, with formation of a compound characterized by a 9 Å spacing.

Note that, except clinotorbermotite, none of the mineral names and species quoted above are officially approved by the Commission on New Minerals and Mineral Names (CNMMN) of the International Mineralogical Association (IMA; cf. the website *www.geo.vu.nl/users/ima-cnmmn/*). On the other side, the complex situation affecting the natural C-S-H phases of the tobermorite group suggests caution in proposing an official nomenclature.

**OD character of the phases in the tobermorite group**

The various compounds in the tobermorite group present OD character (Dornberger-Schiff 1956, 1964, 1966; Ďurovič 1997; Merlino 1997; Ferraris et al. 2004) clearly manifested by their diffraction patterns displaying streaks, diffuse reflections and unusual systematic absences rules. The OD character depends on their peculiar crystal chemistry (which will be thoroughly discussed in following sections), in particular on the metrical relationships between the calcium polyhedral module, with the repeat of 3.65 Å, and the tetrahedral chains with the typical repeat of 7.3 Å. Figure 12 shows that the tetrahedral chain may be connected to the calcium ribbons in two distinct but equivalent positions shifted by 3.65 Å in the **b** direction. Consequently the various compounds in the tobermorite group may be described in terms of OD layers, fully ordered in two dimensions, with **a** and **b** translation vectors ($a$ = 11.3, $b$ = 7.4 Å, $\gamma$ = 90° in all the tobermorite phases), which – thanks to the ambiguity of the connection between the silicon tetrahedral and calcium polyhedral modules – may stack according to two distinct ways along the **c*** direction, giving rise to a whole family of disordered or ordered sequences (polytypes): in all the possible sequences pairs of adjacent layers are geometrically equivalent, no matter whether taken in one member or in different members of the family (principle of OD structures).

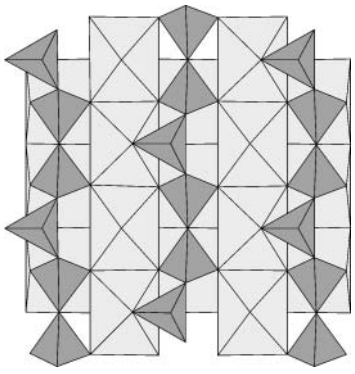

**Figure 12.** Connection between the silicon tetrahedral chain (dark grey) and the calcium polyhedral module (light grey) in the compounds of the tobermorite group.

The possible members of each family present diffraction patterns characterized by a set of common reflections (those with $k = 2n$ in all the tobermorite compounds), which are always sharp and have the same position in the reciprocal space and the same intensity in all the members of the family: they are called family reflections and define the "family cell," subcell in short, and consent to determine the so called "average structure." Table 4 compares the subcells of the various compounds.

The various members of each family may be distinguished on the basis of the characteristic reflections, namely those with $k = 2n+1$, more or less diffuse (sometimes continuous streaks) along **c***; they present different positions and intensities in the different members of the family. Two main polytypes exist in each tobermorite family and OD theory indicates how to single them out. In fact they correspond to the MDO (Maximum Degree of Order) structures, in which not only pairs but also triples (quadruples,…n-tuples) of OD layers are geometrically equivalent (principle of MDO structures). A detailed treatment of the OD features for the various compounds in the tobermorite group, including the derivation of the MDO polytypes, may be found in the papers devoted to their structure determinations (Merlino et al. 1999, 2000, 2001; Bonaccorsi et al. 2005). The cell parameters and space groups of the various MDO structures are collected in Table 5.

**Table 4.** Composition and subcell parameters (in Å and °) of the phases in the tobermorite group.

| *Composition* | *Phase* | *Subcell* | *S.G.* | $a_S$ | $b_S$ | $c_S$ | $\beta_S$ |
|---|---|---|---|---|---|---|---|
| $Ca_5Si_6O_{16}(OH)_2$ | 'clinotobermorite 9Å' | monoclinic | *A*2/*m* | 5.58 | 3.65 | 18.78 | 92.8 |
| | riverseideite (tobermorite 9Å) | orthorhombic | *Pnmm* | 5.58 | 3.65 | 18.78 | |
| $Ca_5Si_6O_{17}.5H_2O$ | clinotobermorite | monoclinic | *A*2/*m* | 5.638 | 3.671 | 22.642 | 97.3 |
| | tobermorite 11Å | orthorhombic | *I*2*mm* | 5.632 | 3.692 | 22.487 | |
| $Ca_5Si_6O_{16}(OH)_2.7H_2O$ | plombierite (tobermorite 14Å) | orthorhombic | *I*2*mm* | 5.63 | 3.71 | 27.99 | |

**Table 5.** The two main polytypes (MDO structures) for each compound of the tobermorite group, and their crystallographic data (in Å and °).

| | *Polytype* | *S.G.* | *a* | *b* | *c* | α | β | γ |
|---|---|---|---|---|---|---|---|---|
| Clinotobermorite | $MDO_1$ | *Cc* | 11.276 | 7.343 | 22.642 | | 97.28 | |
| | $MDO_2$ | *C*1 | 11.274 | 7.344 | 11.468 | 99.18 | 97.19 | 90.02 |
| 'Clinotobermorite 9Å' | $MDO_1$ | *C*2/*c* | 11.161 | 7.303 | 18.771 | | 92.91 | |
| | $MDO_2$ | $C\bar{1}$ | 11.156 | 7.303 | 9.566 | 101.08 | 92.83 | 89.98 |
| Tobermorite 11Å | $MDO_1$ | *F*2*dd* | 11.265 | 7.386 | 44.97 | | | |
| | $MDO_2$ | *B*11*m* | 6.735 | 7.385 | 22.487 | | | 123.25 |
| Riversideite (Tobermorite 9Å) | $MDO_1$ | *Fd*2*d* | 11.16 | 7.32 | 37.40 | | | |
| | $MDO_2$ | $P112_1/a$ | 6.7 | 7.32 | 18.70 | | | 123.5 |
| Plombierite (Tobermorite 14Å) | $MDO_1$ | *F*2*dd* | 11.2 | 7.3 | 56.0 | | | |
| | $MDO_2$ | *B*11*b* | 6.735 | 7.425 | 27.987 | | | 123.25 |

**Genesis and parageneses of the natural compounds**

The minerals of the tobermorite group (tobermorite 11 Å, sometimes together with plombierite and, in a pair of cases, with riversideite) form through the action of hydrothermal fluids mainly at late stages of the evolution of different geological environments.

One of the most recurrent occurrences is in vugs, fissures or veins in basalts, frequently in association with zeolites and gyrolite. Of this type were the first findings, in Scotland, of tobermorite as red material "totally filling small druses in the cliffs of the shore immediately to the north of the pier of Tobermory in the Island of Mull" and in a stone quarry near the pier of Dunvegan, Isle of Skye (Heddle 1880) and at Loch Eynort, Isle of Skye (Heddle 1893); as well as the subsequent findings in Scotland: in the basalt of Ardtornish Bay at Morvern, Argylleshire, within druses which are generally filled by gyrolite (Currie 1905); 1 km north of Portree, Skye, on the "Staffin Road," in a olivine-dolerite, with xonotlite, gyrolite and zeolites (Sweet et al. 1961); in the vugs of a basaltic volcanic plug, at Castle Hill, near Kilbirnie in Ayrshire (Webb 1971); in Italy: at Prà de la Stua (province of Trento), near Malga Cola, in the cavities of an olivine basalt, together with natrolite, analcite, apophyllite and phillipsite (Gottardi and Passaglia 1965); as an inclusion in an olivine basalt on the eastern slope of Mount Biaena (province of Trento), together with gyrolite (Gottardi and Passaglia 1966); in the quarry Campomorto, Montalto di Castro (Viterbo), where it is the most widespread mineral in the cavities of the phonolite (Passaglia and Turconi 1982); in peralkaline pegmatites of the Khibiny massif, Kola peninsula, with thaumasite, apophyllite, saponite and Kovdor massif, Kola peninsula, with calcite and tacharanite; at Mokraya Synya river (Voykaro-Synninsky ultrabasic massif, North Urals), where tobermorite forms, together with gyrolite, late hydrothermal veinlets in the gabbro. In Germany tobermorite has been found by Walenta (1980) in melilite-nephelinite of Howenegg in Hegau, together with phillipsite, harmotome and mountainite; at Zeilberg quarry, Maroldsweisach, Bavaria; in the Eifel, at Arensberg near Zilsdorf (Hentschel 1973).

Tobermorite occupies the core of amygdales, accompanied by small amounts of tacharanite, in alkaline basalts at Puyuhuapi, in Chilean Patagonia (Aguirre et al. 1998). At Goldfield, Nevada, tobermorite has been produced by hydrothermal alteration of dacitic rocks and it is found associated with alunite as pseudomorphs after plagioclase phenocrysts in the most intense zone of alteration (Harvey and Beck 1962). In the Island of Surtsey it was found among the products of the hydrothermal alteration of the tephra (Jakobsson and Moore 1986). At Heguri, Chiba Prefecture, Japan, both tobermorite 11 Å and barium-bearing tobermorite 11 Å occur in veinlets cutting a basic tuff suffering metamorphism of zeolite facies, the first being accompanied by small amounts of calcite and poorly crystallized hydrated magnesium silicate (Mitsuda 1973), the second by thomsonite (Kato et al. 1984).

The minerals of the tobermorite groups may also be found in connection with the occurrence of hydrothermal conditions at the contact between limestones and dolerites or granodiorites, or more generally through the action of hydrothermal fluids on calcium silicate minerals. Of this type was the well-known finding of tobermorite phases at Crestmore, Riverside County, California, in a crystalline limestone at the contact with granodiorite (Eakle 1917), where also riversideite has been identified. Tobermorite minerals also occur in vugs of larnite rocks at the dolerite-chalk contact at Ballycraigy, Larne, County Antrim, Ireland, together with scawtite (McConnell 1954); at Fuka, Okayama, Japan, in a vein (10 mm width) of the altered rock at the contact between limestones and intrusive igneous rocks (Maeshima et al. 2003); in the Wessels mine (north of the town of Kuruman in the Kalahari Manganese Field, South Africa), where tobermorite was found near a dike and had crystallized in altered portions of the wall rock that had been in contact with the intrusion (Gutzmer and Cairncross 1993); in skarns at Cornet Hill, Apuseni Mountains, Romania (Marincea et al. 2001), which

have undergone a late metasomatic event and subsequent hydrothermal events, the late of which resulted in the formation of 11 Å tobermorite, riversideite, as well as thomsonite, gismondine, aragonite and calcite, while the subsequent weathering gave plombierite, portlandite and allophane. Tobermorite 11 Å occurs in garnet-pyroxene skarns at Okur-tau, Uzbekistan, and in garnet-wollastonite skarns at Arimao-Norte, Cuba, with plombierite, riversideite, scawtite (Zadov et al. 1995); in xenoliths of calcite-bearing rocks in basic magmatic rocks, as at Vechec, Eastern Slovakia, and at Ozersky massif, near Baikal lake, together with calcite, plombierite, kilchoanite.

Tobermorite 11 Å has been found (Němec 1982) in the basic Ransko Massif, in the contact parts of the massif or in the xenolith-containing zone, closely associated with apophyllite. Tobermorite 11 Å and plombierite have been found in the rodingites of the Bazhenovskoe deposit of chrysotile, Urals, Russia (Zadov et al. 1995). At Bingham, Utah, a suite of mineral species including, together plombierite, also thaumasite, apophyllite, gyrolite, okenite, stilbite, thomsonite "has formed as hydrothermal alteration product of silicated limestone adjacent to the disseminated copper deposit" (Stephens and Bray 1973).

In one of the most widespread rock types, mainly composed of calcite and spurrite, of the so-called "Mottled Zone," in the Hatrurim region and at the Beersheba Valley in the northern Negev, near Ramleh in the coastal plain (Israel) and at Maaleh Adumin in the Jordanian part of the Judean Desert, minerals of the tobermorite group have been identified in small veinlets, together with a number of other uncommon minerals which include vaterite, portlandite, bayerite, thaumasite, minor ettringite and possibly jennite (Bentor et al. 1963).

In the Maqarin area (North Jordan) tobermorite 11 Å and plombierite were found as secondary minerals filling cavities of weathered marbles, together with ettringite, calcite, jennite and thaumasite, and were probably "precipitated during the weathering of the high grade metamorphic minerals directly from the high pH-water" (Abdul-Jaber and Khoury 1998).

Plombierite has also been collected at Carneal, Co. Antrim, Ireland, in veinlets and cavities in larnite-rich rocks at the chalk-dolerite contact (Nawaz 1977).

Clinotobermorite was firstly described as a new mineral from Fuka, Japan (Henmi and Kusachi 1992), in ghelenite-spurrite-bearing skarns occurring at the contact between quartz monzonite dykes and limestones. Later, it was found in fissures of the Wessels mine, in the Kalahari Manganese zone, South Africa, associated with xonotlite and datolite (Hoffmann and Armbruster 1997). More recently, it was also detected in samples from Bazhenov, Urals (Garbev 2004), were it occurs in association with tobermorite 11 Å, plombierite and diopside.

**Synthetic counterparts**

According to Taylor (1964) the first definite synthesis of crystalline tobermorite 11 Å was by Flint et al. (1938), who obtained it by hydrothermal treatment of "amorphous hydrate with $CaO:SiO_2$ molar ratio 0.80 at temperatures between 150°C and 275°C, assigned the formula $4CaO{\cdot}5SiO_2{\cdot}5H_2O$ to their product and pointed to its possible identity with the natural phase. It was subsequently prepared by Heller and Taylor (1951), Kalousek (1955) and Assarsson (1958). Heller and Taylor (1951) synthesized tobermorite 11 Å by hydrothermal treatment, in the temperature range 110-200°C, of mixtures of $Ca(OH)_2$ and silica gel, as well as of ill-crystallized C-S-H preparations (Taylor 1950), in both cases with $CaO:SiO_2$ ratio approximately 1:1, and interpreted the X-ray diffraction pattern on the basis of an orthorhombic cell with $a = 5.62$, $b = 3.66$, $c = 11.0$ Å, corresponding, apart from the halving of $c$, to the parameters of the subcell of the natural tobermorite 11 Å, as reported in Table 4. The identity of the synthetic product with the natural phase has been indicated by Claringbull and Hey (1952) and definitely established by McConnell (1954). Although tobermorite 11 Å has

been prepared from a variety of starting materials, the synthesis procedures most widely used are either hydrothermal reactions of mixtures of CaO or $Ca(OH)_2$ and finely ground quartz (Heller and Taylor 1951; Sasaki et al. 1996) or autoclaving amorphous C-S-H preparations (Hong and Glasser 2003; Garbev 2004) of appropriate $CaO:SiO_2$ ratio. Actually it has been shown by El Hemaly et al. (1977) that the formation of semi-crystalline C-S-H is the first step in the hydrothermal reaction starting from CaO and finely ground quartz, with subsequent formation of normal and afterwards anomalous tobermorite 11 Å, abutting, for temperature higher than 140°C, to xonotlite. Those authors have also defined the factors (short reaction times, high Ca:Si ratio, presence of $Al^{3+}$ in absence of alkali, low temperature) which tend to stop the reaction at the step of normal tobermorite (El Hemaly et al. 1977).

The possibility to accommodate Al in substitution for Si in tobermorite 11 Å has been firstly shown by Kalousek (1957). The tetrahedral coordination of the aluminum cations has been confirmed by X-ray diffraction (Diamond et al. 1966) and by $^{27}Al$ and $^{29}Si$ MASNMR spectroscopy (Komarneni et al. 1985); the upper limit of Al substitution was indicated as Al:(Al+Si) = 0.13–0.14 by Sakiyama et al. (2000).

Normal tobermorite 11 Å may also be obtained by heating tobermorite 14 Å at 55–120°C. The first synthesis of tobermorite 14 Å has been made by Kalousek and Roy (1957) by processing lime and silicic acid, Ca:Si ratio 1:1, at 60°C for six months. Afterwards it was prepared by Hara et al. (1978) and Hara and Inoue (1980) by autoclaving mixtures of lime and amorphous silica (Ca:Si ratios 0.8, 0.9, 1.0) at 140°C for 20 hours and then keeping the product at 60°C for ten months; for some preparations alumina was added, with Al:(Al+Si) = 0.1, and in these cases tobermorite 11 Å was obtained. It is proper to recall that El Hemaly et al. (1977), in one single experiment of their study, obtained tobermorite 14 Å by hydrothermal reaction of lime-quartz mixtures at 105°C. It has been concluded that "14 Å tobermorite is a stable phase below 100°C in the absence of Al" (Hara et al. 1978).

**General structural aspects**

All the phases of the tobermorite group are clearly distinguished from the other calcium silicate hydrate minerals by the presence of the common structural "complex module," built up by a calcium polyhedral layer (a continuous layer—in the (001) plane —of sevenfold coordinated calcium cations), with tetrahedral chains of wollastonite-type grasped on both sides of it. The "complex module" is *C* centered with periods $a \approx 11.2$ Å, $b \approx 7.3$ Å and width $c_0 \approx 11.2$ Å (Merlino et al. 1999, 2000, 2001) and is represented in Figure 12.

The coordination polyhedron of the cations in the calcium layer may be described as a monocapped trigonal prism or, alternatively, as consisting of a pyramidal part on one side and a domatic part on the other side. The polyhedra are connected through edge sharing to build columns running along **b**. As illustrated in Figure 13, there are two types of polyhedra, which alternate along **b**: in one, the pyramidal apical site is occupied by a

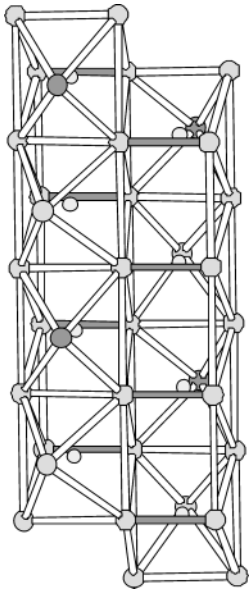

**Figure 13.** Columns of $CaO_7$ polyhedra. The short dome edges are drawn in dark grey. The pyramidal apical sites occupied by $O^{2-}$ or $OH^-$ anion are represented as light grey circles, whereas those occupied by $H_2O$ molecules are represented as dark grey circles. The calcium cations are represented as small circles.

water molecule, in the other the apical site is occupied by an $O^{2-}$ or $OH^{-}$ anion and the corresponding Ca-O bond is significantly displaced from the normal position; in both types of calcium polyhedra the dome edge is substantially shorter (about 2.6 Å) than the two edges of the pyramidal basis parallel to it (nearly 3.0 Å). The polyhedral columns are joined, again through edge sharing, along the **a** direction to build infinite layers. The important aspect of the polyhedral connection is that adjacent columns present the apical ligands (the capping ligands in the "monocapped trigonal prism" description) on opposite sides of the layer and, similarly, the short "dome" edges are placed on opposite sides in adjacent columns, with relative displacement of **b**/4 (Merlino et al. 2000).

Infinite silicate chains of the wollastonite-type ("Dreierketten") run along **b** on both sides of the calcium polyhedral layers. They are built up by "paired" tetrahedra connected by a "bridging" tetrahedron (the terminology of the cement chemists is here used). The chains are linked to the calcium layer with the paired tetrahedra attached to it by sharing the "dome" edges and the bridging tetrahedron sharing the pyramidal $O^{2-}$ (or $OH^{-}$) apices. This kind of connection explains well both the shortness of the dome edges, which must conform to the length of the $SiO_4$ tetrahedral edge, and the deviation from the normal position of the Ca-$O_{ap}$ bond involving the apical oxygen atom, a deviation which is necessary to form Si-$O_{ap}$ bonds of proper distance in the bridging tetrahedra.

It is important to stress that there are two geometrically distinct ways to place the tetrahedral chains on the two sides of the calcium sheet, thus giving rise to two distinct types of "complex module": in the first one, the bridging tetrahedra are placed at right on one side and at left on the other side (or *vice versa*), with respect to the disilicate groups of the corresponding chain, so that the (010) projection of the chains are inclined in the same direction on both sides of the central calcium sheet (complex layer of type A, Fig. 14a); in the second one, the bridging tetrahedra on both sides are all placed at left (or all placed at right) with respect to the corresponding disilicate groups, so that the (010) projection of the chains are inclined in nearly orthogonal directions (complex layer of type B, Fig. 14b).

We shall now examine the occurrence of the complex layers in the various phases of the tobermorite group and how the distinct ways of assembling the layers give rise to the whole series of tobermorite phases. We shall not always specify which kind of complex layer (A or B) we are dealing with, but it is easy to check that types A and B occur in the phases with monoclinic and orthorhombic subcells (Table 4), respectively.

There is a second aspect of modularity which has been briefly discussed previously. In fact the structures of the various compounds, plombierite (tobermorite 14 Å), tobermorite 11 Å, riversideite (tobermorite 9 Å), clinotobermorite and its dehydration product "clinotobermorite 9 Å," occur in two main polytypic variants. In the following, we shall compare the structural

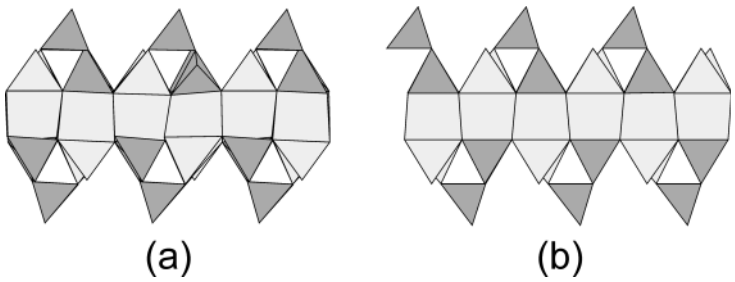


**Figure 14**. Complex layers of type A (a) and B (b), as seen down **b** (**a** horizontal).

arrangements of the various compounds considering only one polytype for each of them, as the crystal chemical properties and thermal behavior are largely independent on the polytypic form.

**11 Å phases: clinotobermorite and tobermorite 11 Å**

***Clinotobermorite.*** In the crystal structure of clinotobermorite the complex layers are stacked in the direction normal to them and the wollastonite-type chains are condensed through apical oxygens of the bridging tetrahedra, thus giving rise to double chains of $[Si_6O_{17}]^{10-}$ composition. These hold firmly adjacent calcium layers together, thus building a strong scaffolding hosting additional calcium cations and water molecules (Ca2, W5, W7 and W8, according to the notations used in Merlino et al. 2000) in its cavities. W5 is placed in the center of the eight-membered ring of the silicate double chains; Ca2, W7 and W8 are located in the central zone of the channels running along **b** and limited by adjacent tetrahedral chains.

Figure 15 shows the position of these "zeolitic" components, with indication of the strong bonds (average length 2.35 Å) between Ca2 and the three "zeolitic" water molecules and two oxygen atoms of the polyhedral framework. Through careful consideration of the hydrogen-bond system involving the "zeolitic" water molecules and the actual geometry of the calcium polyhedra, it was concluded that O6 and O6A are $O^{2-}$ anions and the composition of the polyhedral framework has been derived as $[Ca_4(Si_6O_{17})\cdot 2H_2O]^{2-}$, the negative charge being compensated by the corresponding positive charge of the "zeolitic" part $[Ca\cdot 3H_2O]^{2+}$. The resulting crystal chemical formula of clinotobermorite is $Ca_5Si_6O_{17}\cdot 5H_2O$.

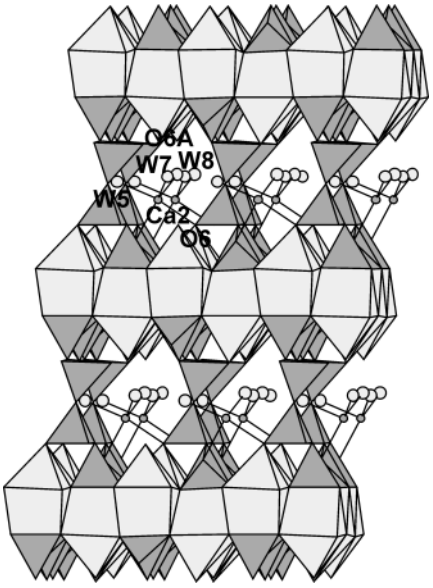


**Figure 15.** Crystal structure of clinotobermorite (triclinic polytype $MDO_2$ in Table 5), as seen along **b**, **a** horizontal. The projection axis is inclined by 7° to favor a better appreciation of the structural arrangement.

***Tobermorite 11 Å.*** Also in tobermorite 11 Å the complex layers are connected through condensation of the wollastonite chains to build $Si_6O_{17}$ double chains. However the double chains present different shapes and symmetries (2/*m* in clinotobermorite, 2*mm* in tobermorite 11 Å) in the two compounds (Fig. 16).

As we previously recalled, two varieties of tobermorite 11 Å are known, normal and anomalous. The crystal structures of the anomalous (specimen from Wessels Mine, South Africa) and normal (specimen from Bazhenovskoe

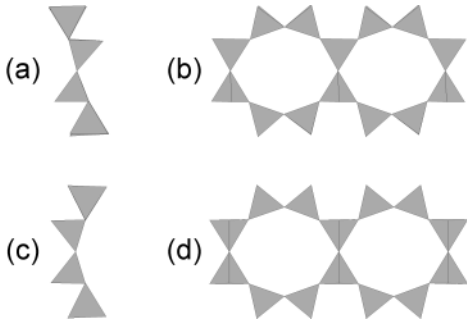


**Figure 16.** Silicate double chains in clinotobermorite, (a) and (b), displaying 2/*m* symmetry, and in tobermorite 11 Å, (c) and (d), displaying 2*mm* symmetry.

deposit, Urals, Russia) tobermorite 11 Å (Merlino et al. 2001) are compared in Figure 17. In both cases the polytype $MDO_2$ of Table 5 is illustrated.

In the anomalous variety only water molecules are located in the cavities of the structure, in positions corresponding to those of the water molecules in clinotobermorite: W2 in the center of the eight-membered rings of the silicate double chains, as W5 in clinotobermorite; W1 and W3 in the central zone of the channels, as W7 and W8 in clinotobermorite; the three molecules lie on the symmetry plane. Due to the absence of the "zeolitic" cation and the weakness of the hydrogen bonding of the water molecules with the oxygen atoms of the framework, it was concluded that O6 is a hydroxyl anion, the composition of the polyhedral framework is $[Ca_4(Si_6O_{15})(OH)_2 \cdot 2H_2O]$ and the crystal chemical formula of the anomalous tobermorite from Wessels Mine is $Ca_4Si_6O_{15}(OH)_2 \cdot 5H_2O$.

As regards the normal tobermorite from Urals, the results of the structural studies point to the presence of "zeolitic" calcium cations Ca2 in general position with occupancy 1/4, in addition to water molecules W2, with full occupancy and in position similar to that of the corresponding molecule in the anomalous variety, and W1, W3 with half occupancy and located in positions not too different from those occupied by the corresponding molecules in anomalous tobermorite 11 Å, apart a small (0.4 Å) displacement from the symmetry plane. Because of the particular composition of the normal tobermorite from Urals with 0.5 "zeolitic" cations per unit formula (Ca:Si = 4.5:6), two situations occur: *a*) the "zeolitic" calcium cation Ca2 is located on one side of the reflection plane, whereas W1 and W3 are located on the other side (Fig. 18); exactly as in the case of clinotobermorite, the O6 oxygen atom on one side of the mirror plane is strongly linked to Ca2, whereas the O6 atom on the other side is hydrogen bonded to W1 and W3 water molecules; consequently both O6 sites are occupied by $O^{2-}$ anions; *b*) Ca2 is absent and possibly the W1 and W3 molecules shift their position

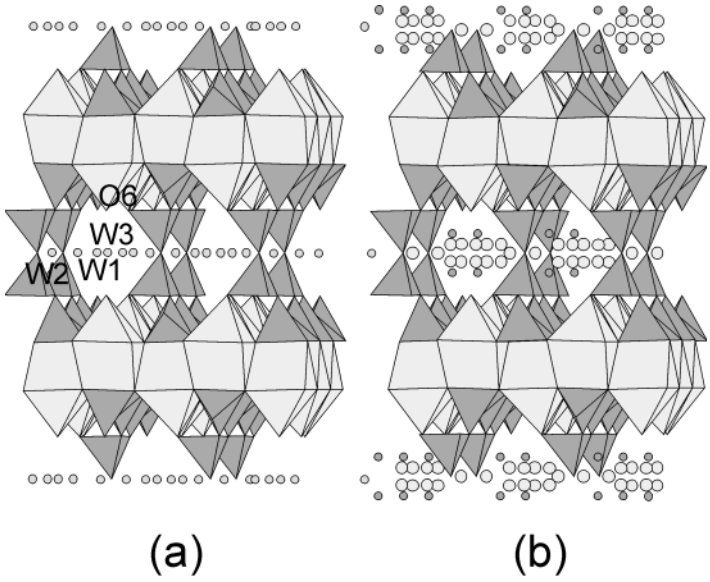


**Figure 17.** (a) The crystal structures of anomalous tobermorite from Wessels mine (only water molecules in the cavities). (b) The crystal structure of normal tobermorite from Urals (water molecules, large circles, and calcium cations, small dark grey circles, in the cavities). In both cases the monoclinic polytype $MDO_2$ of Table 5 is represented, as seen along **b**, **c** vertical, with an inclination (10°) of the projection axis to favor a better appreciation of the structural arrangement.

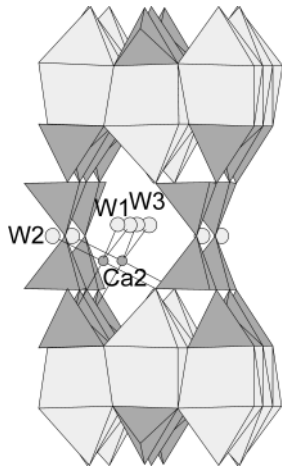


**Figure 18.** The situation a) in normal tobermorite from Urals, discussed in the text, is here illustrated: Ca2 cation (small dark grey circle) is located on one side and W1 and W3 are located on the opposite side of the plane passing through the bridging oxygen atoms which connect the wollastonite chains into double chains, as well as through the W2 water molecules.

toward the mirror plane (as it happens in the anomalous variety) and both O6 sites are occupied by hydroxyl anions. As the two situations occur with the same frequency, the composition of the polyhedral framework is $[Ca_4Si_6O_{16}(OH)\cdot 2H_2O]^{1-}$, the negative charge being compensated by the corresponding positive charge of the "zeolitic" part $[Ca_{0.5}\cdot 3H_2O]^{1+}$. The resulting crystal chemical formula of the normal tobermorite from Urals is $Ca_{4.5}Si_6O_{16}(OH)\cdot 5H_2O$.

Tobermorite specimens from different localities present different amounts of "zeolitic" calcium cations: their increasing causes an increasing occurrence of the situation *a*) described above, till the attainment of the extreme composition $Ca_5Si_6O_{17}\cdot 5H_2O$. At that composition, exactly corresponding to that of clinotobermorite, only the situation *a*) occurs and the distribution of calcium cations and water molecules in the cavities is substantially similar to that realized in clinotobermorite and described by Figure 18.

The whole compositional range for tobermorite 11 Å, excluding substitution of silicon by aluminum in the tetrahedra, spans between $Ca_4Si_6O_{15}(OH)_2\cdot 5H_2O$ and $Ca_5Si_6O_{17}\cdot 5H_2O$. Both in natural and in synthetic compounds, silicon may be partly substituted by aluminum [up to Al:(Al+Si) = 0.13–0.14, according to Sakiyama et al. (2000)], a substitution which may be balanced by a higher Ca content and/or higher $O^{2-}$ by $OH^-$ substitution. That has been confirmed by the structural study carried on a synthetic specimen of tobermorite 11 Å of composition near to $Ca_5Si_{5.5}Al_{0.5}O_{16}(OH)\cdot 5H_2O$, through Rietveld refinement of synchrotron radiation powder diffraction data (Yamazaki and Toraya 2001).

**9 Å phases: "clinotobermorite 9 Å" and riversideite**

"Clinotobermorite 9 Å" and riversideite, are obtained by heating, at 300°C, clinotobermorite and tobermorite 11 Å, respectively. In "clinotobermorite 9 Å" (Fig. 19) adjacent complex layers are now wedged together, the ridges of one fitting into the hollows of the other: the apical oxygen atoms of each single tetrahedral chain on one complex layer are connected to the calcium sheet of the adjacent complex layer just at the positions which in clinotobermorite are occupied by water molecules (and which are now occupied by hydroxyl anions). All the water molecules are lost in the dehydration process and Ca2 is now firmly linked to six oxygen atoms of the framework, with four shorter (2.32–2.36 Å) and two longer (2.62–2.67 Å) bonds. A careful examination of the bond lengths and calculation of the bond-valence balance indicate that all the oxygen sites correspond to $O^{2-}$ anions, except the hydroxyl anion previously mentioned; thus, the crystal chemical formula is $Ca_5[Si_3O_8(OH)]_2$.

The comparison between the crystal structures of clinotobermorite and that of its dehydration product lets guess the following path of the dehydration: a) decondensation of the double chains through action of water molecules, namely $[Si_6O_{17}]^{10-} + H_2O = 2[Si_3O_8(OH)]^{5-}$, and consequent disconnection of adjacent complex layers; b) loss of water molecules and tight reconnection of the layers, after parallel shifting of alternate layers by **b**/2. The whole transformation does not require rearrangements inside the complex layers and proceeds topotactically (Merlino et al. 2000).

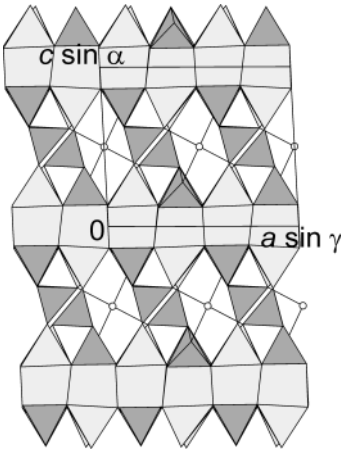


**Figure 19.** Crystal structure of "clino-tobermorite 9 Å" (triclinic polytype $MDO_2$ of Table 5) as seen along **b**. The four shortest Ca2-O bonds are indicated.

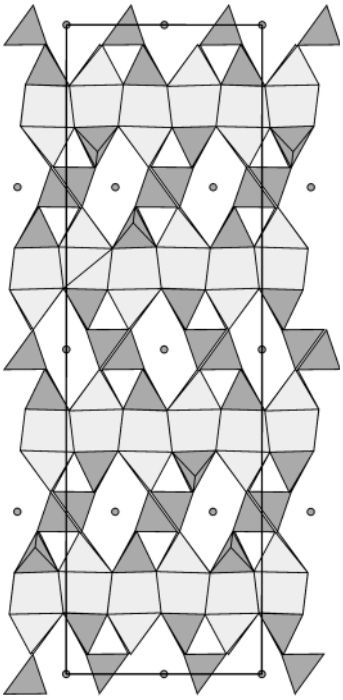

**Figure 20.** Structural model of riversideite (orthorhombic polytype $MDO_1$ of Table 5) as seen along **b**, **a** horizontal.

The structure of tobermorite 11 Å is built up by complex modules of type B and after the decondensation of the double chains, which constitutes the first step of the dehydration process, the complex layers facing each other cannot reconnect without a rearrangement of the tetrahedral chains, driven by the "zeolitic" water molecules. An ordered rearrangement occurring on both sides of each second complex layer, with subsequent reconnection of alternating unaltered and rearranged layers gives rise to the structure of riversideite (tobermorite 9 Å) as represented in Figure 20.

The structural details of riversideite are still unknown; in fact only the set of reflections with $k = 2n$, corresponding to the "subcell" structure, may be measured, the reflections with $k = 2n+1$ appearing as continuous diffuse streaks, indicative of high disorder in the sequence of the OD layers. Moreover some diffuseness observed also in the "subcell" reflections indicates that the ordered rearrangement we have sketched in Figure 20 is sometimes interrupted by alternate rearrangements.

**14 Å phase: plombierite**

The crystal structure of plombierite (tobermorite 14 Å) is built up by the same complex module of type B which characterizes tobermorite 11 Å. However the wollastonite-type chains facing each other on adjacent layers are not condensed into double chains; moreover they show a relative shift of **b**/2. The unconnected complex modules are moved apart and the space in between contains calcium cations and a larger amount of water molecules with respect to the 11 Å phase. The monoclinic $MDO_2$ polytype of plombierite (Table 5) is represented in Figure 21.

The water molecules in the interlayer region (W2, W3 and W4) as well as Ca2 calcium cations have half occupancies, whereas W1 is fully occupied; two W1, one W2, one W3 water molecules and two O5 anions (the apical oxygen atoms of the bridging silicon tetrahedra on the wollastonite chains) complete a nearly regular octahedron around Ca2. Two distinct ordering schemes may be sketched, in which $Ca(H_2O)_4O_2$ octahedra and W4 water molecules regularly alternate in columns along [010]. Each one may be realized in the space group $B1$ (Fig. 22). The random distribution of the two ordering schemes in the crystal restores the $B11b$ symmetry. The crystal chemical formula indicated by the structural study (Bonaccorsi et al. 2005) is $Ca_5Si_6O_{16}(OH)_2 \cdot 7H_2O$ in agreement with chemical (Mitsuda and Taylor 1978; Maeshima et al. 2003),

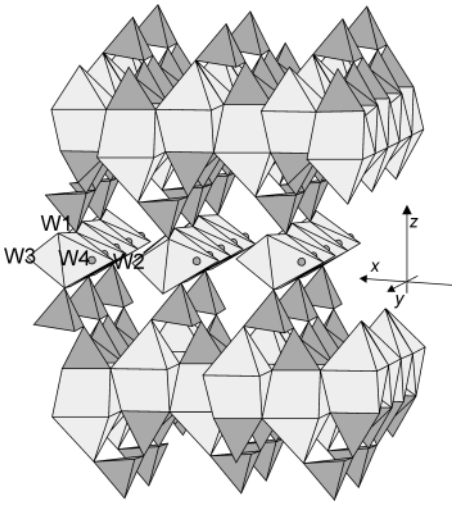


**Figure 21.** Structure of plombierite, monoclinic polytype $MDO_2$. In the interlayer sheet the half occupied $CaO_2(H_2O)_4$ octahedron drawn in light grey; the half occupied W4 molecules are represented by dark grey circles.

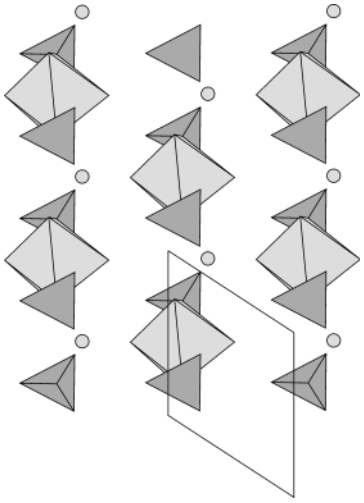

**Figure 22**. Ordering of interlayer material, in the structure of plombierite (monoclinic polytype $MDO_2$) as seen along **c**, **b** vertical.

thermal (Farmer et al. 1966; Maeshima et al. 2003) and MASNMR data (Wieker et al. 1982; Komarneni et al. 1987a; Cong and Kirkpatrick 1996; Maeshima et al. 2003).

**Thermal behavior**

The thermal study carried on tobermorite 14 Å, $Ca_5Si_6O_{16}(OH)_2{\cdot}7H_2O$, from Crestmore (Farmer et al. 1966) points to a first weight loss at 55°C, when the 11 Å phase, $Ca_5Si_6O_{17}{\cdot}5H_2O$, forms. The new phase persists, with continuous loss of water, till 250°C, at which temperature the 9 Å phase, $Ca_5Si_6O_{16}(OH)_2$, appears. This phase persists till 450°C; at 450 to 650°C the hydroxyl groups are lost through a gradual process leading to a phase with increased layer thickness (9.7 Å), at least in the Crestmore specimen. Then, between 850 and 900°C, wollastonite, $CaSiO_3$, forms, after an intermediate (730 to 775°C) wollastonite-like phase. The sketched sequence of steps, the water losses and the consequent structural rearrangements are in keeping with the structural aspects presented for the various phases in the preceding chapter.

Two relevant points deserve careful consideration and comment. The formation of the 9 Å phase from tobermorite 11 Å (*normal behavior*) in the dehydration process, is not straightforward; in fact, some natural and synthetic specimens do dehydrate at 250-300°C without shrinking, namely preserving the basal spacing of 11.3 Å (*anomalous behavior*). This distinct behavior had been previously explained with the presence of "interlayer Si-O-Si linkages" (double chains) in "anomalous" tobermorites and their absence (single chains) in "normal" tobermorites, an absence consenting an approach of adjacent calcium layers on dehydration, with corresponding decrease of the basal spacing. This explanation is obviously untenable since the structural studies have shown that double chains occur in both "normal" and "anomalous" tobermorites, as well as in clinotobermorite which, similarly, transforms to a 9 Å phase on dehydration at 300°C. In keeping with the present structural knowledge, an alternative explanation may be put forward. In clinotobermorite, $Ca_5Si_6O_{17}{\cdot}5H_2O$, "zeolitic" calcium cations in the cavities of the structure are strongly bonded to oxygen atoms of the "complex layers" and to "zeolitic" water molecules. By heating at

300°C the water molecules are lost and a wide rearrangement is required to properly complete the calcium coordination: as the missing ligands may be offered only by atoms of the complex layers, chain decondensation occurs to consent the proper approach of adjacent layers.

As regards tobermorite 11 Å, we have already said that the composition spans between $Ca_4Si_6O_{15}(OH)_2 \cdot 5H_2O$ (no "zeolitic" cations) and $Ca_5Si_6O_{17} \cdot 5H_2O$ (one "zeolitic" calcium cation per unit formula, as in clinotobermorite). In the latter case, as well as in the general case of substantial "zeolitic" calcium content, the loss of water upon heating has the same consequences just described for clinotobermorite, with formation of tobermorite 9 Å. On the contrary, when no (or very few) "zeolitic" calcium cations occur in the cavities of tobermorite 11 Å, no requirement of proper calcium coordination is caused by the dehydration, no chain decondensation takes place and the specimen preserves the basal spacing of 11.3 Å.

The preceding explanation may be generalized in the following way: the normal-anomalous behavior depends on the nature and amount of "zeolitic" cations. Ferreira et al. (2003) prepared novel microporous sodium lanthanide silicates with the structure type of tobermorite 11 Å and with idealized crystal chemical formula $KNa_2Ln_2Si_6O_{16}(OH) \cdot 4H_2O$, actually $KNa_{0.44}(Na_{1.72}Ln_{2.28})Si_6O_{17} \cdot 3.56H_2O$, (*Ln* = Eu, Tb, Sm, Ce, Gd). These compounds display the structure type of tobermorite 11 Å, with layers of alternating $Ln^{3+}$ and $Na^+$ polyhedra substituting for the calcium layers and with $K^+$ "zeolitic" cations located in the cavities of the structure together with water molecules. They have anomalous behavior, as do not shrink on dehydration. This may be explained with the presence of $K^+$ instead than $Ca^{2+}$ as extra-framework cation; $K^+$ cation, with a sensibly larger ionic radius, has satisfactory coordination also without extra-framework water molecules; moreover, and more important, its radius is too large for a proper positioning of $K^+$ in a shrunk 9 Å phase (the Ca2 calcium cation in "clinotobermorite 9 Å" has four Ca-O distances at 2.3 Å and two longer distances at 2.6 Å).

**Technological properties**

The cation exchange and selectivity properties of tobermorite 11 Å have been firstly reported by Komarneni et al. (1982) and Komarneni and Roy (1983). These authors observed that an exchange capability is mainly exhibited by (Al+alkali)-substituted tobermorite 11 Å, which, moreover, shows high selectivity for cesium cations.

The exchange behavior of Al-substituted tobermorite was the subject of several studies, for example by Shrivastava et al. (1991), Al-Wakeel et al. (2001), Šiačiūnas et al. (2002). These last authors have determined the sorption capacity of the compound for $Co^{2+}$, $Ni^{2+}$, $Cu^{2+}$ and $Zn^{2+}$ under static and dynamic conditions, and suggested its use for the elimination of heavy metals from waste water.

The high selectivity of (Al+Na)-substituted tobermorite for cesium has been confirmed by Komarneni et al. (1987b), Komarneni and Guggenheim (1988), Tsuji and Komarneni (1989), Miyake et al. (1989), who defined the detailed ion-exchange characteristics of (Al+Na)- and (Al+K)-substituted tobermorites for $K^+$ and $Cs^+$ cations, respectively, as regards their kinetic, equilibrium, and thermodynamic aspects. Tsuji et al. (1991) determined the exchange properties of (Al+Na)-substituted tobermorites for $Cs^+$ and $Li^+$ cations, as well as their water sorption capacity as a function of the aluminum for silicon substitution.

The high selectivity of Al-substituted tobermorites may find very useful application "in decontaminating circulation water in nuclear reactors and radioactive waste solutions" (Komarneni et al. 1987b). Moreover these compounds are stable in cement and therefore "may be incorporated in cement or concrete for use in nuclear as well as hazardous waste disposal" (Komarneni and Roy 1983).

The exchange, selectivity, sequestration features of (Al+alkali)-substituted tobermorite have been so far interpreted on the basis of incompletely known structural models. According

to the present knowledge of the real structure of tobermorite 11 Å, in both its normal and anomalous forms, the previous interpretations require substantial revisions and new experimental studies are highly recommended.

The interesting photoluminescence properties presented by the sodium lanthanide silicates with the structure-type of tobermorite 11 Å (Ferreira et al. 2003) discussed above, are considered in the chapter by Rocha and Lin (2005) in this volume.

## NATURAL AND SYNTHETIC COMPOUNDS OF THE GYROLITE GROUP

The known natural and synthetic phases in the gyrolite group are presented in Tables 6 and 7, with indication of their chemical compositions and crystallographic properties. It may be observed that the synthetic phases are C-S-H compounds *s.s.*, whereas in the natural

**Table 6.** Crystal chemical formulae of the natural and synthetic compounds of the gyrolite group and related mineral phases.

| *Mineral phases* | | *Synthetic compounds* | |
|---|---|---|---|
| gyrolite | $NaCa_{16}Si_{23}AlO_{60}(OH)_8{\cdot}14H_2O$[1] | gyrolite | $Ca_{16}Si_{24}O_{60}(OH)_8{\cdot}(14+x)H_2O$ |
| truscottite | $Ca_{14}Si_{24}O_{58}(OH)_8{\cdot}2H_2O$[2] | truscottite | $Ca_{14}Si_{24}O_{58}(OH)_8{\cdot}2H_2O$[2] |
| reyerite | $(Na,K)_2Ca_{14}Si_{22}Al_2O_{58}(OH)_8{\cdot}6H_2O$ [3] | | |
| fedorite | $(Na,K)_2(Ca,Na)_7(Si,Al)_{16}O_{38}(F,OH)_2{\cdot}3.5H_2O$[4] | K-phase | $Ca_7Si_{16}O_{38}(OH)_2$[5] |
| | | Z-phase | $Ca_9Si_{16}O_{40}(OH)_2{\cdot}14H_2O$[6] |
| *Related mineral phases* | | | |
| minehillite | $(K,Na)_2Ca_{28}Zn_5Al_4Si_{40}O_{112}(OH)_{16}$[7] | | |
| tungusite | $Ca_{14}Fe_9Si_{24}O_{60}(OH)_{22}$[8] | | |
| martinite | $(Ca,Na)_6Na_7(Si,S)_{14}B_2O_{38}(OH,F,Cl)_4{\cdot}6H_2O$[9] | | |
| orlymanite | $Ca_4Mn_3Si_8O_{20}(OH)_6{\cdot}2H_2O$[10] | | |

[1]The composition refers to the specimen from Qarusait; most gyrolite samples are quite well accounted for by the simpler formula $Ca_{16}Si_{24}O_{60}(OH)_8{\cdot}(14+x)H_2O$, with minor substitutions of sodium and aluminum in calcium and silicon sites respectively and water in the hydroxyl sites, and $0 \le x \le 3$ (Merlino 1988a)

[2]Lachowski et al. 1979
[3]Merlino 1972, 1988b
[4]Mitchell and Burns 2001
[5]Gard et al. 1981a,b
[6]Merlino 1988a
[7]Dai et al. 1995
[8]Ferraris et al. 1995
[9]McDonald and Chao 2002
[10]Peacor et al. 1990

**Table 7.** Crystallographic data of the phases of the gyrolite group (Å and °).

| | *S.G.* | *a* | *b* | *c* | α | β | γ | *References* |
|---|---|---|---|---|---|---|---|---|
| gyrolite | $P\bar{1}$ | 9.74 | 9.74 | 22.40 | 95.7 | 91.5 | 120.0 | Merlino 1988a |
| reyerite | $P\bar{3}$ | 9.765 | | 19.067 | | | | Merlino 1988b |
| truscottite | $P\bar{3}$ | 9.731 | | 18.84 | | | | Lachowski et al. 1979 |
| fedorite | $P\bar{1}$ | 9.630 | 9.639 | 12.612 | 102.42 | 96.23 | 119.89 | Mitchell and Burns 2001 |
| K-phase[1] | $P\bar{1}$ | 9.70 | 9.70 | 12.25 | 101.9 | 96.5 | 120.0 | Gard et al. 1981a,b |
| Z-phase[2] | $P\bar{1}$ | 9.70 | 9.70 | 15.24 | 90.94 | 93.19 | 120.0 | |

[1] The transformation matrix [110/$\bar{1}$00/001] has been applied.
[2] Structural model discussed in this paper.

phases limited Al for Si substitutions occur, being the charge compensation obtained through introduction of alkali cations. Table 6 presents also some minerals which display a more complex composition but deserve consideration because of their close structural and crystal chemical relationships with the other phases, as it will be shown below.

**Natural phases: occurrences and composition**

***Gyrolite.*** Gyrolite has long been of interest to mineralogists and chemists, in particular those concerned with the chemistry of cement, who tried to define its crystal chemistry and establish its relationships with reyerite, truscottite and Z-phase of Assarsson. It was first found in Skye, Scotland, by Anderson (1851), who indicated its approximate composition and was subsequently identified in several other localities, generally in association with calcite, zeolites and other calcium silicate hydrates, as okenite, tacharanite, tobermorite, xonotlite. It mainly occurs in vugs and amygdules related to the latest crystallization stages of basaltic rocks; but it was also found within andesitic tuffs (Kobayashi and Kawai 1974); in drill cores from Yellowstone Park, USA, within hydrothermally altered sediments, pyroclastites and rhyolitic flows (White et al. 1975; Bargar et al. 1981) together with zeolites and calcium silicate hydrates; as very uncommon mineral in some ore deposits, as in the iron sulfides ore deposit of Ortano, Island of Elba, Italy (Garavelli and Vurro 1984) and in hydrothermally metamorphosed limestone at Bingham copper mine, Utah, USA (Stephens and Bray 1973).

Indication of gyrolite occurrences, together with the chemical data of the specimens, may be found in Merlino (1988a) and in general compilations, as Handbook of Mineralogy (Anthony et al. 1995) and Dana's New Mineralogy (Gaines et al. 1997).

On the basis of X-ray diffraction data, chemical analysis and dehydration study of samples from Bombay, India, Mackay and Taylor (1953) indicated that gyrolite is a sheet silicate with a structure based on hexagonal or pseudo-hexagonal structural modules, with $a$ = 9.72, $c$ = 22.1 Å, and chemical composition $Ca_{16}Si_{24}O_{60}(OH)_8 \cdot 12H_2O$. Various structural arrangements were hypothesized: Mackay and Taylor (1953) assumed that the hexagonal or pseudo-hexagonal modules are stacked with successive angular displacements of 60°. Strunz and Micheelsen (1958) maintained they found a trigonal one-layer crystal of gyrolite, with $a$ = 9.80, $c$ = 22.08 Å and chemical composition $Ca_{18}Si_{24}O_{60}(OH)_{12} \cdot 12H_2O$, and Cann (1965), who studied gyrolite closely associated with reyerite from Mull, Scotland, suggested that "the structure was made up of three layers of relatively low symmetry to give a trigonal structure with $a$ = 9.76, $c$ = 67.0 Å," and proposed the ideal formula $Ca_{16}Si_{24}O_{60}(OH)_8 \cdot 14H_2O$. A different structural arrangement has been hypothesized by Mamedov and Belov (1958), who sketched for gyrolite and truscottite a succession of octahedral calcium layers and tetrahedral silicon layers, these last built up through connections of parallel wollastonite chains building up alternating rows of pentagonal and octagonal rings.

The crystal structure of gyrolite, its crystal chemical features and relationships with the other natural and synthetic members of the group were elucidated by Merlino (1988a) who found a triclinic cell, space group $P\bar{1}$, $a$ = 9.74, $b$ = 9.74, $c$ = 22.40 Å, $\alpha$ = 95.7, $\beta$ = 91.5, $\gamma$ = 120.0°, crystal chemical formula $NaCa_{16}Si_{23}AlO_{60}(OH)_8 \cdot 14H_2O$ for a specimen from Qarusait, Greenland; moreover, on the basis of the best analytical data reported in the literature for gyrolites from different localities, the following general formula has been proposed: $(Ca,Na,Mg,Fe,\square)_{17}(Si,Al)_{24}O_{60}(OH,H_2O)_8 \cdot (14+x)H_2O$.

***Reyerite.*** This rare mineral has been firstly found, according to Bøggild (1908), by Giesecke in 1811 at Niakornak, Greenland and was studied by Bøggild himself and Cornu and Himmelbauer (1906). Its troubled history as a mineral species, identified from time to time with gyrolite and truscottite, has been reported by Chalmers et al. (1964) in their comprehensive study of reyerite from the type locality, presenting chemical analysis, infrared

absorption, X-ray powder and single crystal diffraction data and thermal weight loss study. They indicated a trigonal symmetry, space groups *P*3 or $P\bar{3}$, with $a = 9.74$, $c = 19.04$ Å, and a cell content $KCa_{14}Si_{24}O_{60}(OH)_5 \cdot 5H_2O$, with minor substitution of Si by Na+Al.

Reyerite has been subsequently found in few other places. At 'S Airde Beinn, Isle of Mull, Scotland, it was found in amygdales, together with analcime, thomsonite, natrolite and gyrolite, just within the metamorphic aureole of the volcanic plug of the plateau basalt (Cann 1965). According to Cann (1965) it was formed by mild metamorphism of gyrolite and it was suggested that the formation in the type locality was similar. Reyerite was later found in "chlorite-containing amygdales in a diabase dike in Rawlings quarry, Brunswick County, Virginia, that has been subjected to an episode of low-grade regional metamorphism" (Clement and Ribbe 1973), who confirmed the chemical and crystallographic data of Chalmers et al. (1964). Reyerite was found, together with tobermorite 11 Å, with minor chlorite, calcite, pectolite and thomsonite, in central zones within amygdales in olivine basalt at Allt Coir' a' Ghobhainn, near Drynoch, Isle of Skye, Scotland, by Livingstone (1988), who maintains it formed through the action of a Ca- and Si-rich fluid within the deepest and hottest zones of the lava pile during zeolitization.

Merlino (1972, 1988b) determined the crystal structure of reyerite on a specimen of the type locality, indicating the space group $P\bar{3}$, with $a = 9.765$, $c = 19.067$ Å and cell content **(**Na, $K)_2Ca_{14}Si_{22}Al_2O_{58}(OH)_8 \cdot 6H_2O$, and stressing the distinctions between reyerite and truscottite.

***Truscottite.*** Truscottite was firstly found by Hövig (1914) in the Lebong Donok mine, Benkulen, Sumatra. The specimen was studied by Mackay and Taylor (1954) who found a Laue symmetry $\bar{3}$ or $\bar{3}m$ with $a = 9.72$, $c = 18.71$ Å, and pointed to an ideal chemical content $12CaO \cdot 24SiO_2 \cdot 6H_2O$.

It was subsequently found in one of the auriferous quartz veins cutting Miocene pyroclastic rocks at Toi mine, Shizuoka prefecture, Japan, by Minato and Kato (1967), who, taking into consideration the experimentally established stability range under low pressure (see succeeding section), supposed that the vein including truscottite had been formed under temperatures above 180°C and possibly below 355°C, and probably in the lower part of the stability range (Minato and Kato 1967). Truscottite was also found in drill cores from hot spring and geyser areas of Yellowstone National Park (Bargar et al. 1981); at Hishikani deposit, Kagoshima Prefecture, Japan (Izawa and Yamashita 1995); in deep drill hole at Kilauea Volcano (Grose and Keller 1976).

Lachowski et al. (1979) carried out a wide chemical and crystallographic study on specimens of natural and synthetic truscottite and, taking into account the results of the structural study of reyerite (Merlino 1972), definitely established the crystal chemical formula $Ca_{14}Si_{24}O_{58}(OH)_8 \cdot 2H_2O$.

***Fedorite.*** Fedorite has been firstly found by Khukarenko et al. (1965) in fenitized sandstone of the Turiy Peninsula, Kola, Russia, as fine veinlets, in association with narsarsukite, and partly replaced by quartz and apophyllite. It was later found also in metasomatic-hydrothermal charoite-carbonatite rocks of the Little Murun potassic complex, Siberia, Russia (Konyev et al. 1993).

The structure of fedorite has been determined by Sokolova et al. (1983) and subsequently refined with X-ray and neutron diffraction data by Joswig et al. (1988); the studies were carried out with a specimen from Turiy in the space group $C\bar{1}$, with $a = 9.650$, $b = 16.706$, $c = 13.153$ Å, $\alpha = 93.42$, $\beta = 114.92$, $\gamma = 90.0°$. Mitchell and Burns (2001) refined the crystal structures of specimens from both known localities, in the space group $P\bar{1}$, with $a = 9.630$, $b = 9.639$, $c = 12.612$ Å, $\alpha = 102.42$, $\beta = 96.23$, $\gamma = 119.89°$ (specimen from Turiy); the unit cell

given by Mitchell and Burns (2001) may be obtained from the cell of Sokolova et al. (1983) and Joswig et al. (1988) through the transformation matrix [−½ −½ 0 / −½ ½ 0 / 1 0 1].

**Synthetic phases: preparation and composition**

***Gyrolite.*** Gyrolite was firstly synthesized by Flint et al. (1938) from glasses and gels characterized by Ca:Si ratios 0.50–0.66 in the temperature range 150–400°C; actually the product they obtained at the higher temperatures was most probably truscottite (Taylor 1964). It was subsequently prepared by Mackay and Taylor (1954) by autoclaving mixtures of calcium hydroxide and moist silica gel (Ca:Si ratio 0.66) at 150°C for 76 days, and afterwards by several other research groups, who defined the temperature conditions and the preparation procedures to obtain well crystallized products, as well as the stability field with respect to truscottite and xonotlite.

Recently the formation of gyrolite has been the subject of wide and relevant investigations (Shaw et al. 2002; Garbev 2004; Šiačiūnas and Baltakys 2004). Garbev (2004) carried out a wide study on the hydrothermal syntheses of C-S-H phases from mechano-chemically prepared gels with various C:S ratios. Gyrolite has been obtained by hydrothermal treatment from 110 to 220°C of preparations with C:S ratios 0.5 and 0.66. It was clearly shown how the crystallization of gyrolite was preceded by the formation of the Z-phase and a reliable mechanism for its formation was presented. Similar results were obtained by Šiačiūnas and Baltakys (2004) and by Shaw et al. (2002) who studied dynamically, at 190-240°C, by energy dispersive powder diffraction, with X-rays from a synchrotron source, the hydrothermal crystallization of gyrolite. This is a continuous process starting with the formation of a C-S-H gel with well ordered $Ca(O,OH)_2$ layers in the (001) plane, proceeding with progressive ordering in the **c** direction and formation of Z-phase which finally transforms to gyrolite.

***Truscottite.*** As remarked by Taylor (1964) "the earliest report of the synthesis of truscottite, as distinct from gyrolite, was by Buckner et al. (1960), who obtained it together with other products from a hydrothermal run at 295°C and about 2000 kg/cm$^2$," although it had probably already been obtained by Jander and Franke (1941) and by Funk and Thilo (1955). Subsequently it was prepared by Funk (1961) and Meyer and Jaunarais (1961) who indicated the composition $2CaO{\cdot}4SiO_2{\cdot}H_2O$, whereas Harker (1964) proposed the composition $3CaO{\cdot}5SiO_2{\cdot}1.5H_2O$. Lachowski et al. (1979) presented the results of hydrothermal syntheses carried out for 7 days at saturated steam pressure and temperatures between 300 and 345°C, with different starting mixtures at C:S ratio *ca*. 0.6; some preparations had $Al(OH)_3$ or KOH as additional components. By careful examination of the products through analytical electron microscopy and X-ray powder diffraction, and by taking into account the results of the structural study of reyerite (Merlino 1972, 1988b), the crystal chemical formula $Ca_{14}Si_{24}O_{58}(OH)_8{\cdot}2H_2O$ was established. It was also shown that truscottite can accommodate aluminum, up to ~1.5 atoms per formula unit, and potassium, up to 0.5 atoms per formula unit. With some preparation, in particular when mixtures of CaO and silicic acid are reacted, gyrolite-truscottite intergrowths are formed as intermediate products, as already observed by Meyer and Jaunarais (1961) and Harker (1964).

***Z-phase.*** This compound, with composition assumed as $CaO{\cdot}2SiO_2{\cdot}2H_2O$, was first obtained by Funk and Thilo (1955) by autoclaving a C-S-H gel at 180°C. Subsequently Assarsson (1957, 1958) synthesized a similar product by hydrothermal treatment of mixtures of CaO and amorphous $SiO_2$ at 140–240°C and named it Z-phase. The identity of the preparation by Funk and Thilo and Z-phase of Assarson was indicated by Taylor (1962) and confirmed by Funk (1961), who carried out new preparations and, on the basis of a DTA study, concluded that the composition was $2CaO{\cdot}4SiO_2{\cdot}3H_2O$. Z-phase was also obtained by Harker (1964) by autoclaving a mixture of lime and silicic acid at 195°C. It has been recalled in a

preceding section that Z-phase occurs as an intermediate in the formation of gyrolite. A wide study of the Z-phase obtained hydrothermally at 120°C by decomposition of Al-substituted tobermorite was carried out by Gard et al. (1975), who studied the product through X-ray and electron diffraction, thermal and infra-red investigations. They indicated that the phase is built up by hexagonal structural modules with $a = 9.65$, $c = 15.3$ Å, suggested structural relationships with gyrolite and truscottite and proposed for the structural module a composition between $8CaO{\cdot}16SiO_2{\cdot}14H_2O$ and $8CaO{\cdot}16SiO_2{\cdot}16H_2O$. On the basis of the careful analytical data of Gard et al. (1975) and assuming a close structural relationships of Z-phase with gyrolite, Merlino (1988a) proposed the crystal chemical formula $Ca_9Si_{16}O_{40}(OH)_2{\cdot}(14+x)H_2O$, with $0 \leq x \leq 3$. As it will be discussed in another section, a structural model may be sketched for Z-phase in the space group $P\bar{1}$, with $a = 9.70$, $b = 9.70$, $c = 15.24$ Å, $\alpha = 90.94$, $\beta = 93.19$, $\gamma = 120.0°$.

***K-phase.*** It was hydrothermally synthesized by Gard et al. (1981a) from a mixture of CaO and very finely divided reactive silicic acid (Ca:Si ratios 0.2 to 0.6) at temperatures 300 to 400°C. K-phase, if formed, was always mixed with other phases. These almost always included either truscottite, or in short runs, truscottite randomly interstratified with gyrolite. The optimum time for preparing K-phase was about 5 d at 350-375°C, or 5 h at 400°C (Gard et al. 1981a). Through microprobe analyses, transmission electron microscopy, as well as electron and X-ray diffraction studies, Gard et al. (1981a, b) proposed a structural model of K-phase in the space group $P\bar{1}$, with $a = 9.70$, $b = 9.70$, $c = 12.25$ Å, $\alpha = 108.6$, $\beta = 78.1$, $\gamma = 120°$ (by applying the transformation matrix [110/-100/001] we obtain a unit cell with $a = 9.70$, $b = 9.70$, $c = 12.25$ Å, $\alpha = 101.9$, $\beta = 96.5$, $\gamma = 120°$, in agreement with the cell parameters of fedorite, as given in Table 7), and defined the crystal chemical formula $Ca_7Si_{16}O_{38}(OH)_2$. It seems proper to recall here that recently Garbev (2004) has shown that the powder diffraction pattern of the product obtained by Gard et al. (1975) by dehydration of the Z-phase corresponds to that of K-phase, which indicates, according to Garbev (2004) that Gard et al. (1975) had already obtained the K-phase six years before they synthesized it through hydrothermal treatment.

## STRUCTURAL ASPECTS

The various phases of the gyrolite group are built up by the stacking of all (as in gyrolite) or some of the following structural modules: $S_1$ and $S_2$ tetrahedral sheets, O octahedral and X interlayer sheets, all presenting trigonal or hexagonal symmetry, with $a = b \approx 9.7$ Å, $\gamma = 120°$.

The tetrahedral sheet $S_1$ (Fig. 23) may be described as made up by two-dimensional connection of groups of four tetrahedra, characterized by a central tetrahedron and three peripheral tetrahedra, all pointing in one direction; each group of four up-pointing tetrahedra is connected to three groups of four down-pointing tetrahedra (and *vice versa*) to build an infinite sheet with composition $Si_8O_{20}$ and characterized by the presence of two kinds of six-membered rings; the first presents alternatively up- and down-pointing tetrahedra and is denoted as 1,3,5-ring; the second, with oval shape, has three down-pointing tetrahedra, followed by three up-pointing tetrahedra and is denoted as 1,2,3-ring.

Also the tetrahedral sheet $S_2$ (Fig. 24) may be described as built up by connection of groups of four tetrahedra, although in this case the central tetrahedron and the peripheral tetrahedra have opposite directions; the resulting infinite sheet with composition $Si_8O_{20}$ presents two types of six-membered rings: the first is an almost hexagonal ring of tetrahedra pointing in one direction (up pointing in Fig. 24), the second (1,4-ring), with oval shape, is composed of two separated pairs of up-pointing tetrahedra, connected by two single down-pointing tetrahedra.

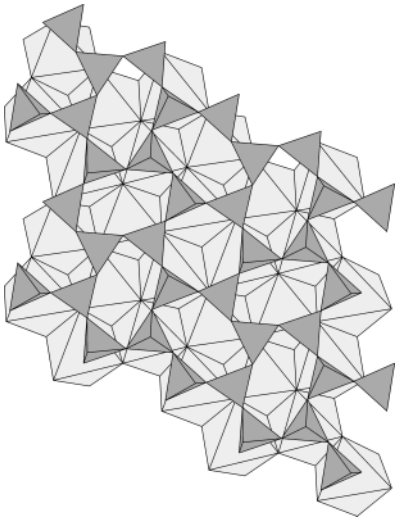

**Figure 23**. The tetrahedral sheet $S_1$ and its connection with the octahedral module O, as seen normal to (001) of gyrolite, **b** vertical.

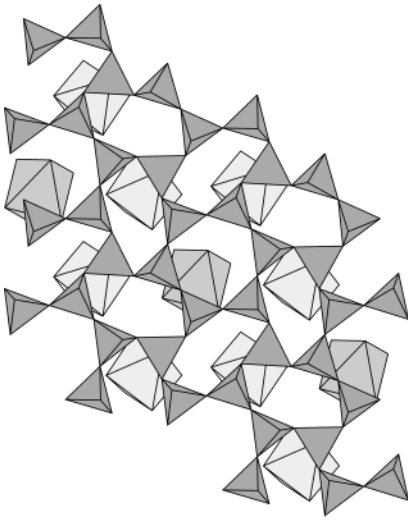

**Figure 24.** The tetrahedral sheet $S_2$ and its connection with the module X, as seen normal to (001) of gyrolite, **b** vertical. The module X is built up, in gyrolite from Qarusait, by calcium (light grey) and sodium (dark grey) octahedra.

The $S_1$ and $S_2$ sheets may also be described as formed by the connection of four-repeat tetrahedral chains, the translational unit (9.7 Å long) presenting three tetrahedra pointing in one direction and one tetrahedron pointing in the opposite direction: in the $S_1$ sheet inversion-equivalent chains follow each other, whereas in the $S_2$ sheet similar chains follow each other.

Calcium octahedra are connected by edge sharing to build infinite O sheets (Fig. 23) with seven octahedra within the unit net and chemical composition $Ca_7(O,OH)_{14}$. The nature of the ligands depends on the kind of connection along the stacking direction: the oxygen atoms of the octahedral sheet which are coordinated also to silicon cations of an adjacent tetrahedral sheet correspond to oxide anions, whereas the remaining oxygen atoms correspond to hydroxyl anions.

The interlayer X sheet, which characterizes the structures of gyrolite and Z-phase, is also called "calcium-water layer" and its actual composition may slightly vary in gyrolites from different localities or in different synthetic preparations. Figure 24 represents the particular X layer in gyrolite from Qarusait (Merlino 1988a), with one sodium and two calcium octahedra in the unit net. The calcium cations are coordinated by two oxide anions, the apical oxygen atoms in the $SiO_4$ tetrahedra of the $S_2$ and $\overline{S}_2$ sheets sandwiching the X layer, and four water molecules, whereas the sodium cation is coordinated by six water molecules; the resulting composition of the X layer is $[Ca_2Na{\cdot}14H_2O]^{+5}$. In most natural and synthetic samples the X layer presents only two calcium cations and the corresponding composition may be expressed as $[2Ca{\cdot}(14+x)H_2O]^{+4}$.

It is now possible to describe (Table 8) the structures of the various natural and synthetic phases of the gyrolite group just indicating the stacking of the constituting modules in the [001] direction (cf. Ferraris et al. 2004) and presenting, where necessary, the additional features which characterize the phase under consideration. The polytypic aspects are not considered here, but will be shortly discussed in a successive section.

**Table 8.** Modular schemes, crystal chemical formulae, space group symmetry and $d_{001}$ distances (Å) for the various natural and synthetic phases of the gyrolite group.

| *Modular scheme* | *Phase* | *Crystal chemical formula* | *S.G.* | $d_{001}$ |
|---|---|---|---|---|
| $S_1\,O\,S_2\,\bar{S}_2\,\bar{O}\,S_1$ | Reyerite | $(Na,K)_2Ca_{14}Si_{22}Al_2O_{58}(OH)_8{\cdot}6H_2O$ | $P\bar{3}$ | 19.07 |
| | Truscottite | $Ca_{14}Si_{24}O_{58}(OH)_8{\cdot}2H_2O$ | $P\bar{3}$ | 18.84 |
| $S_1\,O\,S_2\,X\,\bar{S}_2\,\bar{O}\,S_1$ | Gyrolite | $Ca_{16}Si_{24}O_{60}(OH)_8{\cdot}(14+x)H_2O$ | $P\bar{1}$ | 22.20 |
| $O\,S_2\,\bar{S}_2O$ | Fedorite | $(Na,K)_2(Ca,Na)_7(Si,Al)_{16}O_{38}(F,OH)_2{\cdot}3.5H_2O$ | $P\bar{1}$ | 11.91 |
| | K-phase | $Ca_7Si_{16}O_{38}(OH)_2$ | $P\bar{1}$ | 11.59 |
| $O\,S_2\,X\,\bar{S}_2\,O$ | Z-phase | $Ca_9Si_{16}O_{40}(OH)_2{\cdot}(14+x)H_2O$ | $P\bar{1}$ | 15.30 |

***Gyrolite.*** The crystal structure of gyrolite (Merlino 1988a) is represented in Figure 25: two centrosymmetrically related octahedral sheets O and $\bar{O}$ are present in the unit cell, both sandwiched between two tetrahedral sheets of different kind, building up a complex layer $\bar{S}_2\,\bar{O}\,S_1\,O\,S_2$, with ideal composition $[Ca_{14}Si_{24}O_{60}(OH)_8]^{-4}$ and trigonal symmetry. This symmetry is not preserved in the whole structure in which the complex layer and the X interlayer sheet, $[2Ca{\cdot}14H_2O]^{+4}$, regularly alternate giving rise to a triclinic arrangement $S_1\,O\,S_2\,X\,\bar{S}_2\,\bar{O}\,S_1$, with composition $Ca_{16}Si_{24}O_{60}(OH)_8{\cdot}14H_2O$. When Al for Si substitutions occur, the charge balance may be restored by introduction of sodium cations in the X interlayer sheet.

***Reyerite and truscottite.*** The crystal structure of reyerite (Merlino 1972, 1988b) is represented in Figure 26 and may be described by the scheme $S_1\,O\,S_2\,\bar{S}_2\,\bar{O}\,S_1$, which is valid also for truscottite: two inversion related octahedral sheets, O and $\bar{O}$, are present in the unit cell, both sandwiched between a single $S_1$ and a double $S_2\,\bar{S}_2$ tetrahedral sheets. In reyerite, as indicated in Figure 26, two aluminum cations per unit cell are perfectly ordered in the $S_2\,\bar{S}_2$ double sheet; the whole tetrahedral-octahedral scaffolding has composition $[Ca_{14}Si_{22}\,Al_2O_{58}(OH)_8]^{2-}$ and the charge balance is restored by "zeolitic" alkali cations which are placed, together with water molecules, in the cavities of the structure at the level of the double tetrahedral sheet; the resulting composition is $(Na,K)_2\,Ca_{14}Si_{22}Al_2O_{58}(OH)_8{\cdot}6H_2O$.

Notwithstanding the common structural scheme, reyerite and truscottite present significant differences in their infrared absorption spectra, in the region at 600–850 $cm^{-1}$, associated with Si-O-Si linkages, and in the band at 1640 $cm^{-1}$, attributed to molecular

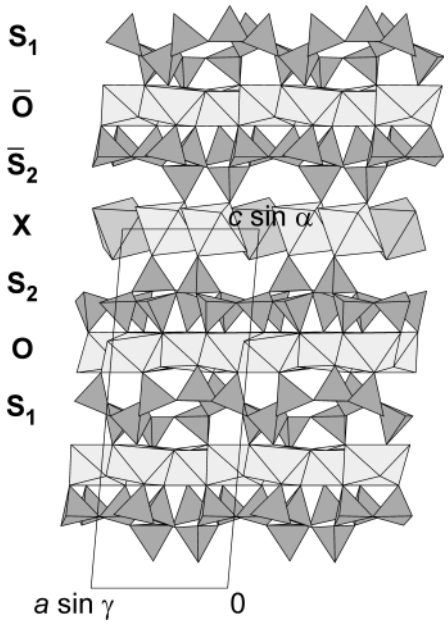


**Figure 25.** Crystal structure of gyrolite from Qarusait, as seen along **b**. The sequence of the modules is indicated. In the X sheet the calcium and sodium octahedra are drawn light and dark grey, respectively.

water (Chalmers et al. 1964), and in chemical composition, with higher water, alkali and aluminum contents in reyerite, and also in the length of their *c* parameters. All the differences in chemistry, infrared spectra, as well as in the *c* parameter, may be easily explained assuming that reyerite is characterized, in comparison with natural and synthetic truscottite, by the presence of two ordered Al cations in the unit cell. This clearly explains the chemical features of reyerite: the Si by Al substitution requires the introduction of alkali cations in the cavities of the $S_2$ $\overline{S}_2$ sheet, to restore the charge balance, and also the introduction of water molecules to complete their coordination. The differences in the band at 1640 $cm^{-1}$ are dependent on the different water content in the two phases, whereas the differences in the region 600-850 $cm^{-1}$ are related to the presence of Si-O-Al linkages in reyerite.

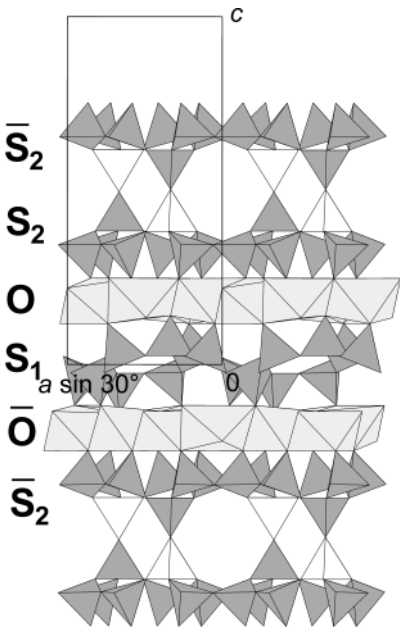


**Figure 26**. Crystal structure of reyerite, as seen along **b**. The sequence of the modules is indicated. In the $S_2$ sheet the $AlO_4$ tetrahedra are drawn white. The disordered distribution of the "zeolitic" alkali cations and water molecules is not indicated.

***Fedorite and K-phase***. The crystal structure of fedorite (Sokolova et al. 1983; Joswig et al. 1988; Mitchell and Burns 2001) is represented in Figure 27 and may be described by the scheme O $S_2$ $\overline{S}_2$ O, which is valid also for the K-phase (Gard et al. 1981a, b). There are between fedorite and K-phase the same relationships already described in the case of reyerite and truscottite: Si by Al substitution in the tetrahedral sheet and Ca by Na substitution in the octahedral sheet are compensated by the introduction of "zeolitic" alkali cations in the cavities of the $S_2$ $\overline{S}_2$ sheet, together with water molecules to complete their coordination.

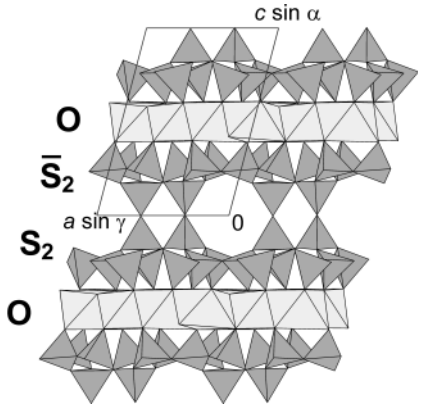


**Figure 27.** Structure of fedorite, as seen along **b.** The alkali cations and water molecules distributed inside the cavities are not represented.

***Z-phase.*** Although its structure has not yet definitely established, the structural scheme O $S_2$ X $\overline{S}_2$ O has been proposed (Gard et al. 1975; Merlino 1988a) and a reliable model may be derived on the basis of our knowledge of the structures of K-phase and gyrolite and the available crystallographic information collected by Gard et al. (1975) through electron diffraction investigations. They obtained an electron diffraction pattern that could be indexed on a pseudo-hexagonal unit cell with $a$ = 9.65 Å and estimated a $c$ period between 15 and 16 Å, with an angle between **c** and **c*** of 4±1°. In building the structural model for Z-phase we find, in the sequence of the modules, two points of possible ambiguity, namely in fixing the relative position of $\overline{S}_2$ and $S_2$ layers on both sides of the O module and of the X module. As regards the first point we may assume the same positioning as

found in K-phase (and fedorite); as regards the second point there are six possible stacking ways equivalent to that realized in gyrolite, but only one gives an angle between **c** and **c*** (4.3°) corresponding to the value obtained by Gard et al. (1975). For the structure so derived, represented in Figure 28, the calculated intensities are in satisfactory agreement with those of the *hk*0 electron diffraction pattern presented by Gard et al. (1975).

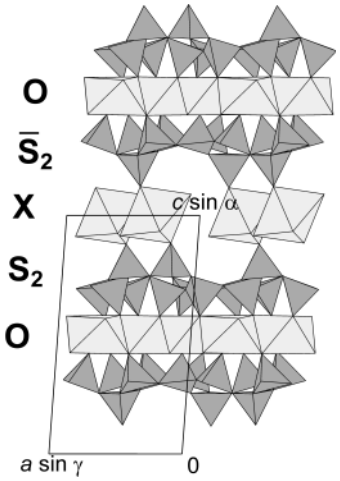


**Figure 28.** The structural model of Z-phase, as seen along **b**. The interlayer X module is built up by $CaO_2(H_2O)_4$ octahedra.

**Thermal behavior**

The thermal studies carried on the various phases may be easily interpreted on the basis of the structural arrangements just discussed. By weight loss studies of reyerite, Chalmers et al. (1964) determined that water is lost in two steps, the first, corresponding to the loss of 5.8 water molecules is completed at 400°C, the second one, which begins at 650°C, corresponds to the loss of 3.6 water molecules; they attribute the two steps to the loss of water molecules and hydroxyl anions respectively, which is in good agreement with the six water molecules and the eight hydroxyl anions indicated by the structure analysis (Merlino 1988b).

Similarly the dehydration curve presented by Mackay and Taylor (1954) for truscottite indicates a total weight loss of 4.6%, 1.5% in the temperature range 110 to 350°C, corresponding to the two water molecules in the crystal chemical formula, and 3.1% from 350 to 650°C, corresponding to the eight hydroxyl anions in the formula (Table 6).

The thermal behavior of gyrolite was firstly described for a specimen from Bombay by Mackay and Taylor (1953): also in this case the result of the study clearly shows that the water is lost in two stages, the first completed at 450°C, the second completed by 850°C; the weight losses in the two stages closely correspond to the water molecules and hydroxyl anions in the crystal chemical formula. A careful thermal study of gyrolite from Ortano (Italy) was carried out by Garavelli and Vurro (1984) and the results were carefully discussed and convincingly explained on the basis of the structural arrangement.

A thermal study of the Z-phase has been presented by Garbev (2004) who maintains that at 500°C the phase has lost all the molecular water and the transformation into the K-phase (see the discussion in the following paragraph) has been completed.

Very interesting results were obtained by following the dehydration processes of gyrolite and Z-phase through X-ray powder diffraction. Gard et al. (1975) found that by heating Z-phase at 500°C the basal (001) spacing, 15.3 Å, shortens to 11.8 Å; they also collected the powder diffraction pattern of the heated material, which, as we have already said, was subsequently shown by Garbev (2004) to correspond to the pattern of the K-phase. The Z-phase to K-phase transformation on dehydration at 400°C has been definitely proved and discussed by Garbev et al. (2004). They have also shown that, similarly, synthetic gyrolite transforms to truscottite at 400°C. In both transformations the water content of the X layer is lost and the separated $S_2$ and $\bar{S}_2$ sheets are condensed to form the characteristic double sheet of K-phase and truscottite. They also discuss about the possible location, in the dehydrated phases, of the two calcium cations of the interlayer X sheet, indicating that most probably they behave as the "zeolitic" alkali cations in fedorite and reyerite and that the charge balance may be restored through

combination of the "redundant" oxide anions resulting from the condensation process and water molecules to give hydroxyl anions: $2\ O^{2-} + 2\ H_2O = 4\ OH^-$.

The dehydration process of a crystal of gyrolite from Qarusait has been also studied on a single crystal X-ray diffractometer equipped with heating device (Bonaccorsi and Merlino 2004). Structural refinements were carried out with data collected from the same crystal at room temperature and at 250°C, then again at room temperature after placing the crystal in water for three weeks. The crystal heated at 250°C has the structure-type of reyerite, with trigonal symmetry and $c$ = 19.1 Å, with calcium and sodium cations distributed in the cavities of the $S_2\,\bar{S}_2$ double sheet; after wetting, partial rehydration occurs, but the structure-type does not change. Gyrolite specimens from other localities (for example Antrim, Ireland; Ortano, Italy; Poona, India) present a different behavior on heating: their basal spacing remain unchanged at ≈ 22 Å on dehydration; it is possible that small differences in composition—we guess in the aluminum content—may explain the distinct behavior (Bonaccorsi and Merlino 2004).

**Related mineral phases**

Four other natural phases are known which may be classified as members of the gyrolite group: minehillite (related to reyerite), tungusite (related to gyrolite), martinite (related to Z-phase), and orlymanite, whose structure is still unknown.

***Minehillite.*** It was described from Franklin, New Jersey, by Dunn et al. (1984) who suggested it is "a secondary, relatively low-temperature, hydrothermal, replacement mineral" with close relationships with reyerite. The results of the structural study, carried on by Dai et al. (1995) in the space group $P\bar{3}c1$, with $a$ = 9.777, $c$ = 33.293 Å, lead to the crystal chemical formula $(K,Na)_2Ca_{28}Zn_5Al_4Si_{40}O_{112}(OH)_{16}$. The structure is illustrated in Figure 29 and its relationships with that of reyerite may be understood on the basis of the following scheme:

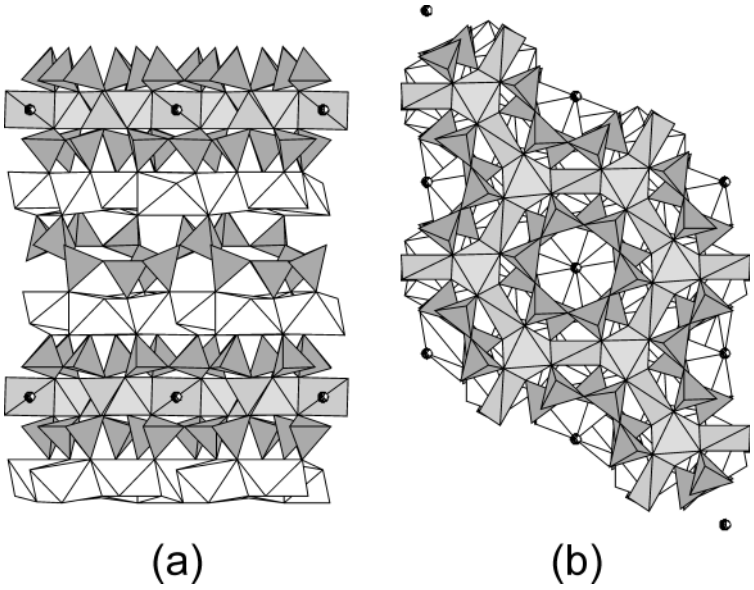


**Figure 29**. (a) The crystal structure of minehillite as seen along **b**, **c** vertical. The figure illustrates the sequence of the layers. (b) The figure represents the complex layer built up by sheets of hexagonal silicate rings, with the sheet of Al octahedra and Zn tetrahedra in between, as seen along **c**. The small circles in both (a) and (b) represent the $K^+$ cations located at 0, 0, 0.

| | | | | |
|---|---|---|---|---|
| (K,Na) | $Ca_{14}$ | $Zn_{2.5}\square_{0.5}Al_2$ | $Si_{20}O_{56}(OH)_8$ | minehillite |
| $(Na,K)_2$ | $Ca_{14}$ | $Si_2Al_2O_2$ | $Si_{20}O_{56}(OH)_8{\cdot}6H_2O$ | reyerite |

The structure of minehillite may be derived from that of reyerite by substituting, in the $S_2\,\bar{S}_2$ double layers, the pairs of inverted tetrahedra sharing common apices (Si-O-Al), with Al octahedra which build up an infinite layer through interconnection, by edge sharing, with Zn tetrahedra. The alkali cations are located in the centers of the rings of Al and Zn polyhedra. As clearly shown by Figure 29b, the slab built up by the sheets of silicate hexagonal rings and the sheet of Al and Zn polyhedra in between, is closely similar to that occurring in beryl, with zinc substituting for beryllium, or in the minerals of the osumilite group, with various cations substituting for Al and Zn. The thickness of this slab is drastically smaller than the thickness of the double tetrahedral layer $S_2\,\bar{S}_2$ in reyerite, thus reducing the size of the cavities; this explains why only a single alkali cation is present and the water molecules are absent. The presence of zinc in the hydrothermal solutions from which the mineral formed was probably responsible for the crystallization of minehillite instead than reyerite.

***Tungusite.*** It was firstly found (Kudriashova 1966) in pillow lavas on the right-hand bank of the Lower Tunguska river, Tura, East Siberia, as radially fibrous flakes on the walls of amygdales, with intergrown reyerite and gyrolite. New findings were reported by Anastasenko (1978) in basalts of the North-West Siberian platform (basins of rivers Eramchino, Tutonchana and Kureyka). On the basis of chemical data, and electron and X-ray powder diffraction studies, a structural model closely related to the structure-type of gyrolite and the ideal crystal chemical formula $Ca_{14}Fe_9Si_{24}O_{60}(OH)_{22}$ have been proposed by Ferraris et al. (1995), who assumed the space group symmetry $P\bar{1}$, with $a$ = 9.714, $b$ = 9.721, $c$ = 22.09 Å, α = 90.13, β = 98.3, γ = 120.0°. The structural relationships between tungusite (Fig. 30) and gyrolite are described by the following scheme:

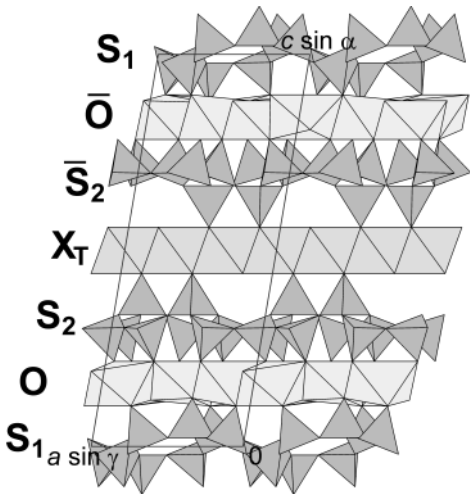


**Figure 30.** Crystal structural model of tungusite, as seen along **b**. The sequence of building modules is indicated.

| | | |
|---|---|---|
| $Ca_{14}Si_{24}O_{60}(OH)_8$ | $Fe_9(OH)_{14}$ | tungusite |
| $Ca_{14}Si_{24}O_{60}(OH)_8$ | $Ca_2{\cdot}(14+x)H_2O$ | gyrolite |

the X layer of gyrolite being substituted in tungusite by a continuous sheet $X_T$ of edge sharing iron octahedra.

***Martinite.*** It was discovered as last-stage phase in sodalite syenite xenoliths at the Poudrette quarry, Mont St. Hilaire, Quebec, by McDonald and Chao (2002), who determined and refined its crystal structure in the space group $P\bar{1}$, $a$ = 9.544, $b$ = 14.027, $c$ = 9.535 Å, α = 71.06, β = 119.79, γ = 105.85° and defined its crystal chemical formula. The structure of martinite is related to that of the Z-phase and their relationships are described by the scheme:

| | | | |
|---|---|---|---|
| $(Ca,Na)_7$ | $(Si,S)_{14}B_2O_{38}(OH,F,Cl)_4$ | $Na_6{\cdot}6H_2O$ | martinite |
| $Ca_7$ | $Si_{16}O_{40}(OH)_2$ | $Ca_2{\cdot}14H_2O$ | Z-phase |

The $S_2$ and O modules present in martinite a more complex composition than in Z-phase, whereas the X layer of Z-phase is substituted by a layer of sodium cations and water molecules.

***Orlymanite.*** This mineral has been found at the Wessels Mine, South Africa, as dark brown spherules in association with inesite and minor calcite. The species was defined by Peacor et al. (1990) who proposed the crystal chemical formula, $Ca_4Mn_3Si_8O_{20}(OH)_6{\cdot}2H_2O$, and determined its unit cell parameters $a$ = 9.60, $c$ = 35.92 Å, space group $P3$ or $P\bar{3}$. The structure has not been solved, but the cell parameters and the chemical composition point to a close relationships with the phases of the gyrolite group.

**Ambiguities in the layer stacking and polytypism**

Zvyagin (1997) carried on a study of the possible polytypes in the phases of the gyrolite group. In reyerite (and truscottite as well) the so called complex modules R = $\bar{S}_2$ $\bar{O}$ $S_1$ O $S_2$ are directly connected through the double sheet $S_2$ $\bar{S}_2$. The different periodicity of the O and S sheets (both $S_1$ and $S_2$ unit nets contain seven unit nets of the O sheet) is the cause of the possible polytypism in reyerite. Four distinct polytypes are derived, all presenting the common "complex layer" R; the R modules follow each other in different ways in the different polytypes, giving rise to the known reyerite structure with space group $P\bar{3}$ and $c$ = 19 Å, and to three other possible arrangements, presenting two R modules in the unit translation $c$ = 38 Å and space group $P6_3$, $P\bar{3}1c$, $P\bar{3}c1$ . This last structure is closely related to that of minehillite through substitution of the $S_2$ $\bar{S}_2$ double sheet by the aluminum-zinc module which characterizes the crystal structure of minehillite.

In gyrolite the X module may have six different azimuthal orientations around the symmetry axis of the R complex layer. A careful analysis by Zvyagin (1997) has derived the possible homogeneous polytypes which comprise, besides the one-layer triclinic structure we have described in a previous section and represented in Figure 25, one trigonal three-layer ($c$ = 66.5 Å) and one hexagonal six-layer ($c$ = 135.0 Å) polytype, as well as several other triclinic and monoclinic two-layer polytypes.

In fedorite and in K phase, ...O $S_2$ $\bar{S}_2$ O $S_2$…, there are three distinct ways for positioning $S_2$ and $\bar{S}_2$ sheets on both sides of O: one of them is realized in the actual structures of fedorite and K-phase. In the more complex structure of Z-phase, … $\bar{S}_2$ O $S_2$ X $\bar{S}_2$ O $S_2$…, if we assume that the $S_2$ and $\bar{S}_2$ sheets on both sides of the O sheet are placed as in the actual structure of fedorite, the problem is similar to that already met in gyrolite. As we have already said in a previous section, it was possible to derive the correct azimuthal orientation of the X module by comparing the calculated crystallographic parameters for each case with the crystallographic information by Gard et al. (1975).

## ACKNOWLEDGMENTS

The authors are grateful to K. Garbev for his careful reading of the text and his valuable suggestions. The research was supported by MIUR (Rome) through the FIRB project "Properties and technological applications of minerals and their synthetic analogues" and the PRIN project "Microstructural and modular aspects in minerals: analyses and applications."

## REFERENCES

Abdul-Jaber QH, Khoury H (1998) Unusual mineralisation in the Maqarin Area (North Jordan) and the occurrence of some rare minerals in the marbles and the weathered rocks. N Jb Geol Paläont Abh 208: 603-629

Aguirre L, Dominguez-Bella S, Morata D, Wittke O (1998) An occurrence of tobermorite in tertiary basalts from Patagonia, Chile. Can Mineral 36:1149-1155
Al-Wakeel EI, El-Korashy SA, El-Hemaly SA, Rizk MA (2001) Divalent ion uptake of heavy metal cations by (aluminum + alkali metals)-substituted synthetic 1.1nm-tobermorites. J Mater Sci 36:2405-2415
Anastasenko GF (1978) Boron-bearing traps of the North-West Siberian platform. Leningrad University Press. Leningrad (in Russian)
Anderson T (1851) Description and analysis of gyrolite. Philos Mag Sect IV 1:111-115
Anthony JW, Bideaux RA, Bladh KW, Nichols MC (1995) Handbook of Mineralogy. Vol. II Silica, silicates. Mineral Data Publishing, Tucson, Arizona
Assarsson GO (1957) Hydrothermal reactions between calcium hydroxide and amorphous silica; the reactions between 180 and 220°C. J Phys Chem 61:473-479
Assarsson GO (1958) Hydrothermal reactions between calcium hydroxide and amorphous silica; the reactions between 120 and 160°C. J Phys Chem 62:223-228
Baerlocher Ch, McCusker LB Database of Zeolite Structures: *http://www.iza-structure.org/databases/*
Ballirano P (1994) Crystal chemistry of cancrinites. Plinius 11:81-86
Ballirano P, Bonaccorsi E, Maras A, Merlino S (1997) Crystal structure of afghanite, the eight-layer member of the cancrinite group: evidence for long-range Si,Al ordering. Eur J Mineral 9:21-30
Ballirano P, Bonaccorsi E, Maras A, Merlino S (2000) The crystal structure of franzinite, the ten-layer mineral of the cancrinite group. Can Mineral 38:657-668
Ballirano P, Bonaccorsi E, Merlino S, Maras A (1998) Carbonate groups in davyne: structural and crystal-chemical considerations. Can Mineral 36:1285-1292
Ballirano P, Maras A (2004) The crystal structure of a "disordered" cancrinite. Eur J Mineral 16:135-141
Ballirano P, Maras A, Buseck PR (1996a) Crystal chemistry and IR spectroscopy of Cl- and $SO_4$-bearing cancrinite-like minerals. Am Mineral 81:1003-1012
Ballirano P, Maras A, Caminiti R, Sadun C (1995) Carbonate-cancrinite: In situ real time thermal processes studied by means of energy-dispersive X-ray powder diffractometry. Powder Diffr 10:173-177
Ballirano P, Merlino S, Bonaccorsi E, Maras A (1996b) The crystal structure of liottite, a six-layer member of the cancrinite group. Can Mineral 34:1021-1030
Bargar KE, Beeson MH, Keith TEC (1981) Zeolites in Yellowstone National Park. Min Record 12:29-38
Barrer RM, Cole JF, Villiger H (1970) Chemistry of soil minerals. Part VII. Synthesis, properties, and crystal structures of salt-filled cancrinites. J Chem Soc A:1523-1530
Barrer RM, Falconer JD (1956) Ion exchange in feldspathoids as a solid-state reaction. Proc Royal Soc 236: 227-249
Barrer RM, White EAD (1952) The hydrothermal chemistry of silicates. Part II. Synthetic crystalline sodium aluminosilicates. J Chem Soc (London):1561-1571
Baur WH (1991) The framework of $Na_8Al_6Ge_6O_{24}{\cdot}CO_3{\cdot}2H_2O$ has the LOS topology. Zeolites 11:639
Belokoneva EL, Uvarova TG, Dem'yanets LN (1986) Crystal structure of synthetic Ge-cancrinite $Na_8[Al_6Ge_6O_{24}]Ge(OH)_6{\cdot}2H_2O$. Sov Phys Crystallogr 31:516-519
Bentor YK, Gross S, Heller L (1963) Some unusual minerals from the "mottled zone" complex, Israel. Am Mineral 48:924-930
Bieniok A, Brendel U, Amthauer G (2004) Synthesis and characterisation of a microporous cobaltphosphate with the cancrinite framework structure. Micro- and Mesoporous Mineral Phases (Accad Lincei, Roma). Volume of Abstracts, p 63-64
Bieniok A, Brendel U, Paulus E (1998) Synthese und Struktur eines Zinkphosphat-Cancrinits. Z Kristallogr Suppl. Issue 15:26.
Binon J, Bonaccorsi E, Bernhardt HJ, Fransolet AM (2004) The mineralogical status of "cavolinite" from Vesuvius, Italy, and crystallochemical data on the davyne subgroup. Eur J Mineral 16:511-520
Bøggild OB (1908) On Gyrolite from Greenland. Meddelelser om Grønland 34:91
Bogomolov VN, Efimov AN, Ivanova MS, Poborchii VV, Romanov SG, Smolin YuI, Shepelev YuF (1992) Structure and optical properties of a one-dimensional chain of selenium atoms in a cancrinite channel. Sov Phys Solid State 34:916-919
Bonaccorsi E (1992) Feldspatoidi del gruppo della davyna: cristallochimica, trasformazioni di fase, scambi ionici. PhD Dissertation, Dipartimento di Scienze della Terra, Università di Pisa
Bonaccorsi E (2004) The crystal structure of giuseppettite, the 16-layer member of the cancrinite-sodalite group. Microporous Mesoporous Mater 73:129-136
Bonaccorsi E, Comodi P, Merlino S (1995) Thermal behavior of davyne-group minerals. Phys Chem Minerals 22:367-374
Bonaccorsi E, Merlino S (2004) Calcium silicate hydrate (C-S-H) minerals: structures and transformations. 32nd Int Geol Congr Abs 1:215
Bonaccorsi E, Merlino S, Kampf AR (2005) The crystal structure of tobermorite 14 Å (plombierite), a C-S-H phase. J Am Ceram Soc 88:505-512

Bonaccorsi E, Merlino S, Orlandi P, Pasero M, Vezzalini G (1994) Quadridavyne, $[(Na,K)_6Cl_2][Ca_2Cl_2][Si_6Al_6O_{24}]$, a new feldspathoid mineral from Vesuvius area. Eur J Mineral 6:481-487

Bonaccorsi E, Merlino S, Pasero M (1990) Davyne: its structural relationships with cancrinite and vishnevite. N Jb Mineral Mh 1990:97-112

Bonaccorsi E, Merlino S, Pasero M (1992) Davyne from Zabargad (St. John's) Island: peculiar chemical and structural features. Acta Vulcanol 2 Marinelli Volume:55-63

Bonaccorsi E, Merlino S, Pasero M, Macedonio G (2001) Microsommite: crystal chemistry, phase transitions, Ising model and Monte Carlo simulations. Phys Chem Miner 28:509-522

Bonaccorsi E, Orlandi P (2003) Marinellite, a new feldspathoid of the cancrinite-sodalite group. Eur J Mineral 15:1019-1027

Bresciani Pahor N, Calligaris M, Nardin G, Randaccio L (1982) Structure of a basic cancrinite. Acta Crystallogr B38:893-895

Brown L, Cesbron F (1973) Sur les surstructures des cancrinites. C R Acad Sc Paris Sèrie D 276:1-4

Buckner DA, Roy DM, Roy R (1960) Studies in the system $CaO$-$Al_2O_3$-$SiO_2$·$H_2O$. II: The system $CaSiO_3$-$H_2O$. Am J Science 258:132-147

Buhl J-Ch (1991) Synthesis and characterization of the basic and non-basic members of the cancrinite-natrodavyne family. Thermochim Acta 178:19-31

Buhl J-Ch, Stief F, Fechtelkord M, Gesing TM, Taphorn U, Taake C (2000) Synthesis, X-ray diffraction and MAS NMR characteristics of nitrate cancrinite $Na_{7.6}[AlSiO_4]_6(NO_3)_{1.6}(H_2O)_2$. J Alloys Compd 305:93-102

Burton A, Feuerstein M, Lobo RF, Chan JCC (1999) Characterization of cancrinite synthesized in 1,3-butanediol by Rietveld analysis of powder neutron diffraction data and solid-state $^{23}Na$ NMR spectroscopy. Microporous Mesoporous Mater 30:293-305

Camara F, Bellatreccia F, della Ventura G, Mottana A (2004) A new member of the cancrinite-sodalite group with a 14 layers stacking sequence. Micro- and Mesoporous Mineral Phases (Accad Lincei, Roma) Volume of Abstracts, p 186-187

Cann JR (1965) Gyrolite and reyerite from 'S Airde Beinn, northern Mull. Mineral Mag 35:1-4

Chalmers RA, Farmer VC, Harker RI, Kelly S, Taylor HFW (1964) Reyerite. Mineral Mag 33:821-840

Chorover J, Choi S, Amistadi MK, Karthikeyan KG, Crosson G, Mueller KT (2003) Linking Cesium and Strontium Uptake to Kaolinite Weathering in Simulated Tank Waste Leachate. Environ Sci Technol 37: 2200-2208

Claringbull GF, Hey MH (1952) A re-examination of tobermorite. Mineral Mag 29:960-962

Clement SC, Ribbe PH (1973) New locality, formula, and proposed structure for reyerite. Am Mineral 58: 517-522

Cong X, Kirkpatrick RJ (1996) $^{29}Si$ and $^{17}O$ NMR investigation of the structure of some crystalline calcium silicate hydrates. Adv Cem Bas Mater 3:133-143

Coombs DS, Alberti A, Armbruster T, Artioli G, Colella C, Galli E, Grice JD, Liebau F, Mandarino JA, Minato H, Nickel EH, Passaglia E, Peacor DR, Quartieri S, Rinaldi R, Ross M, Sheppard RA, Tillmanns E, Vezzalini G (1998) Recommended nomenclature for zeolite minerals: Report of the Subcommittee on Zeolites of the International Mineralogical Association, Commission on New Minerals and Mineral Names. Eur J Mineral 10:1037-1081

Cornu P, Himmelbauer A (1906) Reyerit. Tsch Mineral Petr Mitt 25:519-520

Currie J (1905) Note on some new localities for Gyrolite and Tobermorite. Mineral Mag 14:93-95

Dai Y, Post JE, Appleman DE (1995) Crystal structure of minehillite: twinning and structural relationships to reyerite. Am Mineral 80:173-178

Daubrée GA (1858) Sur la relation des sources thermales de Plombières avec les filons métallifères et sur la formation contemporaine des zéolithes. Annales des Mines ser. 5 13:227-256

Deer WA, Howie RS, Wise WS, Zussman J (2004) Rock-forming minerals. Vol. 4B Second Edition. Framework silicates: silica minerals, feldspathoids and the zeolites. The Geological Society, London

Depmeier W (2005) The sodalite family – a simple but versatile framework structure. Rev Mineral Geochem 57:203-240

Diamond S, White JL, Dolch WL (1966) Effects of isomorphous substitutions in hydrothermally-synthesized tobermorite. Am Mineral 51:388-401

Dornberger Schiff K (1956) On the order-disorder (OD-structures). Acta Crystallogr 9:593-601

Dornberger Schiff K (1964) Grundzüge einer Theorie von OD-Strukturen aus Schichten, Abh Deutschen Akad Wiss Berlin, Klasse für Chem Geol Biol 3:1-107

Dornberger-Schiff K (1966) Lehrgang über OD-Strukturen. Akademie-Verlag, Berlin

Dunn PJ, Peacor DR, Leavens PB, Wicks FJ (1984) Minehillite: A new layer silicate from Franklin, New Jersey, related to reyerite and truscottite. Am Mineral 69:1150-1155

Ďurovič S (1997) Fundamentals of the OD theory. EMU Notes in Mineralogy 1:3-28

Eakle AS (1917) Minerals associated with the crystalline limestone at Crestmore, Riverside County, California. Bull Dept Geol Univ Calif 10/19:327-330

Edgar AD (1964) Studies on cancrinites: II – Stability fields and cell dimensions of calcium and potassium-rich cancrinites. Can Mineral 8:53-67

Edgar AD, Burley BJ (1963) Studies on cancrinites I –Polymorphism in sodium carbonate rich cancrinite-natrodavyne. Can Mineral 7:631-642

Eitel W (1922) Über das System $CaCO_3$-$NaAlSiO_4$ (Calcit-Nephelin) und den Cancrinit. N Jb Mineral 2: 45-61

El Hemaly SAS, Mitsuda T, Taylor HFW (1977) Synthesis of normal and anomalous tobermorites. Cem Concr Res 7:429-438

Emiraliev A, Yamzin II (1982) Neutron-diffraction refinement of the structure of a carbonate-rich cancrinite. Sov Phys Crystallogr 27:27-30

Farmer VC, Jeevaratnam J, Speakman K, Taylor HFW (1966) Thermal decomposition of 14 Å tobermorite from Crestmore. *In:* Proc. Symp. 'Structure of Portland cement paste and concrete' Sp. Report 90, Highway Res. Board. Washington DC, p 291-299

Fechtelkord M, Posnatzki B, Buhl J-Ch (2003) Characterization of basic cancrinite synthesized in a butanediol-water system. Eur J Mineral 15:589-598

Fechtelkord M, Posnatzki B, Buhl J-Ch, Fyfe CA, Groat LA, Raudsepp M (2001) Characterization of synthetic Cs-Li cancrinite grown in a butanediol-water system: An NMR spectroscopic and Rietveld refinement study. Am Mineral 86:881-888

Ferraris G, Makovicky E, Merlino S (2004) Crystallography of Modular Materials. IUCr Monographs in Crystallography, Oxford University Press, Oxford

Ferraris G, Pavese A, Soboleva S (1995) Tungusite: new data, relationships with gyrolite and structural model. Mineral Mag 59:535-543

Ferreira A, Ananias D, Carlos LD, Morais CM, Rocha J (2003) Novel microporous lanthanide silicates with tobermorite-like structure. J Am Chem Soc 125:14573-14579

Flint EP, McMurdie HF, Wells LS (1938) Formation of hydrated calcium silicate at elevated temperatures and pressures. J Res Natl Bur Standards 21:617-638

Foit FFJr, Peacor DR, Heinrich EW (1973) Cancrinite with a new superstructure from Bancroft, Ontario. Can Mineral 11:940-951

Funk H (1961) Chemische Untersuchungen von Silicaten. XXVI. Über Calciumsilicathydrate mit der Zusammensetzung $CaO{\cdot}2SiO_2{\cdot}0.5\text{-}2H_2O$ und die Synthese des Reyerit (=Truscottit) ($CaO{\cdot}2SiO_2{\cdot}0.5H_2O$). Z anorg allg Chem 313:1-13

Funk H, Thilo E (1955) Über Hydrogensilicate. IV. Das Calcium-trihydrogenmonosilikat $Ca[OSi(OH)_3]_2$ und seine Umwandlung in das Calciumtetrahydrogendisilikat $Ca[Si_2O_3(OH)_4]$. Z anorg allg Chem 278:237-248

Gaines RV, Skinner HCW, Foord EE, Mason B, Rosenzweig A (1997) Dana's New Mineralogy, 8th Ed. John Wiley & Sons, New York

Garavelli CL, Vurro F (1984) Gyrolite from Ortano (Island of Elba). Rend Soc Ital Mineral Petrol 39:695-704

Garbev K (2004) Structure, properties and quantitative Rietveld analysis of calcium silicate hydrates (C-S-H-phases) crystallized under hydrothermal conditions. PhD Dissertation. Ruprecht-Karls-University, Heidelberg

Garbev K, Black L, Stumm A, Stemmermann P, Gasharova B (2004) Polymerization reactions by thermal treatment of gyrolite-group minerals – an IR spectroscopic and X-ray diffraction study based on synchrotron radiation. *In*: Applied Mineralogy. Pecchio et al (eds) 2004 ICAM-Br, São Paulo, p 245-248

Gard JA, Luke K, Taylor HFW (1981a) $Ca_7Si_{16}O_{40}H_2$, a new calcium silicate hydrate phase of the truscottite group. Cem Concr Res 11:659-664

Gard JA, Luke K, Taylor HFW (1981b) Crystal structure of K-phase, $Ca_7Si_{16}O_{40}H_2$. Sov Phys Crystallogr 26: 691-695

Gard JA, Mitsuda T, Taylor HFW (1975) Some observations on Assarsson's Z-phase and its structure relations to gyrolite, truscottite and reyerite. Mineral Mag 43:325-332

Gesing ThM, Buhl J-Ch (2000) Structure and spectroscopic properties of hydrogencarbonate containing alumosilicate sodalite and cancrinite. Z Kristallogr 215:413-418

Gies H, Kirchner R, van Koningsveld H, Treacey MMJ (1999) Faulted Zeolite Framework Structures. *In*: Proc. 12th International Zeolite Conference, Baltimore, Maryland, USA, July 5-11, 1998, Treacey MMJ, Marcus BK, Bisher ME, Higgins JB (Eds) Materials Research Society, MRS, Warrendale, Pennsylvania, p 2999-3029

Gottardi G, Passaglia E (1965) Tobermorite "non espandibile" di Prà de la Stua (Trento). Period Mineral 35: 197-204

Gottardi G, Passaglia E (1966) Tobermorite "non espandibile" e Gyrolite del Monte Biaena (Trento). Period Mineral 36:1079-1083
Grose LT, Keller GV (1976) Petrology of deep drill hole, Kilauea Volcano. Am Geophys Union Trans 57: 1017
Grundy HD, Hassan I (1982) The crystal structure of a carbonate-rich cancrinite. Can Mineral 20:239-251
Gutzmer J, Cairncross B (1993) Recent discoveries from the Wessels Mine, South Africa. Min Record 24: 365-368
Hackbarth K, Gesing ThM, Fechtelkord M, Stief F, Buhl J-Ch (1999) Synthesis and crystal structure of carbonate cancrinite $Na_8[AlSiO_4]_6CO_3(H_2O)_{3.4}$, grown under low-temperature hydrothermal conditions. Microporous Mesoporous Mater 30:347-358
Hara N, Chan CF, Mitsuda T (1978) Formation of 14 Å tobermorite. Cem Concr Res 8:113-116
Hara N, Inoue N (1980) Thermal behavior of 11 Å tobermorite and its lattice parameters. Cem Concr Res 10: 53-60
Harker RI (1964) Dehydration series in the system $CaO\text{-}SiO_2\text{-}H_2O$. J Am Ceram Soc 47:521-529
Harrison WTA, Gier TE, Stucky GD (1993) Synthesis and structure of $Li_8(HPO_4)(BePO_4)_6{\cdot}H_2O$ – a new zeolite, LOS-type beryllophosphate molecular sieve. Zeolites 13:242-248
Harvey RD, Beck CW (1962) Hydrothermal regularly interstratified chlorite-vermiculite and tobermorite in alteration zones at Goldfield, Nevada. Clays Clay Miner 9:343-354
Hassan I, Antao SM, Parise JB (2005) Cancrinite: structures, phase transition, dehydration, and Na mobilization at high temperatures. Eur J Mineral (accepted)
Hassan I, Buseck PR (1992) The origin of the superstructure and modulations in cancrinite. Can Mineral 30: 49-59
Hassan I, Grundy HD (1984) The character of the cancrinite-vishnevite solid-solution series. Can Mineral 22: 333-340
Hassan I, Grundy HD (1990) Structure of davyne and implications for stacking faults. Can Mineral 28:341-349
Hassan I, Grundy HD (1991) Crystal structure of basic cancrinite, ideally $Na_8[Al_6Si_6O_{24}](OH)_2{\cdot}3H_2O$. Can Mineral 29:377-383
Heddle MF (1880) Preliminary notice of substances which may prove to be new minerals. Mineral Mag 4: 117-123
Heddle MF (1893) On pectolite and okenite from new localities: the former with new appearances. Trans Geol Soc Glasgow 9:241-255
Heller L, Taylor HFW (1951) Hydrated calcium silicates. Part II. Hydrothermal reactions: lime:silica ratio 1: 1. J Chem Soc 1951:2397-2401
Heller L, Taylor HFW (1952) Hydrated calcium silicates. Part III. Hydrothermal reactions of lime:silica molar ratio 3:2. J Chem Soc 1952:1018-1020
Henmi C, Kusachi I (1989) Monoclinic tobermorite from Fuka, Bitchu-cho, Okayama Prefecture, Japan. J Min Petr Econ Geol 84:374-379 (in Japanese)
Henmi C, Kusachi I (1992) Clinotobermorite $Ca_5Si_6(O,OH)_{18}{\cdot}5H_2O$, a new mineral from Fuka, Okayama Prefecture, Japan. Mineral Mag 56:353-358
Hentschel G (1973) Begleitmineralien des Basalts vom Arensberg bei Zilsdorf/Eifel. Notizbl Hess Landesamt Bodenforsch 101:310-316
Hoffmann C, Armbruster T (1997) Clinotobermorite, $Ca_5[Si_3O_8(OH)]_2{\cdot}4H_2O$ – $Ca_5[Si_6O_{17}]{\cdot}5H_2O$, a natural C-S-H(I) type cement mineral: determination of the substructure. Z Kristallogr 212:864-873
Hogarth DD (1979) Afghanite: new occurrences and chemical composition. Can Mineral 17:47-52
Hong S-Y, Glasser FP (2003) Phase relations in the $CaO\text{-}SiO_2\text{-}H_2O$ system to 200°C at saturated steam pressure. Cem Concr Res 34:1529-1534
Hövig P (1914) Truscottiet. Jaarb Mijnwezen Ned Oost-Indië Batavia 41 (for 1912):202
Hund F (1984) Nitrat-, Thiosulfat-, Sulfat- und Sulfid-Cancrinit. Z Anorg Allg Chem 509:153-160
Ivanov VG, Sapozhnikov AN (1975) The first find of afghanite in the U.S.S.R.. Zap Vses Mineral Obs 104: 3328-3331 (in Russian)
Izawa E, Yamashita M (1995) Truscottite from the Hishikari deposit, Kagoshima Prefecture. J Soc Resource Geology 45:251-252
Jakobsson S, Moore JG (1986) Hydrothermal minerals and alteration rates at Surtsey volcano, Iceland. Geol Soc Am Bull 97:648-659
Jamtveit B, Dahlgren S, Austrheim H (1997) High-grade contact metamorphism of calcareous rocks from the Oslo Rift, Southern Norway. Am Mineral 82:1241-1254
Jander W, Franke B (1941) Die Bildung von Calciumhydrosilikaten aus Calciumoxyd und Kieselsauregel bei 300° und 350° und hohen Drucken. Z Anorg Allg Chem 247:161-179
Jarchow O (1965) Atomanordnung und Strukturverfeinerung von Cancrinit. Z Kristallogr 122:407-422

Joswig W, Drits VA, Sokolova GV (1988) Refinement of structure of fedorite. Sov Phys Crystallogr 33:763-765

Kalousek GL (1955) Tobermorite and related phases in the system $CaO$-$SiO_2$-$H_2O$. J Am Concr Inst 51:989-1011

Kalousek GL (1957) Crystal chemistry of the hydrous calcium silicates: I. Substitution of aluminum in the lattice of tobermorite. J Am Ceram Soc 40:124-132

Kalousek GL, Roy R (1957) Crystal chemistry of hydrous calcium silicates: II. Characterization of interlayer water. J Am Ceram Soc 40:236-239

Kanepit VN, Rieder EÉ (1995) Neutron diffraction study of cancrinite. J Struct Chem 36:694-696

Kato A, Matsubara S, Tiba T, Sakata Y (1984) A Barium-bearing Tobermorite from Heguri, Chiba prefecture, Japan. Bull Natn Sci Mus Tokyo, Ser. C, 1984:10131-10140

Khomyakov AP, Nadezhina TN, Rastsvetaeva RK, Pobedimskaya EA (1992) Hydroxycancrinite $Na_8[Al_6Si_6O_{24}](OH)_2{\cdot}3H_2O$: A new mineral. Zap Veseross Mineral Obs 121(1):100-105 (in Russian)

Khomyakov AP, Pobedimskaya EA, Nadezhina TN, Terenteva LE, Rastsvetaeva RK (1991a) Structural mineralogy of high-Si cancrinite. Moscow Univ Geol Bull 46:71-75

Khomyakov AP, Semenov EI, Pobedimskaya EA, Nadezhina TN, Rastsvetaeva RK (1991b) Cancrisilite $Na_7[Al_5Si_7O_{24}]CO_3{\cdot}3H_2O$: A new mineral of the cancrinite group. Zap Vses Mineral Obs 120(6):80-84 (in Russian)

Khukarenko AA, Orlova MP, Bulakh AG, Bagdasarov EA, Rimskaya-Korsakov OM, Nefedov EI, Il'inskii GA, Sergeev AS, Abakumova NB (1965) Caledonian complex of ultrabasic alkaline rocks and carbonatites of the Kola Peninsula and Northern Karelia. Nedra Press, Leningrad, Russia (in Russian)

Klaska R, Jarchow O (1977) Sinthetischer Sulfat-Hydrocancrinit vom Mikrosommit-typ. Naturwiss 64:93

Kobayashi A, Kawai T (1974) Gyrolite found in the andesitic tuffs, near the Sayama lake, Ueda city, Nagano Prefecture, Japan. Geosci Mag 25:367-370

Komarneni S, Breval E, Miyake M, Roy R (1987b) Cation-exchange properties of (Al+Na)-substituted synthetic tobermorites. Clays Clay Minerals 35:385-390

Komarneni S, Guggenheim S (1988) Comparison of cation exchange in ganophyllite and [Na+Al]-substituted tobermorite: crystal-chemical implications. Mineral Mag 52:371-375

Komarneni S, Roy DM (1983) Tobermorites: a new family of cation exchangers. Science 221:647-648

Komarneni S, Roy DM, Fyfe CA, Kennedy GJ (1987a) Naturally occurring 1.4nm tobermorite and synthetic jennite: characterization by $^{27}Al$ and $^{29}Si$ MASNMR spectroscopy and cation exchange properties. Cem Concr Res 17:891-895

Komarneni S, Roy DM, Roy R (1982) Al-substituted tobermorite: shows cation exchange. Cem Concr Res 12:773-780

Komarneni S, Roy R, Roy DM, Fyfe CA, Kennedy GJ, Bothner-By AA, Dadok J, Chesnick AS (1985) $^{27}Al$ and $^{29}Si$ magic angle spinning nuclear magnetic resonance spectroscopy of Al-substituted tobermorites. J Mater Science 20:4209-4214

Konyev AA, Vorobyev YI, Bulakh AG (1993) Charoit – der Schmukstein aus Sibirien und seine seltenen Begleit-minerale. Lapis 1993:13-20

Kudriashova VI (1966) Tungusite, a new hydrous silicate of calcium. Dokl Akad Nauk SSSR 171:163-166

Lachowski EE, Murray LW, Taylor HFW (1979) Truscottite: composition and ionic substitutions. Mineral Mag 43:333-336

Lee Y, Parise JB, Tripathi A, Kim SJ, Vogt T (2000) Synthesis and crystal structures of gallium and germanium variants of cancrinite. Microporous Mesoporous Mater 39:445-455

Leoni L, Mellini M, Merlino S, Orlandi P (1979) Cancrinite-like minerals: new data and crystal chemical considerations. Rend Soc Ital Mineral Petrol 35:713-719

Lindner G-G, Hoffmann K, Witke K, Reinen D, Heinemann C, Koch W (1996) Spectroscopic properties of $Se_2^{2-}$ and $Se_2^{-}$ in cancrinite. J Solid State Chem 126:50-54

Lindner G-G, Massa W, Reinen D (1995) Structure and properties of hydrothermally synthesized thiosulfate cancrinite. J Solid State Chem 117:386-391

Liu C, Li S, Tu, K, Xu R (1993) Synthesis of cancrinite in butane-1,3-diol systems. Chem Comm 1993:1645-1646

Livingstone A (1988) Reyerite, tobermorite, calcian analcime and bytownite from amygdales in a Skye basalt. Mineral Mag 52:711-713

Mackay AL, Taylor HFW (1953) Gyrolite. Mineral Mag 30:80-91

Mackay AL, Taylor HFW (1954) Truscottite. Mineral Mag 30:450-457

Maeshima T, Noma H, Sakiyama M, Mitsuda T (2003) Natural 1.1 and 1.4 nm tobermorites from Fuka, Okayama, Japan: chemical analysis, cell dimensions, $^{29}Si$ NMR and thermal behavior. Cem Concr Res 33:1515-1523

Mamedov KS, Belov NV (1958) The crystal structure of micaceous Ca-hydrosilicates: okenite, nekoite, truscottite, gyrolite. A new silico-oxygen radical $[Si_6O_{15}]$. Dokl Akad Nauk SSSR 121:720-723

Marincea S, Bilal E, Verkaeren J, Pascal M-L, Fonteilles M (2001) Superposed parageneses in the spurrite-, tilleyite- and gehlenite-bearing skarns from Cornet Hill, Apuseni Mountains, Romania. Can Mineral 39: 1435-1453
Mashal K, Harsh JB, Flury M, Felmy AR, Zhao H (2004) Colloid formation in Hanford sediments reacted with simulated tank waste. Environ Sci Technol 38:5750-5756
McConnell JDC (1954) The hydrated calcium silicates riversideite, tobermorite, and plombierite. Mineral Mag 30:293-305
McCusker LB, Liebau F, Engelhardt G (2001) Nomenclature of structural and compositional characteristics of ordered microporous and mesoporous materials with inorganic hosts. (IUPAC Recommendations 2001). Pure Appl Chem 73:381-394
McDonald AM, Chao GY (2002) Martinite, a new borosilicate mineral from Mont Saint-Hilaire, Quebec, Canada: description and crystal structure determination. 18th Gen Meet IMA 1:139
Merlino S (1972) New tetrahedral sheets in reyerite. Nature Phys Sci 238:124-125
Merlino S (1984) Feldspathoids: their average and real structures. *In*: Feldspars and Feldspathoids. Brown WL (ed), Riedel Publishing Company, Dordrecht, p 457-470
Merlino S (1988a) Gyrolite: its crystal structure and crystal chemistry. Mineral Mag 52:377-387
Merlino S (1988b) The structure of reyerite, $(Na,K)_2Ca_{14}Si_{22}Al_2O_{58}(OH)_8.6H_2O$. Mineral Mag 52:247-256
Merlino S (1997) OD approach in minerals. EMU Notes in Mineralogy 1:29-54
Merlino S, Bonaccorsi E, Armbruster T (1999) Tobermorites: Their real structure and order-disorder (OD) character. Am Mineral 84:1613-1621
Merlino S, Bonaccorsi E, Armbruster T (2000) The real structures of clinotobermorite and tobermorite 9 Å: OD character, polytypes, and structural relationships. Eur J Mineral 12:411-429
Merlino S, Bonaccorsi E, Armbruster T (2001) The real structure of tobermorite 11 Å: normal and anomalous forms, OD character and polytypic modifications. Eur J Mineral, 13:577-590
Merlino S, Mellini M, Bonaccorsi E Pasero M, Leoni L, Orlandi P (1991) Pitiglianoite, a new feldspathoid from southern Tuscany, Italy: chemical composition and crystal structure. Am Mineral 76:2003-2008
Meyer JW, Jaunarais KL (1961) Synthesis and crystal chemistry of gyrolite and reyerite. Am Mineral 46: 913-933
Milestone NB, Hughes SM, Stonestreet PJ (1995) Synthesis of zeolites in anhydrous glycol systems. Stud Surf Sci Catal 98:42-43
Minato H, Kato A (1967) Truscottite from the Toi mine, Shizuoka Prefecture. Mineral J (Japan) 5:144-156
Mitchell RH, Burns PC (2001) The structure of fedorite: a re-appraisal. Can Mineral 39:769-777
Mitsuda T (1973) Paragenesis of 11 Å tobermorite and poorly crystalline hydrated magnesium silicate. Cem Concr Res 3:71-80
Mitsuda T, Taylor HFW (1978) Normal and anomalous tobermorites. Mineral Mag 42:229-235
Miyake M, Komarneni S, Roy R (1989) Kinetics, equilibria and thermodynamics of ion exchange in substituted tobermorites. Mater Res Bull 24:311-320
Nadezhina TN, Rastsvetaeva RK, Pobedimskaya EA, Khomyakov AP (1991) Crystal structure of natural hydroxyl-containing cancrinite. Sov Phys Crystallogr 46:325-327
Nawaz R (1977) A second occurrence of killalaite. Mineral Mag 41:546-548
Němec D (1982) Assemblages of fissure minerals in the basic Ransko Massif. N Jb Mineral Abh 145:256-269
Nithollon P, Vernotte MP (1955) Structure cristalline de la cancrinite. Publ Sci Tech Ministère Air, France, Notes Tech 53, 48 pp
Norby P, Krogh Andersen IG, Krogh Andersen E, Colella C, De Gennaro M (1991) Synthesis and structure of lithium cesium and lithium thallium cancrinites. Zeolites 11:248-253
Park M, Choi CL, Lim WT, Kim MC, Choi J, Heo NH (2000) Molten-salt method for the synthesis of zeolitic materials II. Characterization of zeolitic materials. Microporous Mesoporous Mater 37:91-98
Passaglia E, Turconi B (1982) Silicati ed altri minerali di Montalto di Castro (Viterbo). Rivista Mineralogica Italiana 1982:97-110
Pauling L (1930) The structure of some sodium and calcium aluminosilicates. Proc Natl Acad Sci 16:453-459
Peacor DR, Dunn PJ, Nelen JA (1990) Orlymanite, $Ca_4Mn_3Si_8O_{20}(OH)_6{\cdot}2H_2O$, a new mineral from South Africa: A link between gyrolite-family and conventional phyllosilicate minerals? Am Mineral 75:923-927
Peacor DR, Rouse RC, Ahn J-Ho (1987) Crystal structure of tiptopite, a framework beryllophosphate isotypic with basic cancrinite. Am Mineral 72:816-820
Pobedimskaya YeA, Terent'eva LYe, Rastsvetaeva RK, Sapozhnikov AN, Kashaev AA, Dorokhova GI (1991) Kristallicheskaya struktura bystrita. Dokl Akad Nauk SSSR 319:873-878 (in Russian)
Pushcharovskii DYu, Yamnova NA, Khomyakov AP (1989) Crystal structure of high-potassium vishnevite. Sov Phys Crystallogr 34:37-39
Rinaldi R (1982) More stacking variations in cancrinite-related minerals; how many more new minerals? J Microsc Spectrosc Electron 7:76a-77a

Rinaldi R, Wenk H-R (1979) Stacking variations in cancrinite minerals. Acta Cryst A35:825-828
Rocha J, Lin Z (2005) Microporous mixed octahedral-pentahedral-tetrahedral framework silicates. Rev Mineral Geochem 57:173-202
Rozenberg KA, Sapozhnikov AN, Rastsvetaeva RK, Bolotina NB, Kashaev AA (2004) Crystal structure of a new representative of the cancrinite group with a 12-layer stacking sequence of tetrahedral rings. Crystallogr Rep 49:635-642
Sakiyama M, Maeshima T, Mitsuda T (2000) Synthesis and crystal chemistry of Al-substituted 11 Å tobermorite. J Soc Inorg Mater Jpn 7:413-419
Sapozhnikov AN (2004) Influence of the chemical composition on the framework configuration of cancrinite-like minerals. Micro- and Mesoporous Mineral Phases (Accad Lincei, Roma). Volume of Abstracts, p 290-293
Sapozhnikov AN, Levitsky VI, Cherepanov DI, Suvorova LF, Bogdanova LA (2004) About influence of chlorine upon the framework configuration in cancrinite-like minerals. Zap Veseross Mineral Obs 133(5): 93-102 (in Russian)
Sasaki K, Masuda T, Ispida H, Mitsuda T (1996) Structural degradation of tobermorite during vibratory milling. J Am Ceram Soc 79:1569-1574
Shaw S, Clark SM, Henderson CMB (2000) Hydrothermal formation of the calcium silicate hydrates, tobermorite [$Ca_5Si_6O_{16}(OH)_2{\cdot}4H_2O$] and xonotlite [$Ca_6Si_6O_{17}(OH)_2$] an in-situ synchrotron study. Chem Geol 167:129-140
Shaw S, Henderson CMB, Clark SM (2002) In-situ synchrotron study of the kinetics, thermodynamics, and reaction mechanism of the hydrothermal crystallization of gyrolite $Ca_{16}Si_{24}O_{60}(OH)_8{\cdot}14H_2O$. Am Mineral 87:533-541
Shrivastava O P, Komarneni S, Breval E (1991) $Mg^{2+}$ uptake by synthetic tobermorite and xonotlite. Cem Concr Res 21:83-90
Šiačiūnas R, Baltakys K (2004) Formation of gyrolite during hydrothermal synthesis in the mixtures of CaO and amorphous $SiO_2$ or quartz. Cem Concr Res 34:2029-2036
Šiačiūnas R, Palubinskaite D, Ivaunaskas R (2002) Elimination of heavy metals from water by modified tobermorite. Envir Res Engin Manag 3(21):61-66
Sieber W, Meier WM (1974) Formation and properties of Losod, a new sodium zeolite. Helv Chim Acta 57: 1533-1549
Sirbescu M, Jenkins DM (1999) Experiments on the stability of cancrinite in the system $Na_2O$-CaO-$Al_2O_3$-$SiO_2$-$CO_2$-$H_2O$. Am Mineral 84:1850-1860
Smolin YuI, Shepelev YuF, Butikova IK, Kobyakov IB (1981) Crystal structure of cancrinite. Sov Phys Crystallogr 26:33-35
Sokolov YuA, Maksimov BA, Galiulin RV, Ilyukhin VV, Belov NV (1981) Determination of crystal structure of cancrinite-like $Na_8Al_6Ge_6O_{24}(CO_3){\cdot}2H_2O$. Patterson and diffraction pseudosymmetry. Sov Phys Crystallogr 26:161-164
Sokolov YuA, Maksimov BA, Ilyukhin VV, Belov NV (1978) Low-temperature investigation of the crystal structure of sodium aluminogermanate $Na_8Al_6Ge_6O_{24}(CO_3){\cdot}3H_2O$. Sov Phys Dokl 23:789-791
Sokolova GV, Kashaev AA, Drits VA, Ilyukhin VV (1983) The crystal structure of fedorite. Sov Phys Crystallogr 28:95-96
Stephens DJ, Bray E (1973) Occurrence and infrared analysis of unusual zeolitic minerals from Bingham, Utah. Min Record 4:67-72
Strunz H, Micheelsen H (1958) Calcium phyllosilicates. Naturwiss 45:515
Sweet JM, Bothwell DI, Williams DL (1961) Tacharanite and other hydrated calcium silicates from Portree, Isle of Skye. Mineral Mag 32:745-753
Taylor HFW (1950) Hydrated calcium silicates. Part I. Compound formation at ordinary temperatures. J Chem Soc 1950:3682-3690
Taylor HFW (1953a) Crestmoreite and riversideite. Mineral Mag 30:155-165
Taylor HFW (1953b) Hydrated calcium silicates. Part V. The water content of calcium silicate hydrate (I). J Chem Soc 1953:163-171
Taylor HFW (1962) Hydrothermal reactions in the systems CaO-$SiO_2$-$H_2O$ and the steam curing of cement and cement-silica products. *In*: Chemistry of Cement, Proceedings of the Fourth International Symposium. National Bureau of Standards Monograph 43. U.S. Department of Commerce, Washington DC, p 167-204
Taylor HFW (1964) The calcium silicate hydrates. *In:* Chemistry of Cements. Vol. 1. Taylor HFW (Ed) Academic Press, London, p 167-232
Taylor HFW (1986) Proposed structure for calcium silicate hydrate gel. J Am Ceram Soc 69:464-467
Taylor HFW (1992) Tobermorite, jennite, and cement gel. Z Kristallogr 202:41-50
Tsuji M, Komarneni S (1989) Alkali metal ion selectivity of Al-substituted tobermorite. J Mater Res 4:698-703

Tsuji M, Komarneni S, Malla P (1991) Substituted tobermorites: $^{27}$Al and $^{29}$Si MASNMR, cation exchange, and water sorption studies. J Am Ceram Soc 74:274-279

Vaughan DEW (1986) A crystalline zeolite composition having a cancrinite-like structure and a process for its preparation. Eur Patent 0 190 903 A3

Vaughan DEW (1991) Process for preparation of an ECR-5 crystalline zeolite composition. US Patent 5,015,454

Walenta K (1980) Zeolithparagenesen aus dem Melilith-Nephelinit des Howenegg im Hegau. Aufschluss 25: 613-626

Webb ABSJ (1971) Tobermorite from Castle Hill near Kilbirnie, Ayrshire. Mineral Mag 38:253

White DE, Fournier RO, Muffler LJP, Truesdell AH (1975) Physical results of research drilling in thermal areas of Yellowston National Park, Wyoming. U S Geol Survey Prof Paper 892

Wieker W, Grimmer A-R, Winkler A, Mägi M, Tarmak M, Lippmaa E (1982) Solid-state high-resolution $^{29}$Si NMR spectroscopy of synhetic 14 Å, 11 Å and 9 Å tobermorites. Cem Concr Res 12:333-339

Yakubovich OV, Karimova OV, Mel'nikov OK (1994) A new representative of the cancrinite family $(Cs,K)_{0.33}[Na_{0.18}Fe_{0.16}(H_2O)_{1.05}]\{ZnPO_4\}$: preparation and crystal structure. Crystallogr Rep 39:564-568

Yamazaki S, Toraya H (2001) Determination of positions of zeolitic calcium atoms and water molecules in hydrothermally formed aluminum-substituted tobermorite-1.1nm using synchrotron radiation powder data. J Am Ceram Soc 84:2685-2690

Zadov AE, Chukanov NV, Organova NI, Belakovsky DI, Fedorov AV, Kartashov PM, Kuzmina OV, Litzarev MA, Moknov AV, Loskutov AB, Finko VI (1995) New results: the investigations on the minerals of the tobermorite group. Proc Russ Miner Soc 124:36-54

Zhuang J, Flury M, Jin Y (2003) Colloid-facilitated Cs transport through water-saturated Hanford sediment and Ottawa sand. Environ Sci Technol 37:4905-4911

Zvyagin BB (1997) Modular analysis of crystals. EMU Notes in Mineralogy 1:345-372

Zyryanov VN (1982) Cancrinite equilibria in the system Can-Ne-Fsp-$(K,Na),CO_3^{aq}$. Internat Geol Rev 24: 671-676